Chemical Papers (2020) 74:3195–3232
https://doi.org/10.1007/s11696-020-01180-8

REVIEW

Fluorescent, colourimetric, and ratiometric probes based on diverse fluorophore motifs for mercuric(II) ion (Hg^{2+}) sensing: highlights from 2011 to 2019

Stephen Opeyemi Aderinto[1]

Received: 3 January 2020 / Accepted: 28 April 2020 / Published online: 16 May 2020

Abstract
Though it has not been shown to deliver any biological importance, mercuric(II) ion (Hg^{2+}) is a deleterious cation which poses grievous effects to the human body and/or the ecosystem, hence, the need for its sensitive and selective monitoring in both environmental and biological systems. Over the years, there has been a great deal of work in the use of fluorescent, colourimetric, and/or ratiometric probes for Hg^{2+} recognition. Essentially, the purpose of this review article is to give an overview of the advances made in the constructions of such probes based on the works reported in the period from 2011 to 2019. Discussion in this review work has been tailored to the kinds of fluorophore scaffolds used for the constructions of the probes reported. Selected examples of probes under each fluorophore subcategory were discussed with mentions of the typically determined parameters in an analytical sensing operation, including modulation in fluorescence intensity, optimal pH, detection limit, and association constant. The environmental and biological application ends of the probes were also touched where necessary. Important generalisations and conclusions were given at the end of the review. This review article highlights 196 references.

Keywords Mercuric(II) ion (Hg^{2+}) · Fluorescent probes · Colourimetric probes · Ratiometric probes · Hg^{2+}-selective probes · Sensing

Introduction

Mercury (II) (Hg^{2+}) detection

Generating means to detect mercury(II) (Hg^{2+}) is necessary since reports have shown Hg^{2+} to be a health threat to the world environment, this stemming from its highly toxic nature and ubiquitous impact in both the lithosphere and hydrosphere (Coronado et al. 2005). Years of experimental works have shown Hg^{2+} to pose health problems not only to human beings but also to other animal species. Hg^{2+} contamination is being engendered through natural and anthropogenic endeavours, including ocean and volcanic eruptions, mining of metal (especially artisanal and small-scale gold mining, ASGM), incineration of waste, tanning of leather, electroplating, occupational operations, dental care, preventive medical practices, agricultural and industrial operations, and fossil fuel combustion (from coal-burning power plants) (Renzoni et al. 1998; Rice et al. 2014; Bravo et al. 2014; Costa et al. 2016; Martinez-Finley et al. 2014). Elemental mercury and ionic mercury (Hg and Hg^{2+}, respectively) have the tendency to be transformed by microorganisms like bacteria into methylmercury (MeHg), which is a potentially harmful neurotoxin capable of bioaccumulation into the food chain (Nolan and Lippard 2008). Its damaging effect on the placenta of pregnant women has been particularly identified, which thereby poses a developmental problem to foetal brain and central nervous system, resulting in a developmental delay in children (Coronado et al. 2005; Kim et al. 2008; Gibb and OLeary 2014). This can then implicate certain biological processes, inducing a chain of diseases including splanchnic damage, nosebleed, headache, perforation of the stomach, nerve disorder, intestines septum, and acute renal failure (Renzoni et al. 1998; Zhai et al. 2012; Hoyle et al. 2005; Zarlaida 2017). As such, exposure to low concentrations of Hg^{2+} can trigger numerous grievously damaging

✉ Stephen Opeyemi Aderinto
soaderinto1@sheffield.ac.uk

[1] Department of Chemistry, The University of Sheffield, Dainton Building, Brook Hill, Sheffield S3 7HF, UK

effects to the human heart, kidney, stomach, and intestines, resulting in metabolic disorders, motor and cognitive disorders, and sensory malfunctions and disorders (Rice et al. 2014; Hoyle and Handy 2005; Arya and Bhansali 2011; Ghasemi et al. 2018; Wang et al. 2008). This has resulted in stringent regulations imposed on relevant industries to bring about a clean-up system for mercury-laden wastewater before its discharge into waste streams. The maximum permissible limit of total mercury in wastewater discharge is 10 µg/L (US Environmental Protection Agency 2001; Kumar et al. 2012a). US EPA's previously regularised guideline of Hg^{2+} in drinking water of 1 µg/L was changed to 6 µg/L in 2005—the former value being based on methylmercury (MeHg), whilst the recent guideline is based on inorganic mercury (Frisbie et al. 2015). Amongst the various heavy metals, Hg^{2+} ion shows the most toxicity, hence, the inspiration and need for its monitoring. These obvious environmental and biological threats which (Hg^{2+}) poses have engendered the construction of methods for its detection and measurement in aqueous phases—three of such widely exploited concepts being the fluorescent, colourimetric, and/or ratiometric detection modes due to their pre-eminence over other detection techniques.

The fluorescence, colourimetric, and ratiometric optical detection methods

The past twenty plus years of the arrival of the supramolecular chemistry have recorded stunning successes in the constructions of fluorescent, colourimetric, and ratiometric probes as vibrant, vital tools for the sensing of environmentally and biologically relevant cations and anions, and also for the detection of H^+ (proton) in biological assays (Gunnlaugsson et al. 2006; Lodeiro and Pina 2009; Duke et al. 2010; Georgiev et al. 2011; Park et al. 2020). Compared to conventional analytical detection methods of voltammetry, polarography, X-ray fluorescence analysis, infrared spectroscopy, atomic fluorescence spectrometry, high-performance liquid chromatography, mass spectrometry, atomic absorption spectroscopy, etc., which have been utilised to recognise heavy metal ions like Hg^{2+}, the fluorescence method is a preferred, sought-after, and powerful analytical tool. The fluorescence technique has been employed for molecular recognition since it offers the benefits of high spatial resolution, ultra-high sensitivity and selectivity, real-time detection, local observation, operational simplicity, equipment's inexpensiveness, quick response time, and non-destructive nature (Lee et al. 2015; Carter et al. 2014; Zhang et al. 2014; Kim et al. 2012, 2011; Chen et al. 2012; Yang et al. 2013; Singha et al. 2019). Because of these merits, there have been successful instances of the application of the fluorescent technique in clinical diagnostics, biotechnology, biochemistry and molecular biology, materials and environmental sciences (Mason 1999). It has been used for the monitoring of diverse groups of analytes including heavy metal ions, explosives, peptides, and pesticides (Bigdeli et al. 2019).

The colourimetric method, a powerful analytical technique like the fluorescence method, has also been harnessed in the field of sensing science as it affords the ability for naked-eye monitoring of analytes even before spectrophotometric analytical investigation (Kaur et al. 2018). Colourimetric probes upon interaction with analytes give 'naked-eye' (i.e. visibly detectable) colour changes, which are easily detectable signal outputs that do not need any sophisticated instruments. Diagnostic assays like blood-glucose monitoring and early pregnancy tests are two key instances where the colourimetric method has been successfully applied (Bicker et al. 2011).

The ratiometric detection approach has been put in place to overcome some sensitivity difficulties usually encountered in optical detection (e.g. interference from a variety of analyte-independent factors, including instrumental parameters, the probe's microenvironment, the probe's local concentration, and photobleaching) (Bigdeli et al. 2019; Lee et al. 2015). Ratiometric fluorescence detection method affords the possibility of simultaneous recording of two measurable signals in the presence and absence of analyte (Grynkiewicz et al. 1985). This detection technique is usually both desirable and preferable as it can measure fluorescence signals at two different wavelengths unlike the traditional methods that measure fluorescence intensity only at a single wavelength. Fluorescent resonance energy transfer (FRET) allows for the possibility of precise and quantitative read-outs. Due to this desirable property of FRET, many ratiometric fluorescent probes, such as some discussed in this review, have been designed by adopting the FRET-based ratiometric approach. FRET, in principle, is a distance-dependent physical process involving the non-radiative transfer of energy from an excited molecular fluorophore, i.e. the donor, to another fluorophore, i.e. the acceptor, through an intermolecular long-range, dipole–dipole coupling. FRET can measure molecular closeness at angstrom distances of 10–100 Å and is highly efficient if the donor and acceptor are positioned within the Förster radius (i.e. the distance at which half the excitation energy of the donor is transferred to the acceptor, usually 3–6 nm). FRET is a sensitive technique that could investigate biological processes which induce changes in molecular proximity as it is dependent on the one-sixth of inter-molecular separation (Förster 965; Clegg 1996; Lakowicz 1999; dos Remedios et al. 1987). Apart from FRET, in the context of this review work, other detection mechanisms/strategies including photoinduced electron transfer (PET), internal charge transfer (ICT), twisted intramolecular charge transfer (TICT), electron transfer (ET), energy transfer (eT), through-bond energy transfer (TBET), fluorescence resonance energy transfer (FRET), time-gated fluorescence resonance energy

transfer (TG-FRET), aggregation-induced emission (AIE), through-bond fluorescence resonance energy transfer (TBFRET), etc., have also been employed for the design of some reported probes towards Hg^{2+}detection.

Overview of commonly used molecular motifs for sensing operation

Prompted by the efficacy of the fluorescence, colourimetric, and ratiometric detection techniques, a plethoric number of probes have been developed using various categories of fluorophore motifs. The analytical advantages of small-molecule probes have been recognised, viz high selectivity, bioorthogonality, minimal perturbation to living systems, high sensitivity, simplicity of manipulation, and non-sophistication of instrumentation (Chan et al. 2012; Chen et al. 2011). The year 1845 saw the report of the first fluorescent organic molecule, the sulphate of quinine, which was discovered by Sir John Herschel (1845), whilst the year 1852 saw the advent of the term 'fluorescence', which was conceptualised by Stokes (1845). The discovery of quinine sulphate (Fig. 1) has informed the discovery of many other organic compounds which fluoresce with distinctive colours. These include fluorescein and rhodamine derivatives, boron-dipyrromethene (BODIPY) dyes, cyanine dyes, and others (Fig. 1) (Zheng et al. 2013; Baeyer 1871; Ceresole 1888; Loudet and Burgess 2007; Luo et al. 2011). Dyes which fluoresce with red to near-infrared (NIR) light show great potentials for in vivo imaging in biological systems, owing to their ability to penetrate tissues in the red to near-infrared wavelength region (650–900 nm) (Luo et al. 2011; Weissleder and Ntziachristos 2003). This has implied the development of a new class of dyes, which not only emit red or NIR fluorescence but possess higher extinction coefficients. This class of dyes anchors fluorophores functionalised with additional ring systems or heteroatoms or dye moieties which have been structurally modified. (Umezawa et al. 2008; Yuan et al. 2012; Egawa et al. 2011; Kim et al. 2011; Samanta et al. 2010). Lately, fluorescent dyes with two-photon imaging and super-resolution imaging abilities (Kim and Cho 2009; Krishna et al. 2006; Maçôas et al. 2011) have been gaining momentum for sensing purposes.

Probes based on supramolecular structures usually show superior sensing properties to those based on simple synthetic organic dyes. Common supramolecular structures which are successful in the designs and syntheses of Hg^{2+} probes include 1,4,7,10-tetraazacyclododecanes (cyclen), cyclodextrin, calixarene, porphyrin, crown ethers, helicene, peptidyl, amongst others (Fig. 2) (Kappe 1994; Liu et al. 2008; Lee et al. 2018; Li et al. 2018; Shen and Chen 2012; Tung 2004; Athey and Kiefer 2002; Rothemund 1936; Gierczyk et al. 2013). Many synthetic organic probes have been simply employed in their polymeric forms for improved

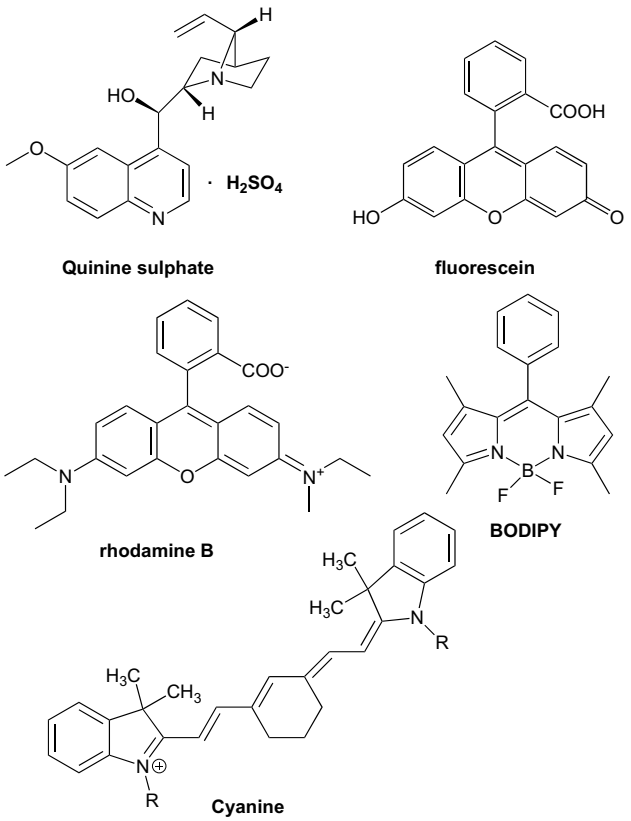

Fig. 1 Structures of some common organic compounds employed as small-molecule probes (Herschel Sir 1845; Zheng et al. 2013; Baeyer 1871; Ceresole 1888; Loudet and Burgess 2007; Luo et al. 2011)

sensing properties. Polymer-embedded optical probes stand out for their several merits, including, signal amplification, ease of use, simplicity of fabrication into devices, and combination of different outputs (Kim et al. 2011).

A burgeoning interest exists in the development of probes based on metal-organic frameworks (MOFs) and covalent-organic frameworks (COFs) as they possess outstanding features of large surface areas, regular pore structures, tunability in their pore sizes and functionalities, and thermal stabilities (Zhang and Yuan 2018; Rudd et al. 2016). These strong merits make them employable as probes for imaging applications. Typically, MOFs have two components: the metal ion or cluster and the organic linker. Common organic linkers used for the constructions of MOFs have been summarised in a paper published by Allendorf's group. The properties of MOFs can be modulated easily by varying the linker, metal, and/or growth conditions (Allendorf et al. 2009). Covalent organic frameworks (COFs) are covalent porous crystalline polymers that enable the elaborate integration of organic building blocks into an ordered structure with atomic precision. COFs possess high thermal stabilities, low mass densities, and long-lasting porosity. These interesting properties of COFs have made them useful

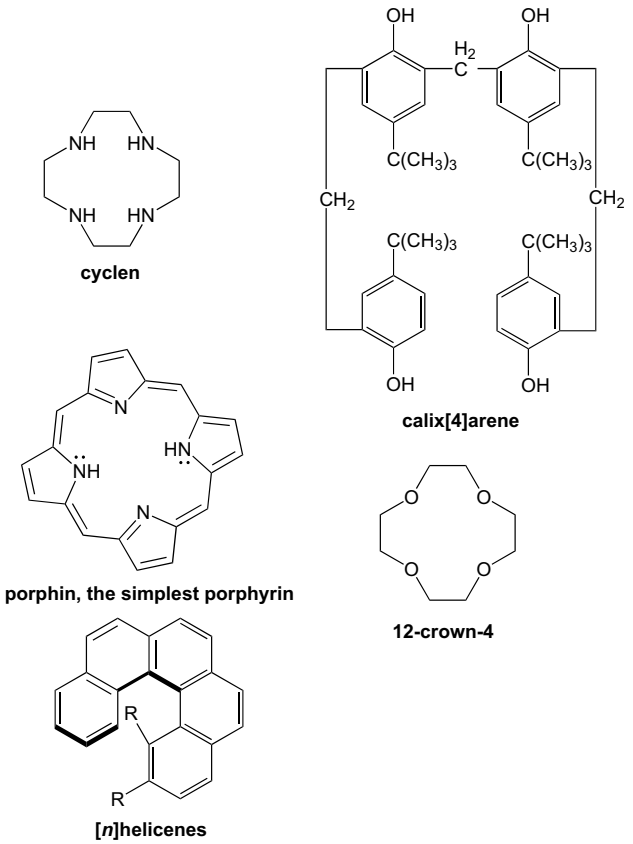

Fig. 2 A few examples of common supramolecular structures employed as probes (Kappe 1994; Liu et al. 2008; Lee et al. 2018; Li et al. 2018; Shen and Chen 2012; Tung 2004; Athey and Kiefer 2002; Rothemund 1936; Gierczyk et al. 2013; Urbano 2003)

towards sensing ends. Both two-dimensional (2D) and three-dimensional (3D) COFs have been recognised (Feng et al. 2012). A diversity of building blocks is available for the development of COFs, and this has been given in a reported literature (James 2003).

Research investigations have found out that some drawbacks of fluorescent dyes can be combated or at the very least ameliorated by the enclosure of the dye in nanoparticle delivery systems (Koo et al. 2007). The distinctive optical and electronic properties of nanomaterials have informed their increasing use as probes and diagnostic agents (Xu et al. 2014). Probes based on nanomaterials possess the advantages of stronger fluorescent emission, large surface-area-to-volume ratio, stability, multifunctionality, target specificity, simplicity, novelty, high selectivity and sensitivity, excellent sensing parameters such as low detection limit and water solubility (Guo et al. 2014; Song et al. 2010). Common examples of nanomaterials include gold nanorods, silver nanoparticles, DNA oligomers, silica nanoparticles (Xu and Suslick 2010; Guo et al. 2009; Ritchie et al. 2007; Shang and Dong 2008; Zhou et al. 2016; Zhang et al. 2015a), quantum dots (QDs) (e.g. CdSe and CdTe), TiO_2 NPs, SiO_2 NPs, and Fe_3O_4 NPs (Lin et al. 2011). Probes based on QDs show superior features of outstanding stability, tunable and minuscule emission spectrum, large quantum yield and Stokes' shifts, wide excitation wavelength, which mirror the merits of synthetic organic probes. Graphene oxides (GOs) show tunable physicochemical properties and good dispersion ability in many solvents, especially in water (Freeman et al. 2009; Abdelhamid and Wu. 2015). Many mercuric (II) (Hg^{2+}) nanoprobes either make use of the change in colour (absorption) or fluorescence intensity ('turn on' and 'turn off') in their detection modes. Some of these can be DNA-functionalised or non-DNA-functionalised.

The purpose, scope, and structure of this current review

To be as brief and direct as possible, the fundamental rules and principles governing the design strategies of probes are left out in this review paper. Insights into these have been given in some other excellent review works (Chan et al. 2012; Kaur et al. 2016). Even though as of the present, a large assembly of fluorescent, colourimetric, and/or ratiometric probes for Hg^{2+}-selective monitoring with suitable applications have been covered in a few previously reported works; however, such exist in rather 'old' references. (Readers are referred to see the review articles by Nolan and Lippard (2008), Mahato et al. (2014), and Chen et al. (2015.) This current review has the purpose of presenting a detailed account of the recent progress made in the designs and syntheses of 'new' optical probes for Hg^{2+} detection from 2011 to 2019.

This article is structured in such a way that the body of the review work is based on four broad categories of selected fluorophore scaffolds used for the structural designs of the probes reported (Fig. 3): 1. simple molecular ligands/synthetic organic dyes; 2. supramolecules: carbohydrates and polymers; 3. metal-organic frameworks (MOFs) and covalent organic frameworks (COFs); and 4. nanoprobes: nanoparticles, quantum dots (QDs), and graphene oxides (GOs) (Fig. 3). The sensing properties of the probes under each subsection have been discussed by emphasising the parameters of the most suitable solvent system, optimum pH value/range, interference property, detection limit, and association constant. Some occasional mentions of the probes' utility in imaging Hg^{2+} in biological systems are also given. Sufficient references, totalling 196 articles, are reviewed in strength to keep abreast of the works done in various labs whilst ensuring succinctness of the report. All reported compounds either employ the fluorescence, colourimetric, and/or ratiometric method in their detection modes (Fig. 3). In some instances, however, the mentioned compounds make use of combined fluorescence or colourimetric or ratiometric

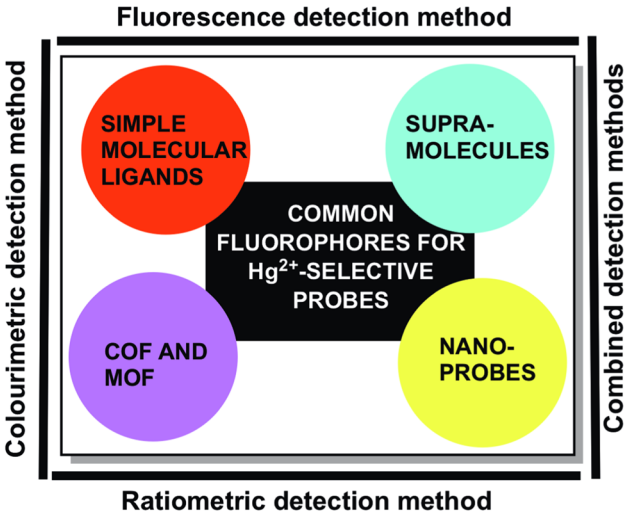

Fig. 3 The future of Hg^{2+} sensing science is bright with key classes of commonly employed fluorophores and signalling methodologies recognised. Source: the author

methods in their sensing technique/detection methodology. This review closes by giving a brief conclusion that will help guide future research works in the chemistry of Hg^{2+} sensing.

Hg^{2+}-selective small-molecule probes based on different fluorophore motifs

Based on different subfluorophores, an account of small-molecule probes for the monitoring of mercuric (II) ion (Hg^{2+}) is detailed below.

Small-molecule Hg^{2+} probes based on simple molecular ligands/synthetic organic dyes

A large percentage of probes that exist to date are based on conventional simple molecular ligands/synthetic dyes constructed from various organic fluorophores such as the 1,8-naphthalimide, rhodamine, coumarin, pentaquinone, boron-dipyrromethene (BODIPY), cinnamaldehyde, Schiff base, anthracene, squaraine, pyrene, azo derivative, amongst many others. Small-molecule probes do not require invasive and often tedious genetic modification of the system and can be applied to many samples, and they, therefore, demonstrate potential clinical applications (Kim and Cho 2015).

Small-molecule Hg^{2+} probes based on naphthalimide fluorophore

The naphthalimide fluorophore possesses several desirable properties including a large Stokes' shift and a high quantum yield that inform its choice as a common fluorophore for the development of probes (Aderinto et al. 2016; Aderinto and Imhanria 2018; Wang et al. 2017). Moreover, its chemistry is versatile, allowing the possibility for distinct functionalisation that confers tailored properties on the probes constructed from this moiety (Moro et al. 2010).

Chen's group recently reported a naphthalimide-based fluorescent and colourimetric probe, **NAP-PS**, that houses the diphenylphosphinothioyl group for Hg^{2+} detection (Chen et al. 2019). In HEPES buffer (1.0 mM, pH = 7.4), amongst the many other ions (Zn^{2+}, Cu^{2+}, Mn^{2+}, Pb^{2+}, Al^{3+}, Ca^{2+}, Cr^{3+}, K^{+}, Fe^{3+}, Fe^{2+}, Cs^{+}, Na^{+}, Ni^{2+}, Mg^{2+}, Sr^{2+}, Cd^{2+}, and Ag^{+}) investigated, only the addition of Hg^{2+} leads to a significant ratiometric response of the fluorescence intensities at 450 nm to 550 nm. The ratiometric fluorescence response of **NAP-PS** is due to its reaction with mercury, which cleaves the thiophosphinate P–O bond in the probe to form the intramolecular charge transfer (ICT) system, **NAP-O**. The linear range of detection was within 0–12 nM, whilst the detection limit was calculated as 43 nM. The probe was also capable of Hg^{2+} monitoring in the solid state. Using two-photon microscopy, the designated probe could bioimage Hg^{2+} in both HeLa live cells and tissues with very low cytotoxicity exhibited.

La's research group reported the design of their newfound 4-Amino-1,8-naphthalimide-based fluorescent probe, **Hg-1** (Fig. 4), for Hg^{2+} monitoring, which could also sense CN^{-} and F^{-} via the colourimetric method, thereby acting as a multianalyte probe (La et al. 2016). The design strategy was based on the combination of both PET and ICT, which allow for a dual analyte monitoring mode. (PET-based probe design involves the fluorophore unit connected to the ionophore unit through a spacer, whilst ICT-based probe design involves the direct connection of the fluorophore unit and ionophore unit to form a single species (Gupta and Kumar 2016.) The reported compound underwent a multiplication in its fluorescence signal intensity after Hg^{2+} was added, whilst the other ions tested together did not modulate the fluorescence signal intensity of the probe significantly. There was a linear response of the probe for Hg^{2+} monitoring with the detection limit reportedly low to the level of 2.40×10^{-7} M (lower than those of previously reported probes), and the association constant reportedly high as 4.12×10^{5} M. The analysis of the Job's plot and ^{1}H NMR results gave the stoichiometric ratio to be 1:1 (Fig. 5).

Two naphthalimide-appended fluorescent probes, **Hg-2** and **Hg-3** (Fig. 4), were devised and reported by Li and his research group members (Li et al. 2016). In phosphate buffer, the two compounds display ultra-high-level sensitivities and selectivities for Hg^{2+} detection. It was observed that **Hg-2** and **Hg-3** could detect Hg^{2+} over a vast expanse of pH, between 7.0 and 10.0. In a 10 μM solution of **Hg-2** in phosphate buffer (pH = 7.5), upon the addition of cations

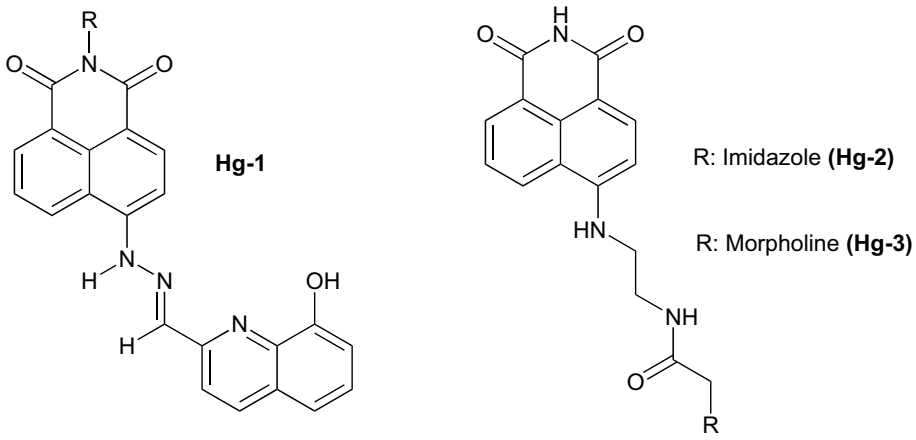

Fig. 4 Structures of Probes **Hg-1**, **Hg-2**, and **Hg-3** (La et al. 2016; Li et al. 2016)

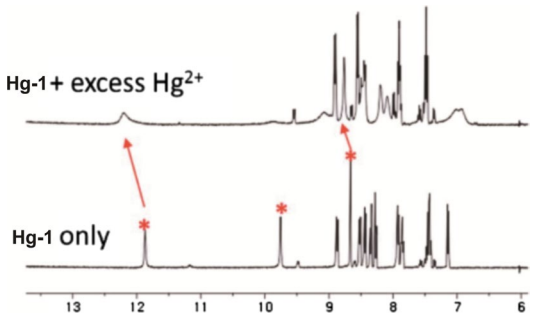

Fig. 5 Proton NMR of Probe **Hg-1** in the absence and presence of excess Hg^{2+}. Key finding: there was an upfield shift in the aromatic protons owing to increased electron density upon protonation (La et al. 2016)

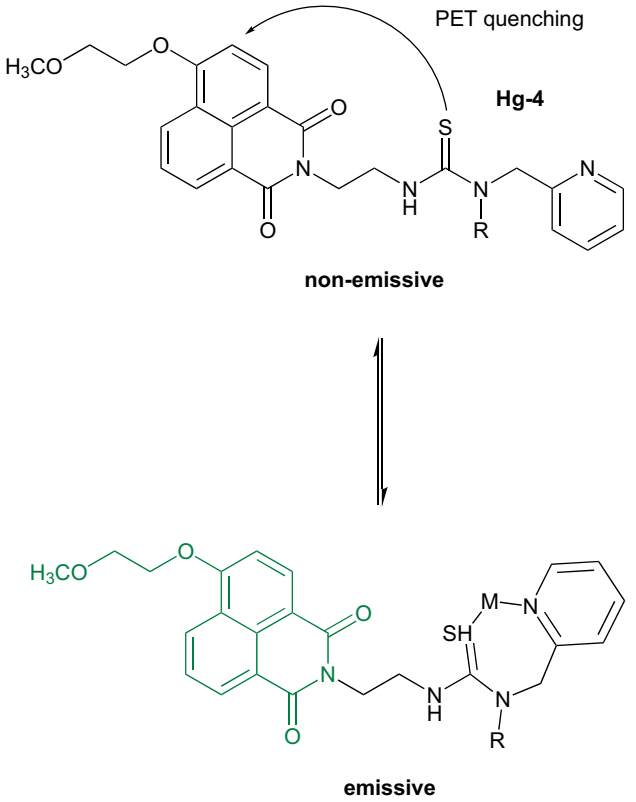

Fig. 6 Scheme of fluorescent Probe **Hg-4** exhibiting the PET mechanism (Vonlanthen et al. 2014)

like Ag^{+}, Al^{3+}, Ba^{2+}, Cd^{2+}, Ca^{2+}, Co^{2+}, Cr^{3+}, Cu^{2+}, Fe^{2+}, Li^{+}, K^{+}, Na^{+}, Mg^{2+}, Zn^{2+}, Mn^{2+}, Pb^{2+}, Ni^{2+}, and Hg^{2+}, only Hg^{2+} led to *ca.* 90% suppression of the fluorescence intensity of **Hg-2**; meanwhile, the other cations impressed only benign effects on the fluorescence intensity. A similar observation went for **Hg-3**. There was linearity in Hg^{2+} monitoring by **Hg-2** between the concentration range of 2 and 10 µM, and the lowest detection limits of **Hg-2** and **Hg-3** for Hg^{2+} detection were 2.1 µM and 3.1 µM, respectively. Analytically, **Hg-2** exhibits higher selectivity and sensitivity towards Hg^{2+} than **Hg-3**, this being accrued to the fact that the conjugation action of morpholine which exists in **Hg-3** makes it to poorly bind to Hg^{2+}. The proton NMR of the binding of **Hg-2** to Hg^{2+} shows the disappearance of a major peak downfield in the NMR spectrum upon the addition of Hg^{2+}.

Work in mercury probes' development has also shifted towards the employment of sulphur-based functional groups (like sulphoxides and thioureas) since they display great affinities for measured analytes in aqueous environments. Vonlanthen and his team members developed a PET thiourea–naphthalimide-based probe, **Hg-4** (Fig. 6) that demonstrates Hg^{2+} sensing over competing metal ions like Na^{+}, K^{+}, Mg^{2+}, Ca^{2+}, Ag^{+}, Zn^{2+}, Cd^{2+}, Hg^{2+}, and Pb^{2+} in CH_3OH (Vonlanthen et al. 2014). At pH 5.5 or lower, in 9:1 H_2O/CH_3OH, no fluorescence enlargement was observed, but there was a massive amplification of the fluorescence in the case of Hg^{2+}. Job's plot establishes a 1:1 stoichiometry of the interaction between the probe and Hg^{2+} ion. Eventually, the compound was applied to image

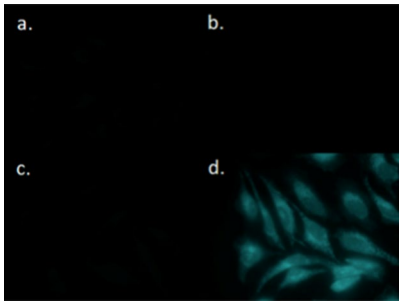

Fig. 7 Fluorescence images showing HeLa cells treated with Probe **Hg-4** and $HgCl_2$. **a** HeLa cells treated overnight with a DMSO control at 37 °C. **b** Cells treated overnight with a DMSO control followed by $HgCl_2$ (200 μM) for 10 min at 37 °C. **c** Cells incubated overnight with Probe **Hg-4** (20 μM) at 37 °C. **d** Cells treated overnight with Probe **Hg-4** (20 μM) followed by $HgCl_2$ (200 μM) for 10 min at 37 °C. Imaging was done on a Zeiss Axio Observer inverted microscope with objective = ×63; excitation wavelength = 365 nm, emission wavelength = 445/50 nm (Vonlanthen et al. 2014)

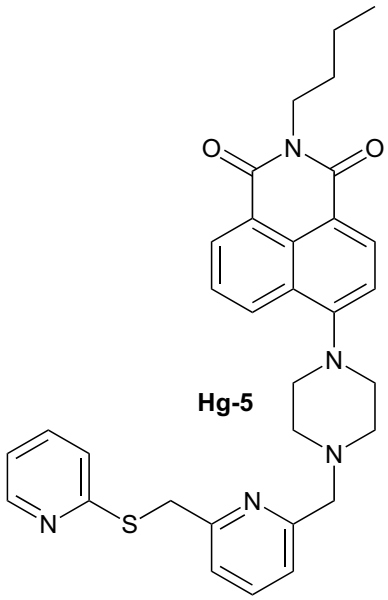

Fig. 8 Structure of Probe **Hg-5** (Un et al. 2014)

Hg^{2+} in living mammalian cells (Fig. 7), indicating its practical utility potential in biological system.

Un et al. introduced a novel, simple, and versatile fluorescent Probe **Hg-5** (Fig. 8) based on the *N*-butyl-4-bromo-1,8-naphthalimide moiety. The probe was employed for a fluorescence 'turn on' monitoring of Hg^{2+} over a wide range of several other cations, including Zn^{2+}, Mn^{2+}, Ba^{2+}, Ni^{2+}, Cu^{2+}, Co^{2+}, Pb^{2+}, Mg^{2+}, Cd^{2+}, Fe^{2+}, Al^{3+}, Ag^{+}, Na^{+}, and Li^{+} (Un et al. 2014). In aqueous solution (THF-H_2O, 1:1, pH = 7.4, 10 mM Tris–HCl), Hg^{2+} addition to a solution of **Hg-5** induced a notable enhancement of fluorescence. The fluorescence detection occurred over the range 1–30 μM, with a detection limit of 6.28×10^{-8} M and an association constant of 5.4×10^{4} M^{-1} calculated. The fluorescence imaging experiments of **Hg-5** for Hg^{2+} tracking in living cells were successfully demonstrated.

Moon et al. employed a new thionaphthalimide-based probe, **Hg-6**, and its two monothio derivatives, **Hg-7** and **Hg-8** (Figs. 9, 10), for the sensitive and selective monitoring of Hg^{2+} through an 'off–on' mode (Moon et al. 2013). In 30% aqueous CH_3CN, the fluorescence intensity of Probe **Hg-6** at 537 nm was escalated upon the addition of 20 equivalents of Hg^{2+}, whereas the effects of other tested cations on the fluorescence intensities of the probes were minuscule. The reported Probe **Hg-6** could allow the detection of Hg^{2+} ion in an amount as low as 2.7 μM. The isomeric probes **Hg-6** and **Hg-7** were demonstrated to exhibit varied sensing behaviours with **Hg-6** showing a faster signalling speed than **Hg-7**. This was explained as due to the carbon resonance of the more electron-rich thiocarbonyl group of **Hg-6** which possesses more electron-rich sulphur and appears in a higher field (192.5 ppm) than that of **Hg-7** which appears in a lower field (194.2 ppm) (Fig. 9). The signalling behaviour of the dithio-derivative, **Hg-8**, was not reported, only that upon interaction with Hg^{2+}, it became desulphurised to the monothiol-derivative, **Hg-7**.

Probe **Hg-9** (Fig. 11) was used by Zhang et al. for the signalling detection of Hg^{2+} amongst several other cations, including Na^{+}, K^{+}, Ca^{2+}, Mg^{2+}, Cu^{2+}, Zn^{2+}, Cr^{2+}, Pb^{2+}, Ni^{2+}, Fe^{2+}, Mn^{2+}, Co^{2+}, and Cd^{2+} (Zhang et al. 2013). In EtOH/H_2O (1/2, v/v), the addition of Hg^{2+} to a solution of the probe led to a marked increase in the fluorescence intensity of **Hg-9**, whilst no obvious disturbance in detection was observed from other tested cations. The binding stoichiometry of **Hg-9** towards Hg^{2+} as furnished by the Job's plot analysis yielded the establishment of a 1:1 complex between Hg^{2+} and **Hg-9**. This was further evidenced by the results of the proton NMR.

Li et al. reported a PET naphthalimide-based probe, **Hg-10** (Fig. 12), that bears a hydrophilic hexanoic acid group (as a solubilising functional group) for the monitoring of Hg^{2+} (Li et al. 2012). Experimental results revealed that the compound was most effective for the tracking of Hg^{2+} within the linear concentration range of 2.57×10^{-7}–9.27×10^{-5} M. Job's plot unveiled a 1:1 stoichiometric mode of Probe **Hg-10** and Hg^{2+}. The calculated detection limit was 4.93×10^{-8} M. In Tris-HNO_3 buffer solution (pH = 7.0), the probe showed a massive enhancement in the intensity of its fluorescence upon Hg^{2+} addition in coexistence with several other investigated cations. The analytical detection response time of Hg^{2+} by **Hg-10** was < 1 min. **Hg-10** exhibited a regeneration ability in its sensing mechanism as ascertained by the release of the unbound probe upon the addition of EDTA to the **Hg-10**/Hg^{2+} complex. The probe was successfully used for Hg^{2+} monitoring in hair samples.

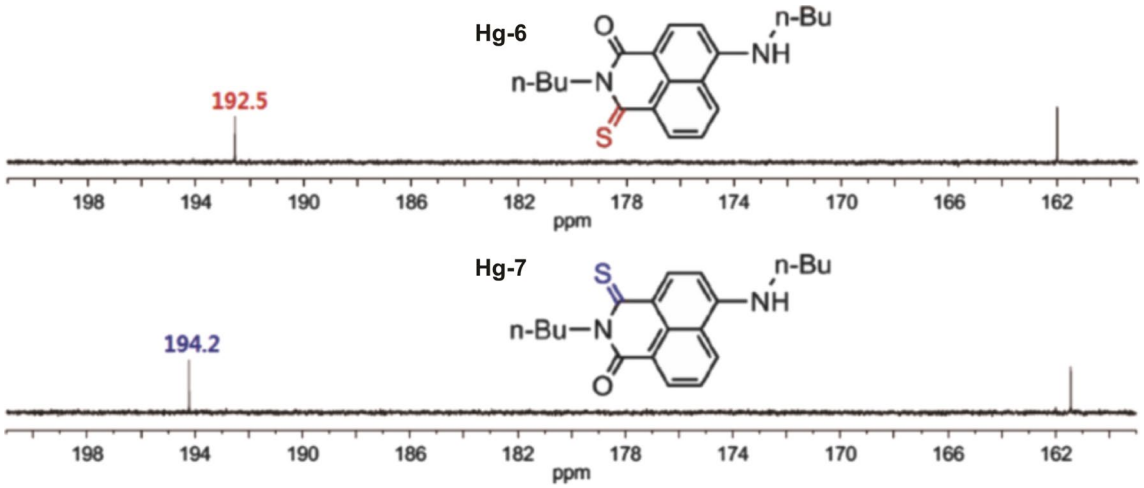

Fig. 9 Partial ^{13}C NMR spectra of Probes **Hg-6** and **Hg-7** in $CDCl_3$ (Moon et al. 2013)

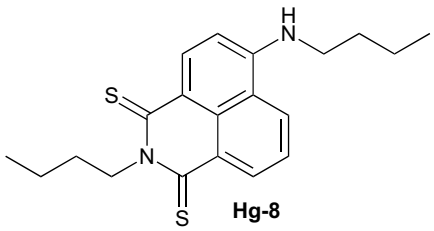

Fig. 10 Structure of Probe **Hg-8** (Moon et al. 2013)

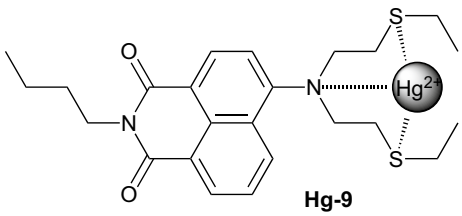

Fig. 11 Structure of Probe **Hg-9** showing its binding mode with Hg^{2+} (Zhang et al. 2013)

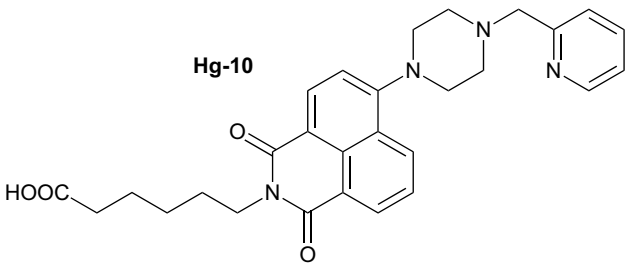

Fig. 12 Structure of Probe **Hg-10** (Li et al. 2012)

Small-molecule Hg^{2+} probes based on rhodamine fluorophore

Since they possess excellent photophysical properties, rhodamines have enjoyed wide applications as fluorescent probes and molecular markers. Rhodamine dyes, which belong to the xanthene class of dyes, represent one of the oldest synthetic dyes used for fabric dyeing. They possess high molar absorptivities in the visible region, and many of their derivatives exhibit strong fluorescence. Moreover, there is a strong influence of their absorption and emission properties by substituents in the xanthene nucleus, thereby making them useful not only as colourants but also as fluorescent markers in photosensitisers, microscopic structural studies, and laser dyes (Arbeloa and Ojeda 1981).

Arivazhagan et al. designed two triazole-appended ferrocene–rhodamine conjugates, $C_{47}H_{45}N_7O_3Fe$ (**Hg-11**) and $C_{49}H_{49}N_7O_3Fe$ (**Hg-12**) (Fig. 13), synthesised as probes for a highly 'turn on' fluorescence detection of Hg^{2+} in CH_3CN/HEPES buffer (2:8, v/v, pH 7.3, 10 μM) (Arivazhagan et al. 2015). It was shown that receptors **Hg-11** and **Hg-12** could be employed for Hg^{2+} monitoring in the near-neutral pH range of 7.3. Upon the addition of Hg^{2+} to the receptors **Hg-11** and **Hg-12**, there was a massive enlargement of the fluorescence intensity, explained based on the spirolactam ring opening of the rhodamine moiety upon chelation with a cation. The addition of alkali, alkaline, transition, and heavier transition metal ions like Na^+, Mg^{2+}, K^+, Ca^{2+}, Cr^{2+}, Mn^{2+}, Fe^{2+}, Co^{2+}, Ni^{2+}, Cu^{2+}, Zn^{2+}, Pb^{2+}, Cd^{2+}, and Tl^+ effected almost no influence on the fluorescence emission spectrum of receptor **Hg-11**, which was further confirmed by competitive experiments, thereby demonstrating the high affinity of receptor **Hg-11** for Hg^{2+}. The same trends of observations went for receptor **Hg-12**. Desirably, experimental results revealed that the receptors were reversible in their monitoring of Hg^{2+}. Since the receptors could image

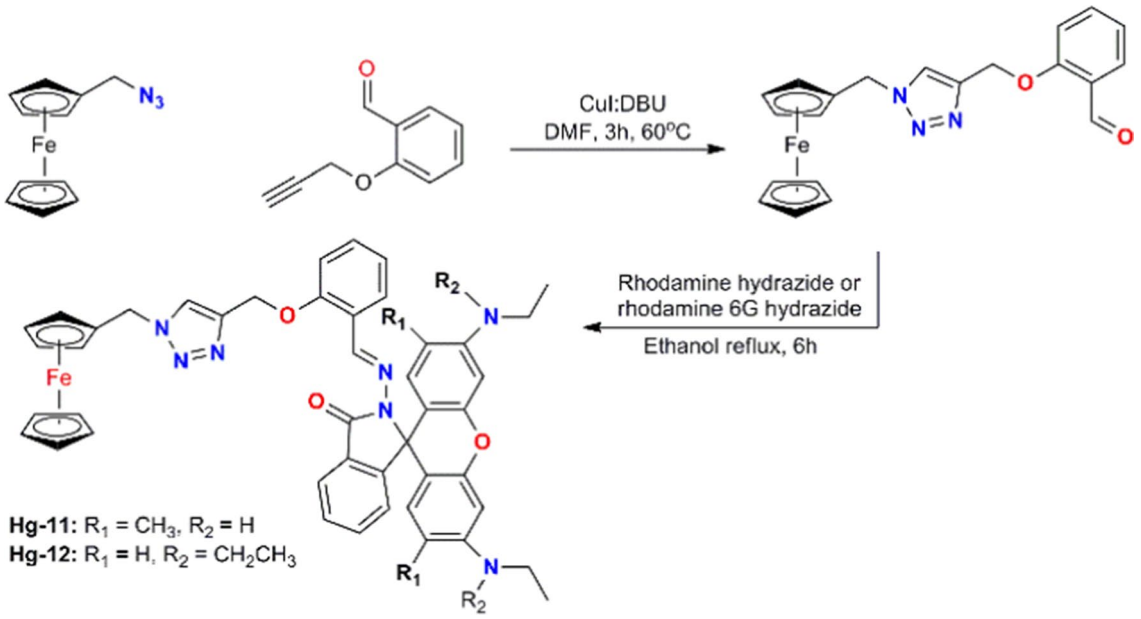

Fig. 13 Structures of Probes **Hg-11** and **Hg-12** (Arivazhagan et al. 2015)

Hg^{2+} ion in living cells using the MTT (5-dimethylthiazol-2-yl-2,5-diphenyltetrazolium bromide) assay without any destruction, their potencies to track intracellular Hg^{2+} ions in MCF-7 breast cancer cells were successfully assessed via fluorescent imaging studies (Fig. 14).

Chen and members of his research laboratory reported a water-soluble fluorescent probe, **Hg-13** (Fig. 15), constructed from rhodamine B derivative (Chen et al. 2013b). The new probe displayed both colourimetric ('naked eye') detection and fluorescent response towards Hg^{2+} in a fully aqueous HEPES buffer solution. The optimum experimental pH range for the sensing of Hg^{2+} by **Hg-13** was found to be 6–11. At 586 nm, a sizeable fluorescent escalation of about 1500-fold increment was noted upon Hg^{2+} addition to the solution of the probe in the presence of other alkali, alkaline earth, and transition metal ions (Na^{+}, K^{+}, Ca^{2+}, Mg^{2+}, Cr^{3+}, Fe^{3+}, Fe^{2+}, Cd^{2+}, Mn^{2+}, Pb^{2+}, Zn^{2+}, Cu^{2+}, Ag^{+}, Co^{2+}, Ni^{2+}) investigated under identical testing conditions. Association constant of $1.21 \times 10^5\ M^{-1}$ was estimated from the binding interaction of the probe and analyte metal ion. Besides the linearity of the relationship between the probe and Hg^{2+}, Job's plot yielded a 1:1 stoichiometric ratio of the probe and the metal ion in the **Hg-13**/Hg^{2+} complex. The reversibility nature of the probe was demonstrated after the addition of EDTA to the complex's solution, which led to the release of free **Hg-13** compound from the bound **Hg-13**/Hg^{2+} complex. A fast response time (there was no apparent time delay) was demonstrated in the tracking of Hg^{2+} by **Hg-13** as justified by the results of the real-time analysis. Utilising the fluorescence imaging experiments, the biological utility of **Hg-13** demonstrated its ability to image Hg^{2+} in living HeLa cells whereby an MTT assay gave cell viability of 95%

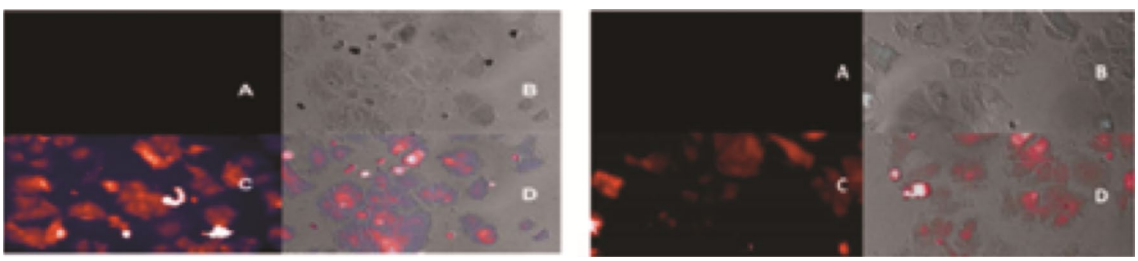

Fig. 14 Fluorescence and bright-field images of MCF-7 cells. **a** Fluorescence image of MCF-7 cells incubated with **Hg-11** (10 μM) for 2 h at 37 °C (left) or **Hg-12** (10 μM) for 2 h at 37 °C (right). **b** Bright-field image of **Hg-11**-treated MCF-7 cells (left) or **Hg-12**-treated MCF-7 cells (right). **c** Fluorescence image of MCF-7 cells incubated with **Hg-11** (10 μM) for 30 min and then treated with (10 μM) $Hg(ClO_4)_2$ for 2 h at 37 °C (left) or **Hg-12** (10 μM) for 30 min and then treated with (10 μM) $Hg(ClO_4)_2$ for 2 h at 37 °C (right). **d** Overlaid images of MCF-7 cells (**b**, **c**) (left: **Hg-11**; right: **Hg-12**) (Arivazhagan et al. 2015)

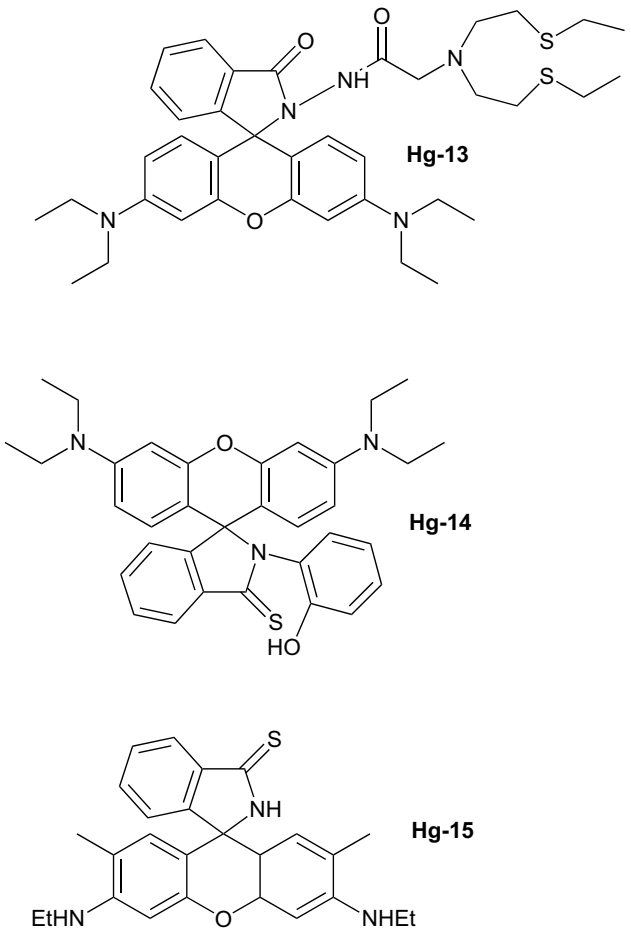

Fig. 15 Structures of Probes **Hg-13**, **Hg-14**, and **Hg-15** (Chen et al. 2013b; Gong et al. 2012; Hu et al. 2013)

after treatment with 10 μM of the compound after 24 h of incubation.

For fluorescence detections of cations, it has been purported that virtually all rhodamine spirolactam fluorescent probes employ the spiro ring-opening reaction either through metal ion coordination or metal ion-catalysed desulphurisation reaction. Having utilised a Hg^{2+}-triggered domino reaction, Gong and his co-workers described the synthesis of a novel rhodamine thiospirolactam derivative, **Hg-14** (Fig. 15), as an 'off–on' fluorescent probe for the detection of Hg^{2+} in neutral H_2O-MeOH (80/20; v/v) solution (Gong et al. 2012). Compound **Hg-14** showed stability of response for Hg^{2+} sensing from 1.0×10^{8}–1.0×10^{6} M. The fairly stable pH range of 3.0–11.0 was chosen for the conduct of the experiments. The fluorescence emission intensity of the rhodamine derivative **Hg-14** underwent a marked increment (of about a 580-fold fluorescence improvement) upon the addition of 1 mM Hg^{2+}. Contrastingly, the addition of 1 mM of Ag^{+} and 50 mM of the coexisting cations left no noteworthy influence on the probe's fluorescence intensity. Whilst Probe **Hg-14** showed linearity of detection response in the range of 10 nM–1 mM and an ultralow detection limit of 3 nM, its response time towards Hg^{2+} was not up to 6 min. As much as the opposite might have been desired, the reported compound **Hg-14** was irreversible in its sensing nature towards Hg^{2+} (i.e. it was a chemodosimeter but not a probe), although it could bioimage Hg^{2+} in living HeLa cells with great sensitivity.

Hu and his teammates developed a simple yet effectual novel fluorescent compound, **Hg-15** (Fig. 15), that anchors the thiorhodamine 6G-amide moiety by the employment of Hg^{2+}-induced desulphurisation reaction and spirolactam opening of rhodamine (Hu et al. 2013). The compound, which functions as a chemodosimeter rather than as a probe, could detect Hg^{2+} in the broad and stable pH range of 6.0–10.0, although with the optimums pH range being 7.2–7.6. In 0.01 M HEPES-buffer ethanol solution (EtOH/H_2O 1:8, v/v, pH = 7.4) solution, the proposed compound **Hg-15** revealed a remarkable increase in its fluorescence intensity only upon contact with Hg^{2+} in the co-presence of several other cations, which induced neither an individual nor a collective effect(s) on the fluorescence intensity of **Hg-15**. 5-min response time for the monitoring of Hg^{2+} by **Hg-15** was observed. The Job's method of continuous variation gives a 1:1 stoichiometric ratio between **Hg-15** and Hg^{2+} in the **Hg-15**/Hg^{2+} complex. An estimated detection limit of 4.2×10^{-8} M was obtained, and **Hg-15** was successfully demonstrated as capable of monitoring Hg^{2+} in living cells via confocal laser scanning microscopy (CSLM).

Based on the spirolactam ring-opening process, Kumar et al. documented the rhodamine B phenyl hydrazide probe, **Hg-16** (Fig. 16), being developed as a novel colourimetric and fluorescent chemodosimeter, for the sensitive, selective, and irreversible Hg^{2+} monitoring (Kumar et al. 2014). The fluorescence emission intensity was quite stable in the pH range of 7–12 upon the addition of various anions and cations. The compound which has the capability for naked-eye detection (from colourless to pink) of Hg^{2+} also displayed a substantial fluorescence increase in its emission intensity. At 580 nm, there was a significant strengthening of the fluorescence emission intensity of **Hg-16** upon the addition of Hg^{2+} amidst several other cations and anions like Ca^{2+}, K^{+}, Mg^{2+}, Pb^{2+}, Ni^{2+}, Zn^{2+}, Fe^{3+}, Cu^{2+}, Cl^{-}, NO_2^{-}, NO_3^{-}, S^{2-}, SO_4^{2-}, and ClO^{-} analysed. The linear detection response lied within the range 1–100 nM, with a detection limit of 0.019 nM calculated. The monitoring of Hg^{2+} by the probe was complete after about 1.5 min of the start of the reaction. The efficacious amphiphilic and fluorescence qualities of the designated compound **Hg-16** were taken advantage of to bioimage Hg^{2+} in living MCF-7 cells by fluorescence microscopic studies. Table 1 summarises the analytical properties of Probe **Hg-16** for Hg^{2+} detection.

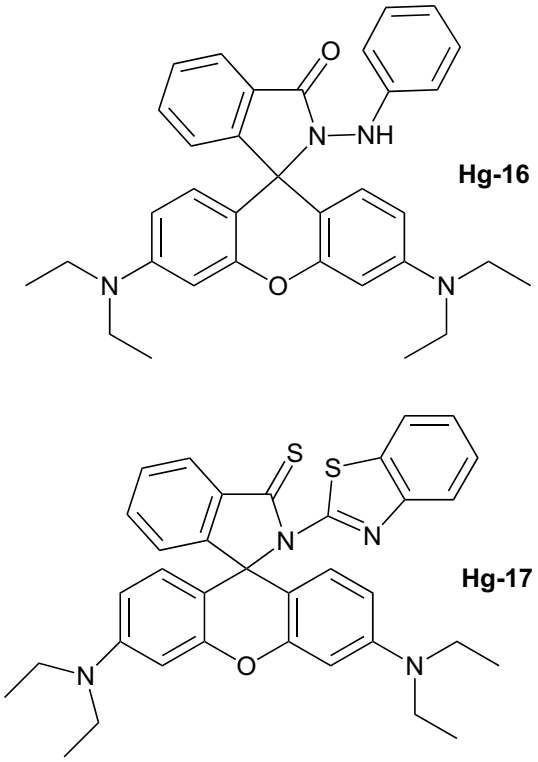

Fig. 16 Structures of Probe **Hg-16** and Chemodosimeter **Hg-17** (Kumar et al. 2014; Wang et al. 2012)

Table 1 Reported analytical properties of Probe **Hg-16** (Kumar et al. 2014)

Analytical feature	nM/mL
Linear range	0.1–50
Limit of detection[a]	0.019
Limit of quantification[b]	0.19
Fluorescence quantum yield (Φ_F)	0.61
RSD ($n=10$) Hg^{2+} = 10 nM	±0.991

A[a] Standard deviation values of 5 reagent blank determinations were used for calculation (3 σ)

A[b]Standard deviation values of 5 reagent blank determinations were used for calculation (10 σ)

Wang and colleagues devised a rhodamine-based compound, **Hg-17** (Fig. 16), that anchors the thiospirolactam and benzimidazole moieties (Wang et al. 2012). The probe, which utilises the spirolactam ring-opening and desulphurisation process, functioned as a highly sensitive and selective 'naked-eye' chemodosimeter for Hg^{2+} sensing. In CH_3CN-HEPES buffer (0.01 M, pH 7.4) (3:7, v/v), the fluorescence intensity of the reported compound underwent a sharp increase in the order of 180-fold enlargement when Hg^{2+} was added to the probe solution, which was attributed to the selective spirolactam ring-opening process followed by desulphurisation. The other added cations like Zn^{2+}, Pb^{2+}, Cd^{2+}, Co^{2+}, Hg^{2+}, Cu^{2+}, Fe^{2+}, Ag^{+}, Al^{3+} and Cr^{3+} Zn^{2+}, Pb^{2+}, Cu^{2+}, Fe^{2+}, Ag^{+}, Li^{+}, Mn^{2+}, Na^{+}, Fe^{3+}, Al^{3+}, and Sr^{2+} induced no influence on the probe's fluorescence emission intensity. The estimated analytical detection limit was found to be 7.4 nM.

Utilising a rosamine scaffold, Taki and co-workers gave an account of the purportedly strongest reversible fluorescent probe compound, **Hg-18** (Fig. 17), designed for Hg^{2+} sensing (Taki et al. 2012). In 50 mM HEPES (pH 7.20, 0.1 M KNO_3) and DMSO (4:1, v/v), **Hg-18** showed a stringent attraction towards Hg^{2+} amidst other foreign cations like Ni^{2+}, Mn^{2+}, Fe^{3+}, Pb^{2+}, Cu^{2+}, Zn^{2+}, Cd^{2+}, and Co^{2+} with an ensuant 20-fold fluorescence increment observed. Cu^{+} and Ag^{+} interfered in the sensing of Hg^{2+} by **Hg-18**, although this was quite minuscule. The existence of a 1:1 stoichiometry between the probe and Hg^{2+} was demonstrated by the analysis of the result of the Job's plot. The dissociation constant of $1.04 \pm 0.05 \times 10^{-16}$ M was calculated for the generation of the complex between the said probe compound and Hg^{2+} analyte ion. The imaging ability of **Hg-18** for Hg^{2+} HeLa cells was feasible.

Small-molecule Hg^{2+} probes based on coumarin fluorophore

The coumarins, or benzo-α-pyrones, constitute a huge and important class of organic compounds. The structure of the simplest coumarin is made up of fused pyrone and benzene rings, with their position 2 harbouring a pyrone carbonyl group. Coumarins are naturally abundant, with the first coumarin isolated in 1820 from a bean variety, and with several

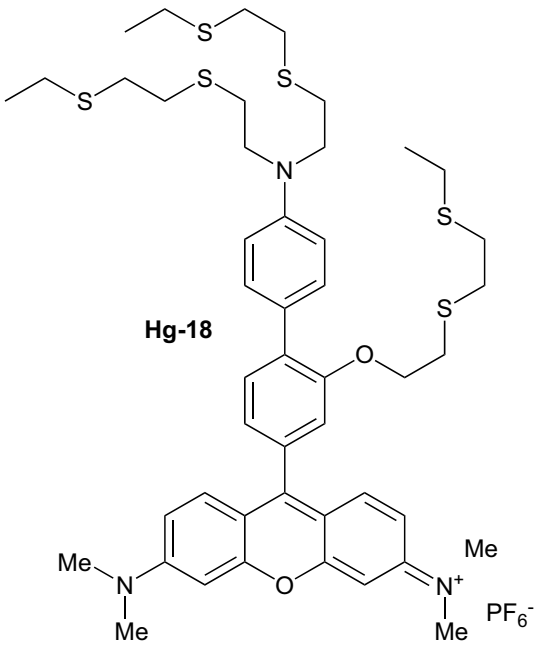

Fig. 17 Structure of Probe **Hg-18** (Taki et al. 2012)

other coumarin derivatives isolated from diverse plant species. The coumarins family exhibits exciting fluorescence properties, including high sensitivity to their local environment—in terms of both polarity and viscosity. This, in turn, led to their extensive application range desirably as sensitive fluorescent probes in a wide range of systems (Wagner 2009; Reddie et al. 2012).

Since the successful synthesis of the first thiocoumarin-derivative fluorescent probe for Hg^{2+} detection which exploits the desulphurisation of thiocoumarin to coumarin (Choi et al. 2009), there has been an upsurge in the subsequent synthesis of more such probes. Drawing inspiration from this, Qin and co-workers (Qin et al. 2018) disclosed a new ICT-based colourimetric and ratiometric fluorescent chemodosimeter, **Hg-19** (Fig. 18), for Hg^{2+} monitoring. When excited at 477 nm and 543 nm, the probe is selective and sensitive towards Hg^{2+} detection in PBS buffer solution (10 mM, pH 7.4, containing 1% DMSO) in the coexistence of several other analytically relevant cations investigated (Na^+, K^+, Ca^{2+}, Mg^{2+}, Zn^{2+}, Co^{2+}, Cr^{3+}, Cu^{2+}, Fe^{2+}, Fe^{3+}, Ni^{2+}, Pb^{2+}, and Sn^{4+}) . The probe's analytical detection range was between 1.0 and 15.0 with a low detection limit of 1.85 ppb. Furthermore, the probe was successfully used for the fluorescence imaging of Hg^{2+} in live cells. The in vitro and in vivo application of the probe towards HeLa cells was ascertained.

Based on Hg^{2+}-induced cyclisation reaction, a simple 7-hydroxycoumarin-based compound, **Hg-20** (Fig. 19), which acts as a 'turn-on' probe for the sensing of Hg^{2+} in aqueous media ($CH_3CN/H_2O = 9{:}1$, pH 7.0), was developed by Gao's laboratory members (Gao et al. 2012). The probe is most effective in its sensing nature between the pH value of 6.2 and 8.0, whilst it could also maintain enough stability in this range (Fig. 19). Results revealed that there was a tremendous improvement in the compound's fluorescence intensity upon the addition of Hg^{2+}. However, in the absence of the competing metal ions, there was an insignificant variation in **Hg-20**′s fluorescence intensity, except for the quenching effect displayed by Cu^{2+}. The results of the competition experiments further justified the high sensitivity and selectivity of **Hg-20** towards Hg^{2+}. The presence of anions also impacted a little effect on the fluorescence response behaviour of **Hg-20** towards Hg^{2+}. Probe **Hg-20**′s detection limit for Hg^{2+} monitoring was calculated to be 5.12×10^{-7} M. The practical usage of the developed compound was demonstrated by its ability to measure Hg^{2+} in tap and well water samples.

Five structurally similar coumarin-based fluorescent probes, **Hg-21**–**Hg-25** (Fig. 20), that could selectively and sensitively monitor Hg^{2+} were developed (Guo et al. 2015). The authors reported that Hg^{2+} detection proceeded through

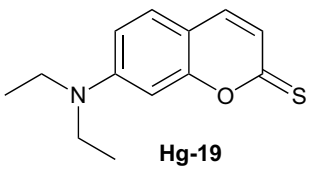

Fig. 18 Structure of **Hg-19** (Qin et al. 2018)

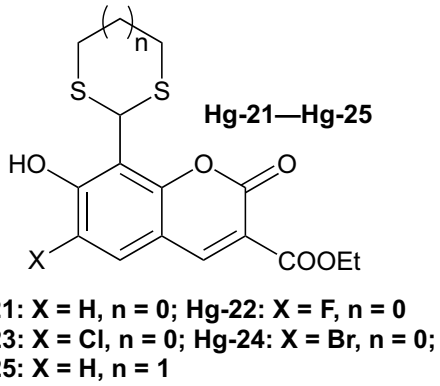

Fig. 20 Structures of Probes **Hg-21–Hg-25** (Guo et al. 2015)

Fig. 19 Structure of Probe **Hg-20** (left), and the changes in the fluorescence of Probe **Hg-20** (black line) and Probe **Hg-20** with Hg^{2+}(red line) in buffer solution as a function of increasing pH value (10 μM $CH_3CN/H_2O = 9/1$, v/v, excitation wavelength = 328 nm, and emission wavelength = 400 nm) (right) (Gao et al. 2012)

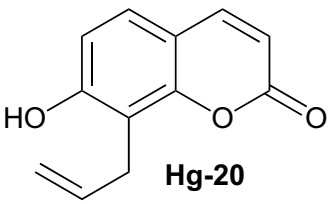

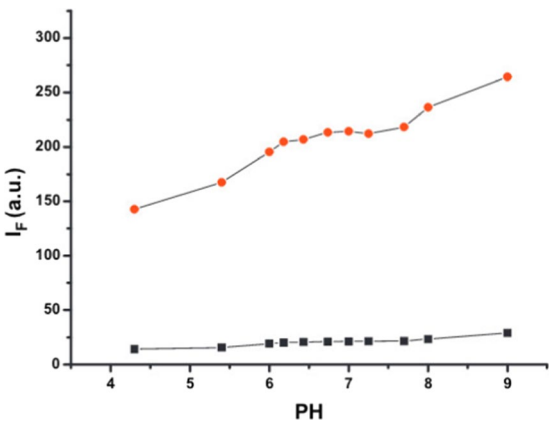

the Hg^{2+}-promoted desulphurisation of the probes—a seldom-used method for the construction of fluorescent probes. All the five probes (especially Probe **Hg-21**) possess excellent selectivity and anti-interference properties towards Hg^{2+} from other co-existing cations present together in the aqueous phase (Fig. 21). The probes showed linearity in their detection mode towards Hg^{2+} over the wide concentration range of 0.06–1.50 mM (0.06–0.90 mM for Probe **Hg-25**). The probes have interesting biological properties towards Hg^{2+}, and the authors tested the efficacies of the probes (especially Probe **Hg-21** because of its superb sensitivity for Hg^{2+} unmatched by the other probes) on MCF-7 cells. The in vitro cytotoxicity experiment revealed that Probe **Hg-21** had little cytotoxicity on MCF-7 cells' proliferation within the 0–10 mM concentration range. The binding mechanism was purported to have occurred via the Hg^{2+}-promoted hydrolysis desulphurisation.

The design of a water-soluble probe, **Hg-26** (Fig. 22), which bears a coumarin unit as the fluorophore and a vinyl ether group as the receptor was documented by Wu's lab (Wu et al. 2017). When investigated in HEPES buffer (20 mM, pH 7.0), there was a remarkable magnification of the probe's fluorescence intensity upon the addition of Hg^{2+}. The low detection limit (0.12 M) of **Hg-26** proves that the probe exhibits outstanding selectivity and sensitivity towards Hg^{2+}. The sensing mechanism of the probe with Hg^{2+} was confirmed using proton NMR (Fig. 22). The practical application of the probe as an excellent monitoring tool was demonstrated by its ability to detect traces of Hg^{2+} in real water samples (Table 2).

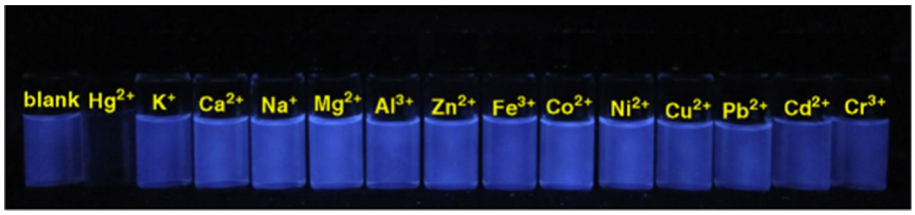

Fig. 21 Visual fluorescence emission of Probe **Hg-21** (1 mM) in the presence of several cations (200 mM, 2.0 mM for Hg^{2+}) on excitation at 365 nm using a UV lamp at ambient temperature (Guo et al. 2015)

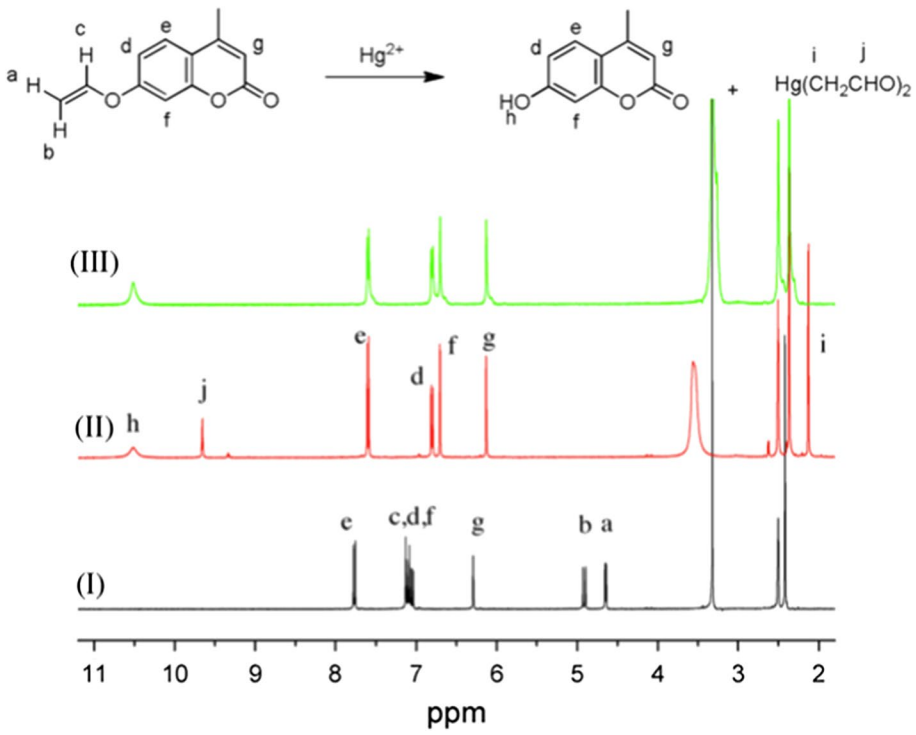

Fig. 22 The partial ^1H NMR (400 M, d_6-DMSO) spectra of Probe **Hg-26** (I), Probe **Hg-26** with Hg^{2+} after 1 h (II), and 7-hydroxy-4-methylcoumarin (III) (Wu et al. 2017)

Table 2 Monitoring of Hg^{2+} by Probe **Hg-26** (Wu et al. 2017)

Sample	Spiked (μM)	Detected (μM)	Recovery (%)	RSD (%)
Tap water	0	Non-detected	–	–
	2	2.09	104.5	1.6
South Lake	0	Non-detected	–	–
	2	2.04	102.0	3.0

Small-molecule Hg^{2+} probes based on naphthalimide and rhodamine hybrid fluorophore

Employing rhodamine 6G and rhodamine B appended to 4-Bromo-1,8-naphthalic anhydride as the fluorophore whilst using ethylenediamine as the spacer, Fang and co-workers successfully developed Probes **Hg-27** and **Hg-28** (Fig. 23) (Fang et al. 2015). Such systems have been proven effective for the highly sensitive and selective sensing of Hg^{2+} in the joint existence of other metal ions when spectroscopically investigated in CH_3CN/HEPES buffer (1:1, v/v, pH = 7.0). There was a 7.09-fold fluorescence enhancement when Hg^{2+} was added to a solution of Probe **Hg-27** (Fig. 24), this being attributed to a Hg^{2+}-chelated spirolactam ring opening. Meanwhile, the association constant and detection limit of Probe **Hg-27** for Hg^{2+} monitoring are 8.31×10^5 M^{-1} and 7.91×10^{-7} mol L^{-1}, respectively. The spectroscopic investigation of Probe **Hg-28**, a more water-soluble probe than Probe **Hg-27**, gave the association constant and detection limit of the binding of **Hg-28** with Hg^{2+} as 4.36×10^5 M^{-1} and 5.46×10^{-6} mol L^{-1}, respectively.

Xu's laboratory synthesised Probe **Hg-29** (Fig. 25), which was employed for the ratiometric detection of Hg^{2+} based on the FRET mechanism (Xu et al. 2017). Robust association constant of 2.75×10^5 M^{-1} was calculated, and minuscule detection limit of 0.059 μM was determined in EtOH/HEPES (v/v, 9:1, pH 7.0) in the analytical presence of other analyte ions, viz K^+, Mg^{2+}, Mn^{2+}, Fe^{2+}, Ni^{2+}, Ba^{2+}, Co^{2+}, Na^+, Zn^{2+}, Cu^{2+}, Pb^{2+}, Ca^{2+}, Cd^{2+}, Ag^+, Cr^{3+}, and Hg^{2+}. Thanks to its high recovery rate, real-time response, and anti-interference property, the probe was reportedly capable of being used for the 'naked-eye' Hg^{2+} monitoring and was also feasibly employed for Hg^{2+} monitoring in actual environmental water samples.

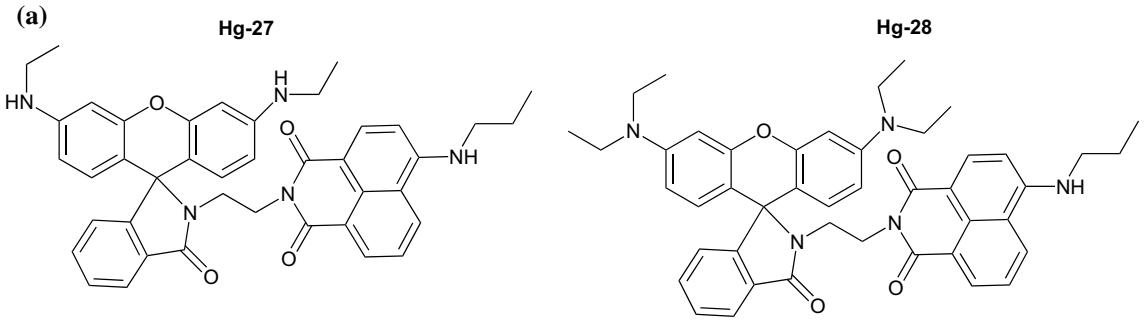

Fig. 23 Structures of Probes **Hg-27** and **Hg-28** (Fang et al. 2015)

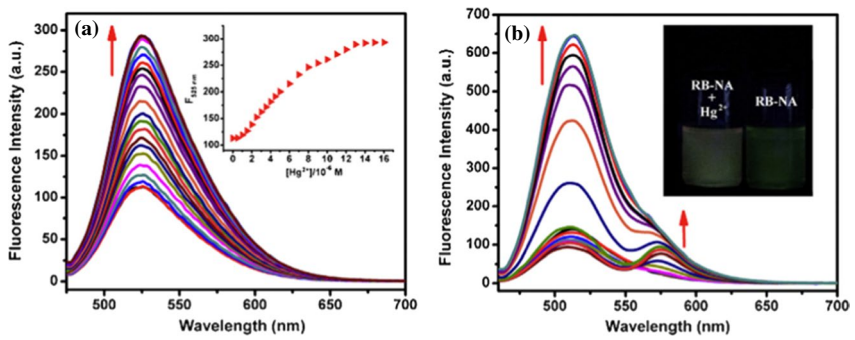

Fig. 24 **a** Fluorescence titration spectra of **Hg-28** (5 μM) in CH_3CN/HEPES buffer (1:1, v/v, pH = 7.0) in the presence of different concentrations of Hg^{2+} (0–16 μM). Inset: the plot of fluorescence intensity at 525 nm versus [Hg^{2+}]. The excitation wavelength was 450 nm. **b** Fluorescence titration spectra of **Hg-28** (5 μM) in pure CH_3CN in the presence of different concentrations of Hg^{2+} (0–24 μM). Inset: the image of fluorescence changes of **Hg-28** (5 μM) before and after upon interaction with Hg^{2+} (24 μM) (Fang et al. 2015)

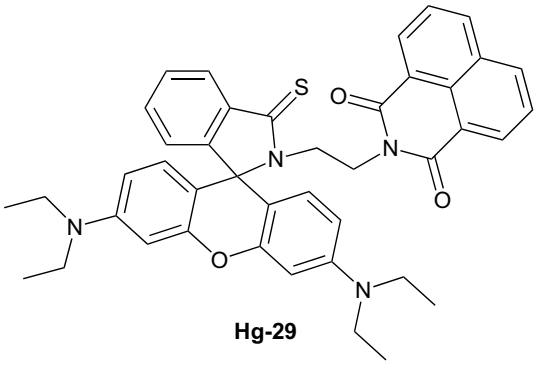

Fig. 25 Structure of Probe **Hg-29** (Xu et al. 2017)

Small-molecule Hg^{2+} probes based on rhodamine and coumarin hybrid fluorophore

Utilising the multiple advantages of ratiometric FRET process as a sensitive, selective, and adaptable detection technique, Zhou et al. (2013) came up with a Hg^{2+}-selective probe, **Hg-30** (Fig. 26), built from the rhodamine–coumarin scaffold. This probe was designed to exhibit a dual-responsive fluorescent and colourimetric analytical detection (Fig. 26) when investigated for Hg^{2+} selectivity when jointly present with common cations like Fe^{2+}, Mn^{2+}, Ni^{2+}, Co^{2+}, Cu^{2+}, Zn^{2+}, Cd^{2+}, Pb^{2+}, and Cr^{3+} in CH_3CN/H_2O system. Upon the addition of these metal ions, there was no noticeable change in the probe's emission intensity. The designated probe was capable of the biological imaging of intracellular Hg^{2+}.

Small-molecule Hg^{2+} probes based on naphthalimide and coumarin hybrid fluorophore

Through a mercury-promoted desulphurisation of thiocarbonyl moiety, a FRET dyad, **Hg-31**, which bears both 1,8-naphthalimide and rhodamine B moieties, was constructed as a ratiometric fluorescent probe for Hg^{2+} detection (Liu et al. 2012). Compound **Hg-31** (Fig. 27) is most appropriate for sensing application within the pH range of 5.7 to 11.0. Meanwhile, the linear range of fluorescence response

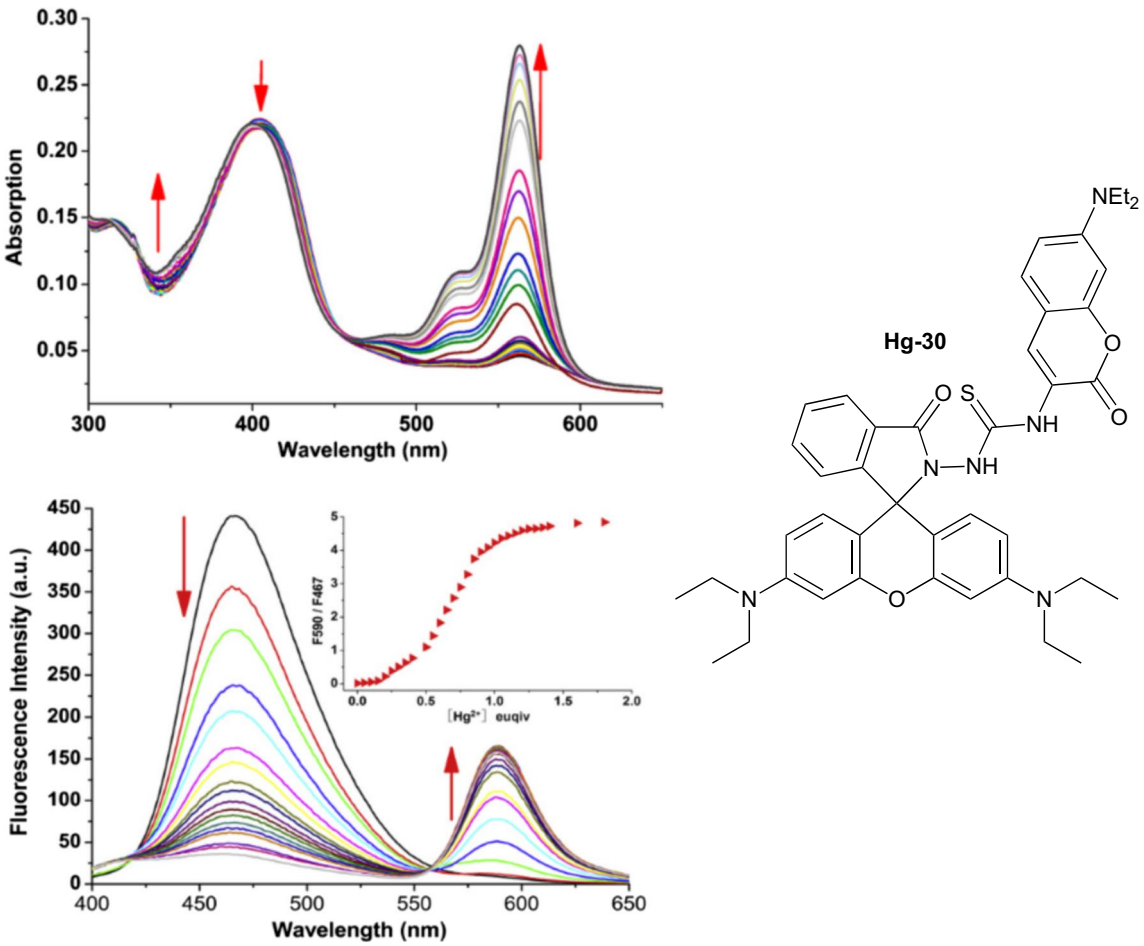

Fig. 26 Absorption (up) and fluorescent (down) spectra of Probe **Hg-30** (2 μM) (inset) (HEPES/CH_3CN, v/v = 20:80; pH 7.0) (Zhou et al. 2013)

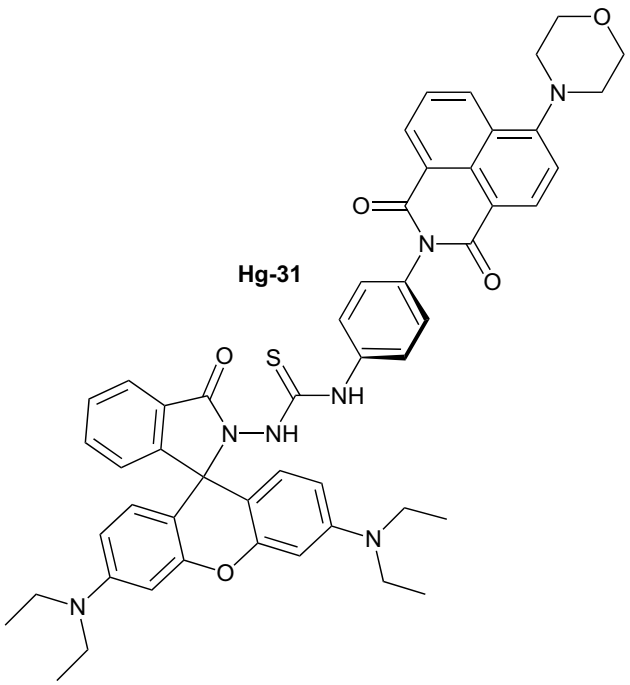

Fig. 27 Structure of Probe **Hg-31** (Liu et al. 2012)

detection was 4.2–10 mM, and the response time for the sensing investigation was 10 min. In (2:1, v/v) MeOH/H_2O solution (10 mM Tris–HCl, pH 7.0), there was a monumental fluorescence intensity increment in **Hg-31** explained as due to the rhodamine B unit ring opening. Cations like K^+, Na^+, Fe^{2+}, Mg^{2+}, Cr^{3+}, Fe^{3+}, Ca^{2+}, Zn^{2+}, Co^{2+}, Cu^{2+}, Pb^{2+}, Ni^{2+}, Cd^{2+}, Ag^+, Au^{3+}, and Pb^2 impacted zero changes on the fluorescence intensity of Compound **Hg-31**, albeit there was a little interference induced by Ag^+.

Small-molecule Hg^{2+} probes based on rhodamine and coumarin hybrid fluorophore

Through a spirocyclisation-modulated process, a rhodamine receptor was fused with a 7-diethylaminocoumarin fluorophore to develop a NIR ratiometric fluorescent Probe **Hg-32** (Fig. 28) (Liu et al. 2013a). The designed compound was stable in the long pH range of 1 to 12: When Hg^{2+} was increasingly added to the solution of the probe in Tris–HCl/CH_3CN (10 mM, pH = 7.4, 1:1, v/v) amidst cations like, K^+, Na^+, Mg^{2+}, Cu^{2+}, Ca^{2+}, Fe^{2+}, Zn^{2+}, Fe^{3+}, Ni^{2+}, Cr^{2+}, Mn^{2+}, Cd^{2+}, Pb^{2+}, Ag^+, and Co^{2+}, there was a massive downward shift in the fluorescence intensity at 480 nm, only for a new emission band positioned at 695 nm to appear. Desirably, the sensing reaction showed completion only after about 10 s of the starting time. A commendable linear ratiometric response (I_{695}/I_{480}) of Hg^{2+} monitoring was observed in the concentration range of 0–30 mM with a detection limit of

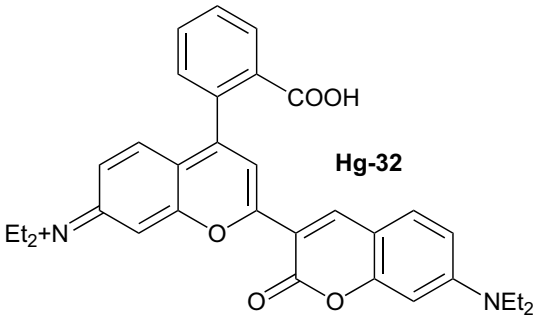

Fig. 28 Synthetic pathway to fluorescent Probe **Hg-32** (Liu et al. 2013a)

2.8×10^{-8} M estimated. Probe **Hg-32** could image Hg^{2+} in living HeLa cells.

Small-molecule Hg^{2+} probes based on rhodamine and pentaquinone hybrid fluorophore

Based on a TBET paradigm, Bhalla et al. documented the first instance of pentaquinone derivatives, **Hg-33** and **Hg-34** (Fig. 29), joined with a rhodamine unit devised for the ultra-high selective and sensitive tracking of Hg^{2+} (Bhalla et al. 2012). The optimum working pH range of the compounds **Hg-33** and **Hg-34** is 4.0–7.0. In THF/H_2O (9.5:0.5, v/v),

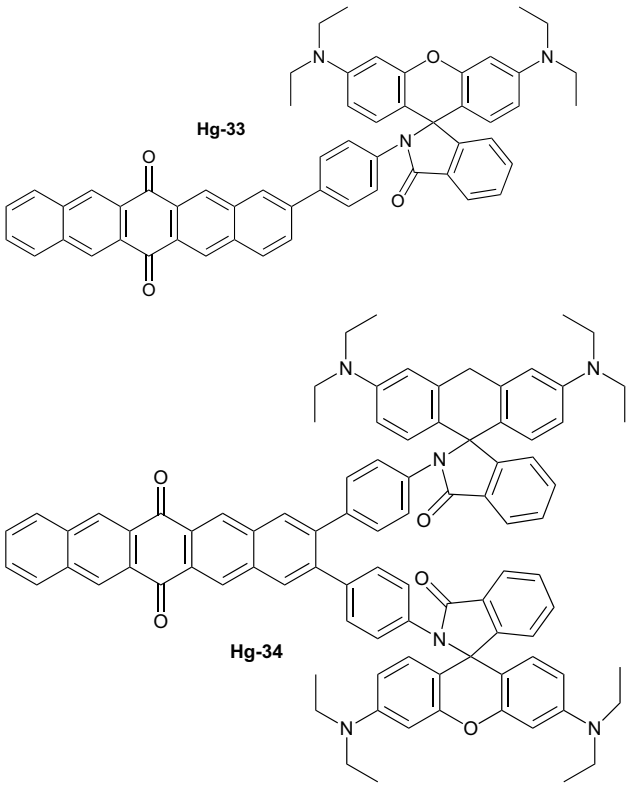

Fig. 29 Structures of Probes **Hg-33** and **Hg-34** (Bhalla et al. 2012)

only Hg^{2+} led to the enhancement of the fluorescence intensities of **Hg-33** and **Hg-34** (56-fold and 160-fold increment, respectively) in the midst of the other co-existent metal ions. The sensing performances of **Hg-33** and **Hg-34** were not affected by counter anions, except for NO_3^- that left a slight decrement in the sensing property of receptor **Hg-34**. The method of continuous variation, i.e. Job's plot, furnishes 1:1 and 1:2 stoichiometric ratios of Hg^{2+} interaction with receptors **Hg-33** and **Hg-34**, respectively. The calculated detection limits of receptors **Hg-33** and **Hg-34** for Hg^{2+} monitoring are 5×10^{-6} and 7×10^{-7} M, respectively. The receptors **Hg-33** and **Hg-34** displayed reversibility in their Hg^{2+} abilities. The receptor **Hg-34** was successfully appraised for in vitro Hg^{2+} monitoring in prostate cancer (PC3) cell lines.

Small-molecule Hg^{2+} probes based on boron-dipyrromethene (BODIPY) fluorophore

The 4,4-difluoro-4-bora-3a,4a-diazas-indacene molecule whose structure can be easily tuned at the carbon positions 1,3,5,7, and 8 is termed boron-dipyrromethene (BODIPY) chromophores, the BODIPY itself being registered under the trademark of Molecular Probes Inc. (Keller et al. 1995; Schade et al. 1996; Jones et al. 1997; Durand et al. 2000; Marme et al. 2003; Traverso et al. 2003). Treibs and Kreuzer 1968 reported the first BODIPY chromophore. The useful photophysical characteristics of BODIPY-based probes have led to their increasing usage. There is operational ease in the tuning of their visible excitation and emission by simply modifying the pyrrole core (Loudet and Burgess 2007; Thoresen et al. 1998; Rurack et al. 2001). They also possess high fluorescence quantum yields ($\Phi_F \approx 1.0$, even in water), high molar absorption coefficients (typically log max > 8.8), narrow emission bandwidths, and excellent photostability. They lack a net ionic charge, and their fluorescence is insensitive to solvent or pH. All these desirable properties constitute additional advantages (Sathyamoorthi et al. 1994; Treibs and Kreuzer 1968; Haugland et al. 1988).

Maity's lab documented a fluorescent probe for Hg^{2+}, **Hg-35** (Fig. 30), which incorporates a 2,2′-(ethane-1,2-diylbis(oxy))bis(*N*,*N*-bis(pyridine-2-ylmethyl)aniline receptor moiety built from a BODIPY derivative (Maity et al. 2015). **Hg-35** exhibited a large variation in its fluorescence within the pH range 4–8. The compound showed both selectivity and sensitivity towards Hg^{2+} (or Cd^{2+}) when present with an array of other cations such as Li^+, K^+, Na^+, Mn^{2+}, Mg^{2+}, Co^{2+}, Ca^{2+}, Fe^{2+}, Ni^{2+}, Zn^{2+}, Cu^{2+}, and Ag^+ in 20% DMSO-H_2O medium. The compliance of the selectivity of the compound for Hg^{2+} was justified by the great fluorescence enhancement noticed upon the addition of Hg^{2+}. The analysis of the Job's plot yielded a 1:1 binding stoichiometry of the **Hg-35**/Hg^{2+} complex. The estimated value of the association constant is 1.8×10^5 M^{-1} for Hg^{2+} (and 3.77×10^4 M^{-1} for Cd^{2+}), and a detection limit of 38 nM was obtained. Compound **Hg-35** detected Hg^{2+} (or Cd^{2+}) well enough in living cells.

The BODIPY derivative, **Hg-36** (Fig. 31), is a fluorescence probe developed for the highly sensitive and selective monitoring of Hg^{2+} in CH_3OH (Vedamalai 2012). An array of cations (Ag^+, K^+, Cd^{2+}, Ca^{2+}, Co^{2+}, Fe^{2+}, Cu^{2+}, Fe^{3+}, Mg^{2+}, Mn^{2+}, Ni^{2+}, Zn^{2+}, and Pb^{2+}) was used to assess the interference property of the compound in the detection of Hg^{2+}. Desirably, these cations impacted only a meagre effect on **Hg-36**′s fluorescence emission intensity. The apparent dissociation constant of **Hg-36**/Hg^{2+} was calculated to be 62 μM. The sensing property of **Hg-36** was tested by mixing

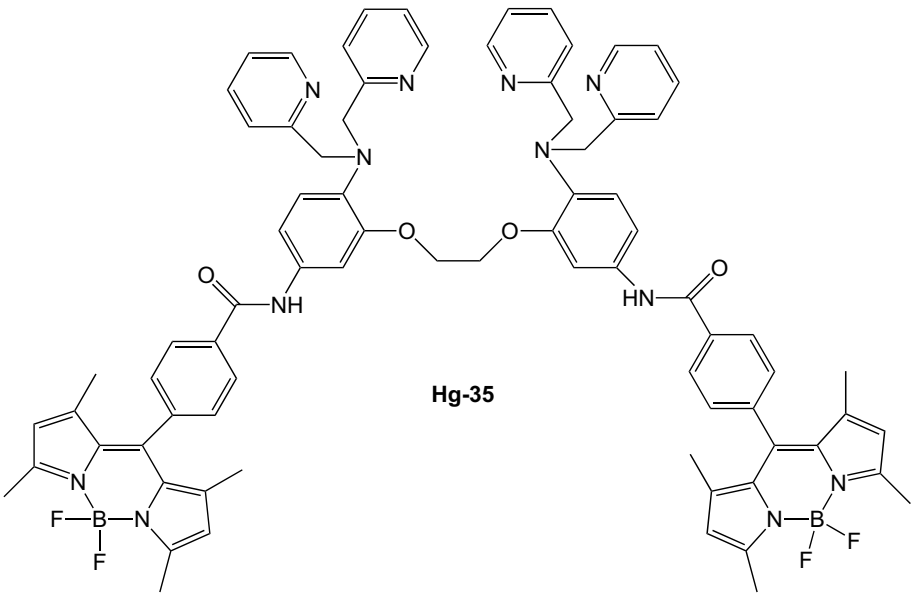

Fig. 30 Structure of Probe **Hg-35** (Maity et al. 2015)

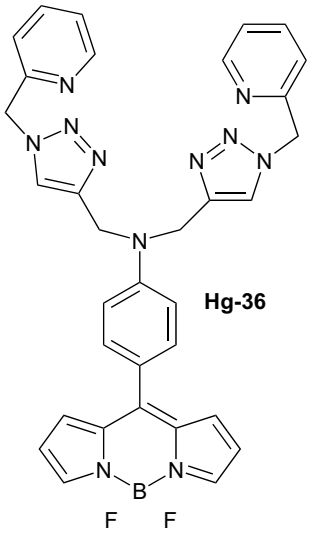

Fig. 31 Structure of Probe **Hg-36** (Vedamalai 2012)

it with other cations like Ag^{+}, Ca^{2+}, Cd^{2+}, Co^{2+}, Cu^{2+}, Fe^{2+}, Fe^{3+}, K^{+}, Mg^{2+}, Mn^{2+}, Ni^{2+}, Pb^{2+}, and Zn^{2+}. Experimental results revealed that the fluorescence emission intensity of the BODIPY derivative underwent a substantial increase upon the addition of Hg^{2+}, but remained unperturbed when other metal ions were added. Job's method indicated a 1:1 binding ratio between the detecting compound and the detected ion. The dissociation constant of 62.1 ± 5.7 µM was obtained. Meanwhile, a detection limit of 2.8 µM was estimated. Utilising the fluorescence rationale, **Hg-36** proves very suitable for Hg^{2+} tracking in living HeLa cells.

Small-molecule Hg^{2+} probes based on cinnamaldehyde fluorophore

Kumar and co-workers synthesised a PET fluorescence 'turn-on' probe, **Hg-37** (Fig. 32), that anchors *N*,*N*-dimethylaminocinnamaldehyde, for the monitoring of Hg^{2+}, whereby the as-prepared complex **Hg-37**/Hg^{2+} was further engaged for the detection of picric acid (Kumar et al. 2012b). In THF/H_2O (9:1, v/v), recognition and competitive experiments

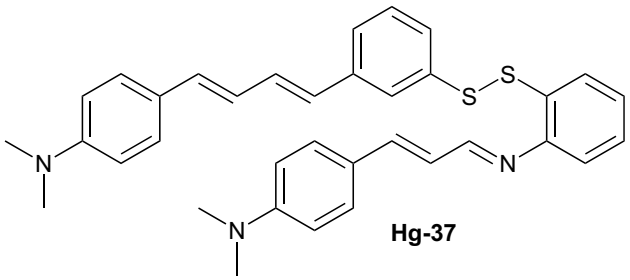

Fig. 32 Structure of Probe **Hg-37** (Kumar et al. 2012b)

revealed that the addition of metal ions to the probe's solution did not induce any substantial change in the fluorescence intensity of the probe, except for Hg^{2+} that impacted a fluorescence quenching phenomenon. The experimental result provides a detection limit of 80×10^{-9} M for Hg^{2+} tracking by the designed compound. Both the linear regression analysis (SPECFIT programme) and Job's plot indicated a 1:2 stoichiometry of chelation between the probe and Hg^{2+} and a binding constant of 9.16 ± 0.03 was estimated. It was demonstrated that the interaction between Hg^{2+} and compound **Hg-37** was reversible.

Small-molecule Hg^{2+} probes based on Schiff base fluorophore

The Schiff base reaction was conceptualised in 1864 by the German chemist, Hugo Schiff, which is a reaction between aldehyde- or ketone-containing compounds and amino groups, leading to the generation of imine groups (–CN–) (Fig. 33). The set of reactions constitute popular chemical reactions due to that their reaction conditions are mild and that their reaction rates are high (Jia and Li2015). Only in the past few years had Schiff base compounds become increasingly applied for the generation of fluorescent and colourimetric probes.

Mandal et al. constructed a series of new imine-based probes, **Hg-38**, **Hg-39**, and **Hg-40** (Fig. 34), for the sharp fluorescence 'turn on' detection of Hg^{2+} in $CHCl_3/CH_3CN$ (1:4, v/v) over other competing metal ions (Mandal et al. 2012). There was a monumental increase in the fluorescence intensities of **Hg-38**, **Hg-39**, and **Hg-40** upon interaction with Hg^{2+}, this being explained as owing to imine isomerisation and inhibited PET mechanism. The composite binding constants of Hg^{2+} by **Hg-38**, **Hg-39**, and **Hg-40** were obtained to be 2.79×10^{9} M^{-2} L^{2} (for **Hg-38**) and 1.29×10^{9} M^{-2} L^{2} (for **Hg-39** and **Hg-40**). Meanwhile, the analysis of the Benesi–Hildebrand plots for **Hg-39** and **Hg-40** gave a 2:1 stoichiometric ratio. **Hg-38** was reversible in its sensing of Hg^{2+} after the addition of KI that led to the recovery of the unbound probe compound from the **Hg-38**/$(Hg^{2+})_2$ complex. Interestingly, **Hg-38** and **Hg-39** were successfully demonstrated for Hg^{2+} detection in living cervical cancer HeLa cells.

Quang reported the synthesis of the ICT aminothiourea-derived Schiff base, **Hg-41** (Fig. 35), for the fluorescent recognition of Hg^{2+} (Quang et al. 2013). In aqueous

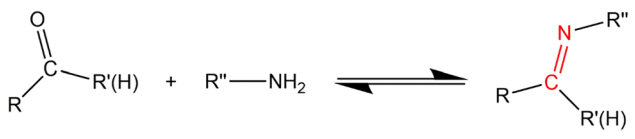

Fig. 33 Schematic demonstration of Schiff base reaction (Jia and Li 2015)

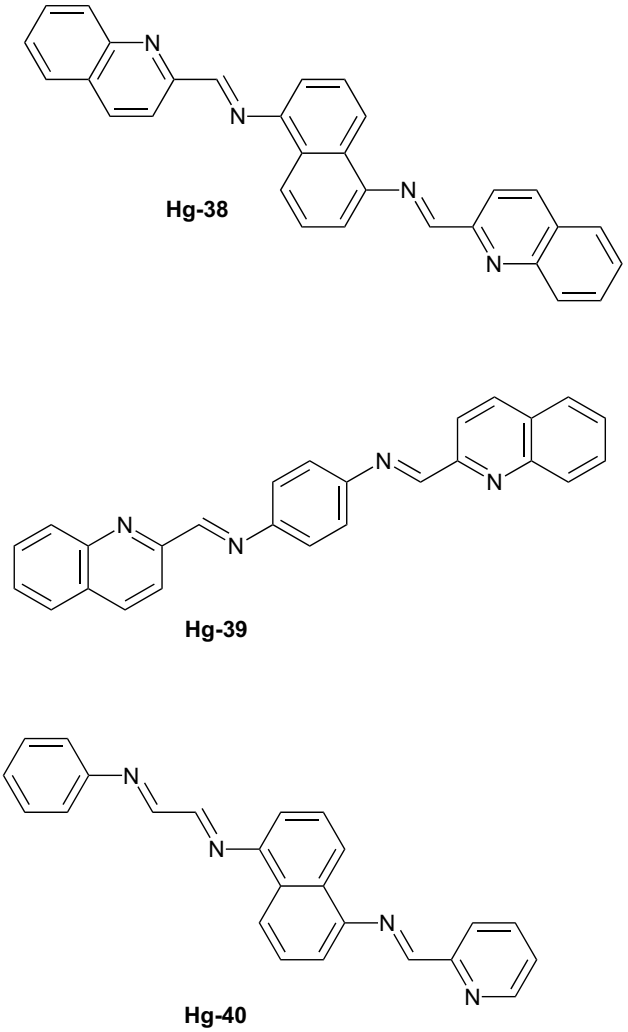

Fig. 34 Structures of imine-based Probes **Hg-38**, **Hg-39**, and **Hg-40** (Mandal et al. 2012)

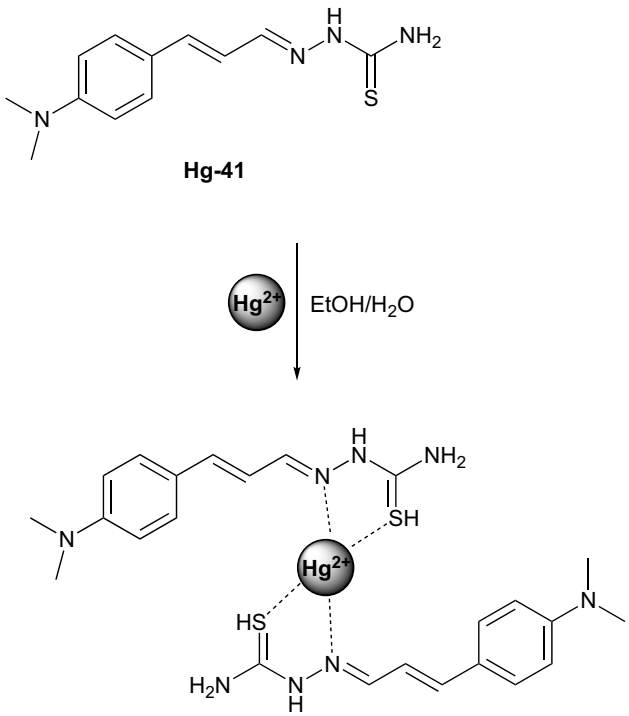

Fig. 35 Proposed interaction mechanism between Probe **Hg-41** and Hg^{2+} (Quang et al. 2013)

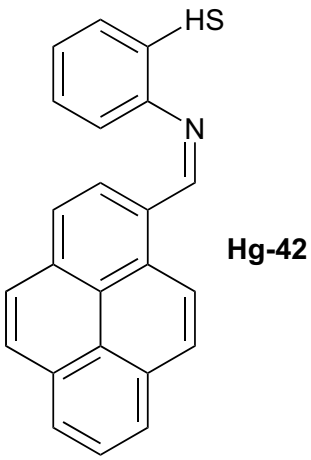

Fig. 36 Structural representation of Probe **Hg-42** (Shellaiah et al. 2015)

solution, the addition of Hg^{2+} to the probe's solution pushed the fluorescence intensity upward at about 30% increment. Contrastingly, competitive cations like K^+, Cd^{2+}, Pb^{2+}, Cr^{3+}, Fe^{2+}, Ni^{2+}, Zn^{2+}, Co^{3+}, Ca^{2+}, Mg^{2+}, and Na^+ led to benign variation in the fluorescence of **Hg-41**. The most desirable working pH range of **Hg-41** for Hg^{2+} determination was from 5 to 9. Moreover, the time required for the reaction to be complete was 30 s. A 2:1 complex of Probe **Hg-41** and Hg^{2+} was derived, which was confirmed by the result of the ESI–MS.

The novel and elegant pyrene-based free thiol probe, **Hg-42** (Fig. 36), that bears the Schiff base was documented by Shellaiah and co-workers (Shellaiah et al. 2015). The developed compound, which utilises a reversible chelation-enhanced fluorescence (CHEF) mechanism, was engaged as a fluorescence 'turn on' probe for the tracking of Hg^{2+} ion in DMSO/H_2O (v/v = 7/3; pH 7.0). The original, strong fluorescence of the devised probe was enhanced when Hg^{2+} was added to it, whereas other cations including Na^+, Ag^+, Ni^{2+}, Co^{2+}, Fe^{3+}, Zn^{2+}, Cd^{2+}, Pb^{2+}, Cr^{3+}, Cu^{2+}, Mg^{2+}, Hg^{2+}, Mn^{2+}, Fe^{2+}, and Al^{3+} did not impact a noticeable effect on the fluorescence intensity of the probe, in either single or dual metal analyses. The only exception was Pb^{2+} and Cd^{2+} that interfered somewhat weakly. Job's plot analysis gives a distinct 2:1 binding ratio of the derived probe-Hg^{2+}complex. The detection limit and association constant

are 2.82×10^{-6} M and 7.36×10^{4} M^{-1}, respectively. Desirably, the usage of **Hg-42** for Hg^{2+} imaging in living HeLa cells was successfully established.

Small-molecule Hg^{2+} probes based on anthracene fluorophore

Srivastava and teammates synthesised an effective PET compound, **Hg-43** (Fig. 37), which anchors anthracene and benzhydryl moieties via a piperazine bridge, as a fluorescent molecular probe for Hg^{2+} sensing (Srivastava et al. 2014). There was observed a large increase in the fluorescence intensity of *ca.* tenfold in HEPES buffer and *ca.* 15% in CH_3CN-H_2O solution, with a consequential colour change from blue to blue-green. Other cations (Na^+, K^+, Ca^{2+}, Zn^{2+}, Pb^{2+}, Ag^+, Cd^{2+}, Co^{2+}, Ni^{2+}, Cu^{2+} Fe^{2+}, Fe^{3+}, Mg^{2+}, Ca^{2+}, and Zn^{2+}) did not engender any noteworthy influence on the fluorescence intensity of Hg^{2+}, except for Fe^{3+} that interfered quite slightly (*ca.* 5 to 7%) on **Hg-43**'s fluorescence emission intensity. The probe existed with Hg^{2+} in **Hg-43**/Hg^{2+} complex in a 1:2 stoichiometry. **Hg-43** was found to be pH insensitive within the range 7–14, with pH 5 being the optimal pH value. Job's plot analysis revealed a 1:2 stoichiometric binding interaction between **Hg-43** and Hg^{2+}. The association constant and detection limit were obtained as 1.06×10^{10} M^{-2} and 10 nM or 2 ppb, respectively. The probe **Hg-43** was successfully applied as a solid probe for Hg^{2+} monitoring on solid surfaces like paper strips and slides coated with silica, as well as to bioimage Hg^{2+} in HeLa cells.

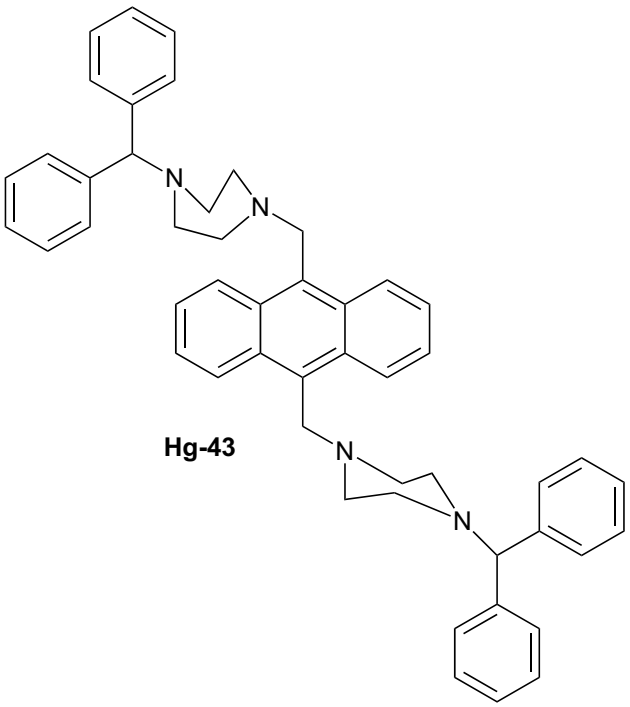

Hg-43

Fig. 37 Structure of Probe **Hg-43** (Srivastava et al. 2014)

Praveen and co-workers constructed the anthracene-oxyquinoline dyad, **Hg-44** (Fig. 38), for Hg^{2+} sensitive and selective sensing (Praveen et al. 2012). In MeCN-H_2O system, Hg^{2+} addition quenched the fluorescence of the reported compound, a phenomenon unobserved in the cases of other co-existed cations. A 1:1 binding stoichiometry was provided by the analysis of the Job's plot, whilst a detection limit of 3.2×10^{-6} M was calculated from the Benesi–Hildebrand plot. Probe **Hg-44** was reversible in its tracking of Hg^{2+}.

A new anthracene-based sensing modality, **Hg-45**, 1-(Anthracen-2-yliminomethyl)-napthalen-2-ol (AIN) (Fig. 39), which features aggregation-induced emission (AIE) was recently disclosed by Shyamal's group (Shyamal et al. 2018). The probe exhibited a suppression in its fluorescence intensity upon selective recognition of Hg^{2+} with a linearity of response within the concentration range 0.3–3.6 M. The sensing ability of the probe was tested in THF/H_2O (7:3, v/v) in the presence of various relevant metal ions. The probe's sensitivity was excellent (a limit of detection limit of *ca.* 3 ppb was estimated), and the quenching constant obtained from Stern–Volmer equation was 2.54×10^{5} M^{-1}. The probe's ability to quantify Hg^{2+} concentration in real water samples was successfully investigated.

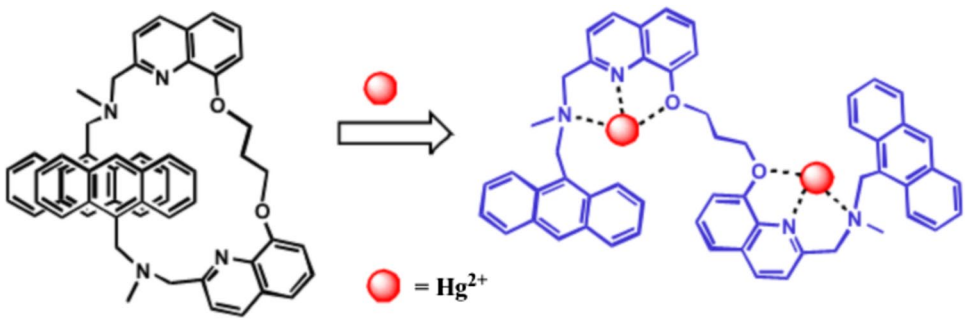

Hg-44

Fig. 38 Plausible binding mode of Probe **Hg-44** with Hg^{2+} (Praveen et al. 2012)

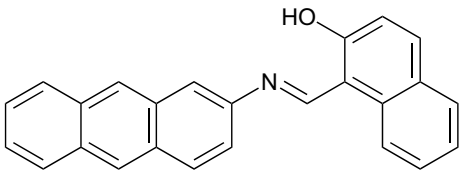

Hg-45

Fig. 39 Structure of Probe **Hg-45**, 1-(Anthracen-2-yliminomethyl)-napthalen-2-ol (AIN) (Shyamal et al. 2018)

Small-molecule Hg^{2+} probes based on squaraine fluorophore

The squaraines are a subclass of the polymethine dyes possessing a zwitterionic structure and constituting one of the most fascinating groups of dyes for the preparation of near-infrared fluorescent probes (Oswald et al. 2000; Kukrer and Akkaya 1999; Dilek and Akkaya 2000). They exhibit outstanding physicochemical properties, including magnificent and sharp absorption bands, (detectable in the visible and NIR regions) as well as intense fluorescence bands (Welder et al. 2003; Kim et al. 2002). These properties make the squarylium fluorophores suitable for sensing purposes. Infusion of substituents into the aromatic ring or on the *N* atom of the terminal heterocyclic moiety could lead to their structural modifications. Such variations can be used to produce a red shift of the absorption and fluorescence bands.

Fan and teammates developed the squaraine-appended colourimetric and fluorescent probe, **Hg-46** (Fig. 40) (Fan et al. 2012), for Hg^{2+}-sensitive and selective sensing. In ethanol–phosphate buffer (EtOH/PB) (50:50, v/v) solution, Hg^{2+} addition amidst several other metal ions led to a gradual dampening of the probe's fluorescence intensity. Job's plot analysis indicates the formation of a 1:1 binding stoichiometry. The calculated association constant and detection limit are 3.05×10^3 M^{-1} and 1.3×10^{-7} M, respectively. Experimental outcomes demonstrated **Hg-46** as reversible in its sensing mode, i.e. the unbound **Hg-46** was regenerated upon EDTA addition to **Hg-46**/metal complex's solution.

Small-molecule Hg^{2+} probes based on pyrene fluorophore

Weng and laboratory members reported a compound, **Hg-47** (Fig. 41), that anchors the pyrene skeleton and diazene architecture (Weng et al. 2012). The designated compound acts as a useful fluorescent probe for tracking Hg^{2+}. In CH_3CN solution, the addition of various cations did not incite any tremendous change in the fluorescence of **Hg-47**, whereas the addition of Hg^{2+} led to a marked decrement in the fluorescence of **Hg-47**, affirming the affinity of the designed probe for Hg^{2+} even in competition with other analytically investigated cations. A 2:1 stoichiometric ratio of the interaction of the probe and Hg^{2+} was furnished by Job's plot analysis, which was corroborated by MS and NMR experimental results. The detection limit was calculated to be 4.69×10^{-6} M.

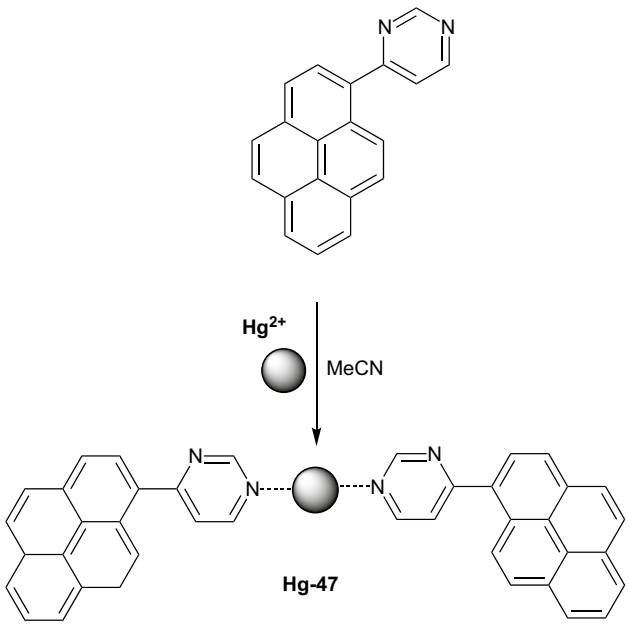

Hg-47

Fig. 41 Possible binding mechanism of Probe **Hg-47** with Hg^{2+} (Weng et al. 2012)

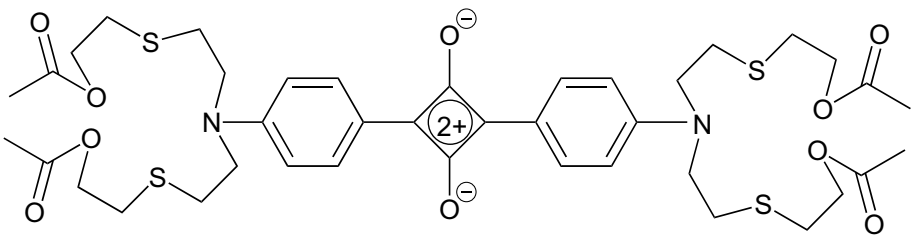

Hg-46

Fig. 40 Structure of the squaraine Probe **Hg-46** (Fan et al. 2012)

Small-molecule Hg^{2+} probes based on rhodamine and pyrene hybrid fluorophore

Being informed by the knowledge that rhodamine and pyrene scaffolds exhibit excellent optical and configurable characteristics, Rui et al. developed two rhodamine–pyrene conjugated probes, **Hg-48** and **Hg-49** (Fig. 42) (Rui et al. 2016), which display strong affinities to Hg^{2+} via FRET process in the existence of other cations tested in EtOH/H_2O (1:1, v/v, pH 7.0). The detection limit of sensing of Hg^{2+} by Probes **Hg-48** and **Hg-49** is 4.34×10^{-7} mol L^{-1} and 1.91×10^{-5} mol L^{-1}, respectively. The experimental results showed that Probe **Hg-48** is a better probe than Probe **Hg-49** due to its shorter response time, lower detection limit, and reversibility. Moreover, Probe **Hg-48** was effectively employed for Hg^{2+} tracking in real water samples.

Two rhodamine–pyrene probes, Probes **Hg-50** and **Hg-51** (Fig. 43), were synthesised by Chu's laboratory (Chu et al. 2013). In EtOH/H_2O (2:1, v/v), both these probes exhibited outstanding sensing properties towards Hg^{2+} when tested in the analytical presence of commonly tested cations. The limit of detection of Probe **Hg-50** for Hg^{2+} monitoring was quantified as 0.72 μM, whilst that of Probe **Hg-51** was obtained as 5.3 μM. Meanwhile, the association constants of these two probes for Hg^{2+} monitoring were 2.74×10^5 M^{-1} and 1.56×10^5 M^{-1}, respectively. It was experimentally confirmed that Probe **Hg-50** had better spectral properties than Probe **Hg-51**, in terms of higher selectivity, excellent

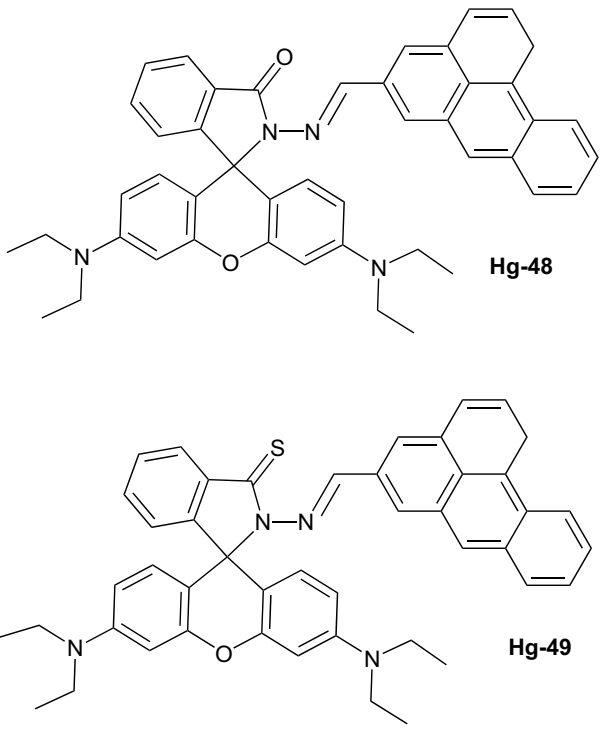

Fig. 42 Structures of Probes **Hg-48** and **Hg-49** (Rui et al. 2016)

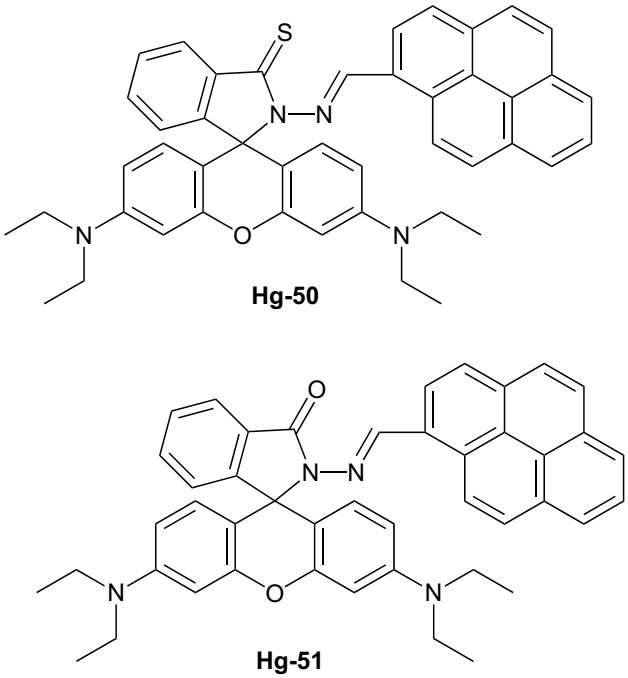

Fig. 43 Structures of Probes **Hg-50** and **Hg-51** (Chu et al. 2013)

reversibility, and lower detection limit than Probe **Hg-51**, due to the thiophilic property of Hg^{2+}. Finally, the utility of Probe **Hg-50** for Hg^{2+} detection in practical biological systems was successfully demonstrated.

Small-molecule Hg^{2+} probes based on azo derivative fluorophore

Tian et al. documented an azo derivative, **Hg-52** (Fig. 44), based on alkynes, which served as a colourimetric and fluorescence probe for the detection of Hg^{2+} (Tian et al. 2014). The probe gave no fluorescence emission in aqueous solution, which is atypical of the azo group of probes. But the addition of Hg^{2+} amongst several other cations and anions led to a 168-fold increase in the probe's fluorescence intensity. The Job's plot provided a 1:1 stoichiometric ratio in the interaction of **Hg-52** with Hg^{2+}. The detection limit and association constant of the probe for the sensing of Hg^{2+} were calculated as 46.50 nM and 3.96×10^6 M^1, respectively. The sensing mechanism of Hg^{2+} by **Hg-52** was demonstrated reversible by the addition of Na_2S. The specificity of Probe **Hg-52** towards Hg^{2+} was determined by fluorescence screening. **Hg-52**′s potency to track Hg^{2+} was successfully demonstrated in living HT-29 cells.

Yu and co-workers designed a thioacetal probe, **Hg-53** (Fig. 44), that anchors both carbazole and azobenzene units (Yu et al. 2016). The spectroscopic characterisation of the compound showed that it functioned effectively in the range of 0–2.5 M and possessed a short response time of 30 s. In

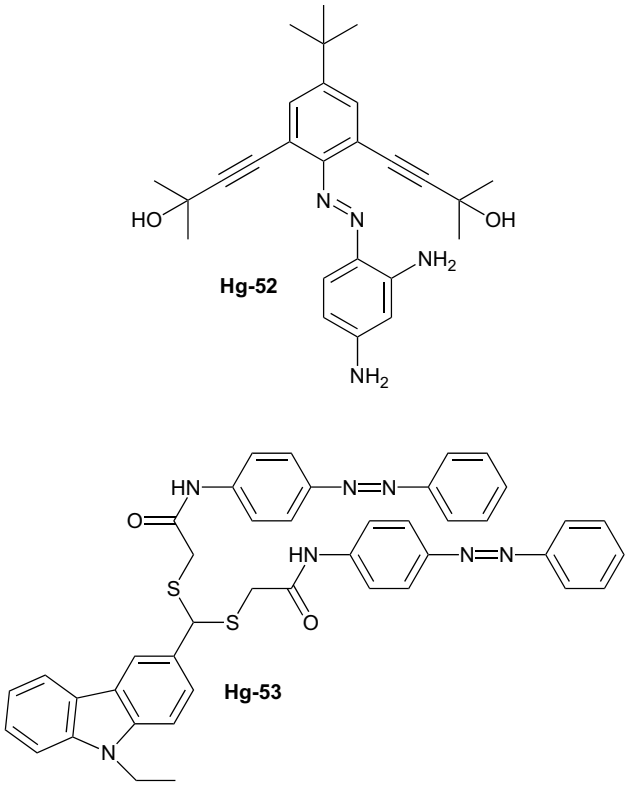

Fig. 44 Structures of Probes **Hg-52** and **Hg-53** (Tian et al. 2014; Yu et al. 2016)

CH_3CN/H_2O solution, various cations (including Na^+, K^+, Ca^{2+}, Mg^{2+}, Ni^{2+}, Li^+, Co^{2+}, Ag^+, Cu^{2+}, Pb^{2+}, Mn^{2+}, Cr^{3+}, Fe^{3+}, Zn^{2+}, Cd^{2+}, Sr^{2+}) impinged no monumental change in **Hg-53′**s fluorescence intensity except for Hg^{2+} that led to a dramatic increment in the fluorescence intensity of the designated compound (about a 24-fold increase). Job's plot indicates a 1:1 binding stoichiometry between the probe **Hg-53** and Hg^{2+}. A detection limit of 1.80×10^{-8} M was calculated.

Small-molecule Hg^{2+} probes based on benzimidazole derivative fluorophore

Hu et al. (2015) reported on a novel Hg^{2+} non-sulphur fluorescent probe, **Hg-54** (Fig. 45) that incorporates the benzimidazole and quinoline moieties as the fluorescence signal groups. The compound exhibited a sharp distinguishing ability for Hg^{2+} over an array of other divalent cations as monitored by fluorescence spectroscopic analysis in H_2O/DMSO (1:9, v/v) solution with a massive colour change from blue to colourless observed when Hg^{2+} was added to the probe's solution in aqueous media. Similar experiments for competitive cations present did not induce any prominent variation in the colour. The analytical limit of detection of the fluorescence response of the probe to Hg^{2+} is low down to 9.56×10^{-9} M. The usage of the probe in the fabrication of test kits which could monitor Hg^{2+} demonstrated the probe's practical application utility in an aqueous environment.

Small-molecule Hg^{2+} probes based on the phenanthroline fluorophore

Shan and co-workers developed a fast, responsive, and highly selective Hg^{2+} probe, **Hg-55** (Fig. 46), based on 2,9-dimethyl-1,10-phenanthroline (2,9-DMP) fluorophore (Shan et al. 2016). The selectivity and sensitivity experiments were carried out in Tris-HNO_3 at the optimum sensing pH value of 2.0. The probe's response to Hg^{2+} was rapid and selective within a good linear range of 0.05–2.00 μM. The reported compound was then utilised to monitor concentrations of Hg^{2+} in aqueous samples of drinking water and Zhujiang River water. Excellent recoveries of 85.42–101.5% and 81.72–96.09%, respectively, were obtained for each of these samples. Fluorescence titration experiment gave a 1:1 complex, demonstrating a 1:1 stoichiometric mode between the probe and Hg^{2+}. This was then further evidenced by the results of Job's plot and single-crystal X-ray diffraction.

Small-molecule Hg^{2+} probes based on miscellaneous fluorophores

Because of limited space, it is difficult to cover all fluorophores used in the development of small-molecule Hg^{2+}

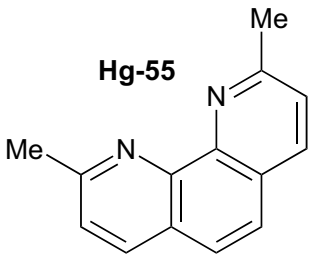

Fig. 46 Structure of 2,9-DMP fluorophore-based Probe **Hg-55** (Shan et al. 2016)

Fig. 45 Synthetic route to Probe **Hg-54** (Hu et al. 2015)

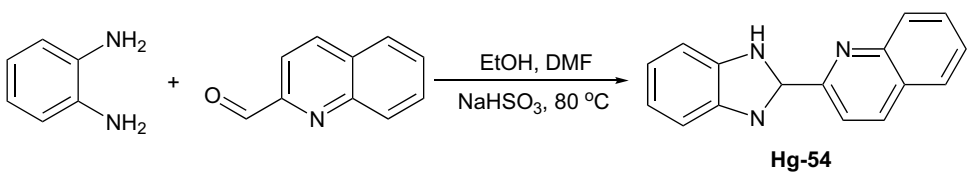

probes in this review work. However, apart from the small-molecule Hg^{2+} probes highlighted above, other fluorophores such as cyanine and fluorescein (Fig. 47) (Zheng et al. 2013; Ando and Koide 2011; Liu et al. 2013b) have been employed as alternative receptors in design and synthesis of small-molecule Hg^{2+} probes. Zheng et al. (2013) provided an overview of fluorescent probes based on the xanthene scaffolds, predominantly the rhodamine and fluorescein moieties. The fluorescent behaviours of these probes towards diverse analytes, including mercuric ion (Hg^{2+}) or methylmercury species (MeHg), were discussed. Ando and Koide (2011) developed a new vinyl ether Hg-selective probe by the reaction of an allyl ether and KO^{t}Bu in DMSO through the oxymercuration reaction. The probe, which functions best at pH 4 in 50 mM phthalate buffer, detects Hg^{2+} at ambient temperature (i.e. 25 °C) and can be applied for Hg^{2+} monitoring in river water and dental amalgam samples. A cyanine-modified nanoprobe (the cyanine dye was assembled on lanthanide UCNPs' surface) which functions as a dual colourimetric and fluorescent probe for $MeHg^+$ sensing was reported by Liu's laboratory (2013b). This probe, whose sensing properties were largely uninfluenced by the presence of other non-mercuric cations, gave the detection limit of *ca.* 200 ppb. The probe showed great potential imaging applications in living cells and also for luminescence in vivo imaging.

The morpholine-based fluorophore possesses a lysosome-targeting capability and has been found efficient as a lysosomal localisation group. Informed by this, Zhang's group developed a PET dual-functional colourimetric and ratiometric fluorescent probe, **Hg-56** (Fig. 48), from the 4-chloro-7-nitrobenzo-2,1,3-oxadiazole (NBD-Cl) moiety (Zhang et al. 2016). The probe is water-soluble, bio-compatible and cell permeable, and could, therefore, monitor Hg^{2+}-related cellular toxicological actions of HeLa cells.

Recently, Gu et al. and Ding and co-workers synthesised and evaluated the optical features of probes based on the 2-(2′-hydroxyphenyl)-9,10-phenanthroimidazole (HPI) and dithioacetal fluorophores, **Hg-57** and **Hg-58** (Fig. 49), respectively (Gu et al. 2015; Ding et al. 2015). Both these probes have superior binding properties towards Hg^{2+} in the coexistence of other analytically investigated cations.

The AIE feature of a π-conjugated cyanostilbene derivative of (Z)-2-(4-nitrophenyl)-3-(4-(vinyloxy)phenyl)acrylonitrile, **Hg-59** (Fig. 50), was advantage taken of by Wang et al. in their design of a new sensing modality (Wang et al. 2015). The sensing properties of the designated probe compound were carried out in THF/H_2O (2:8, v/v). **Probe Hg-59** was selective towards Hg^{2+} amidst an array of metal ions concomitantly investigated, and the fluorescence intensity of **Hg-59** was dampened in a linear fashion with the incremental addition of Hg^{2+} (0–50 μM). The selectivity property of the probe was then tested with the probe's detection limit calculated as 37 nM. These good properties of the probe enabled the quantification of Hg^{2+} in real water samples, thereby lending validity to the probe's good sensing ability.

Hg^{2+} probes based on supramolecular fluorophores

The seminal work of Chen and co-workers (2017) represented the first case of the use of supramolecular polymers in sequestering toxic heavy metal ions. Their supramolecular system was prepared through self-assembly of a thymine-substituted copillar[5]arene, **1**, (catcher) and a tetraphenylethylene (TPE) derivative, **2** (indicator), together with Hg^{2+}. The reversible recognition studies of Hg^{2+} with the thymine moieties of **1** were investigated. The host–guest interaction between **1** and **2** was also examined, and the supramolecular

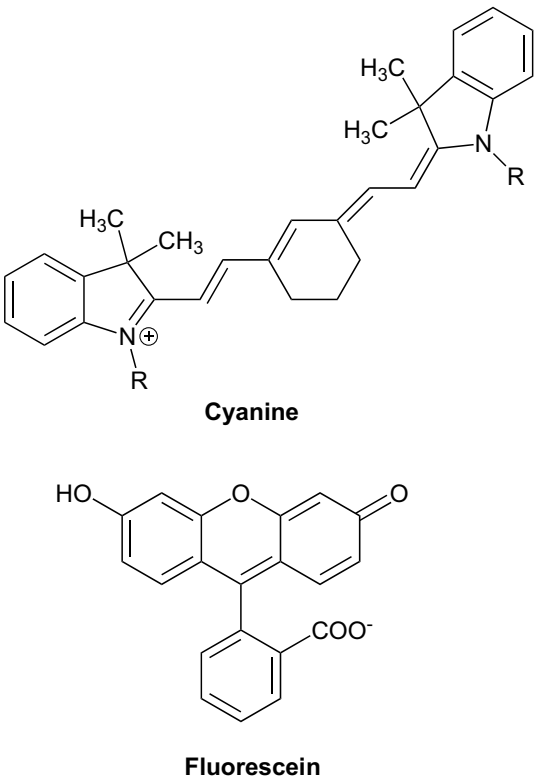

Fig. 47 Simplest structural representations of cyanine and fluorescein moieties (Zheng et al. 2013; Andoand Koide 2011; Liu et al. 2013b)

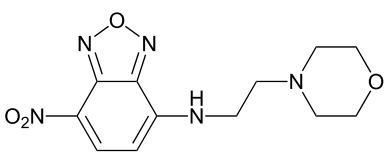

Fig. 48 Structure of Probe **Hg-56** (Zhang et al. 2016)

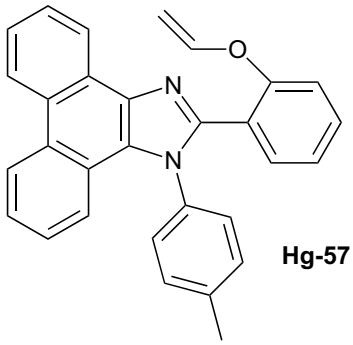

Hg-57

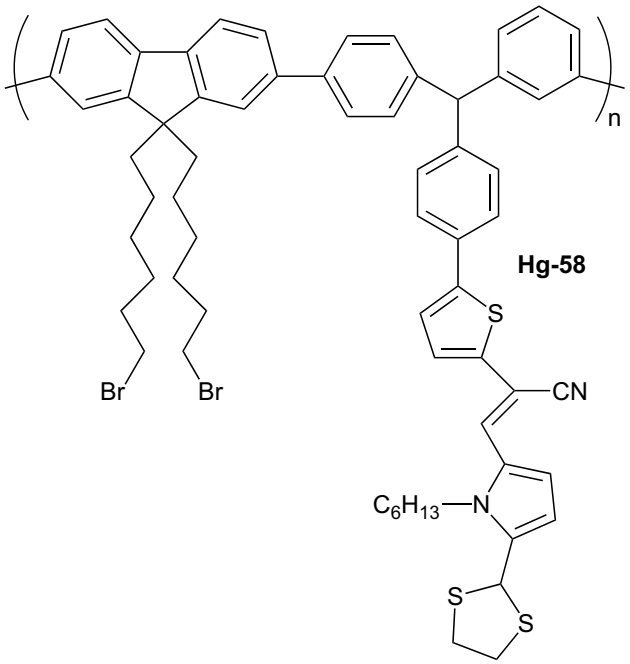

Hg-58

Fig. 49 Structures of Probes **Hg-57** and **Hg-58** (Gu et al. 2015; Ding et al. 2015)

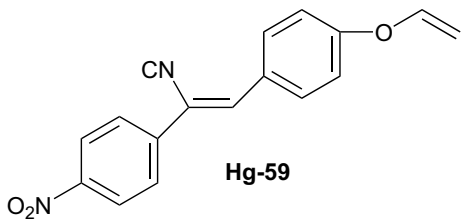

Hg-59

Fig. 50 Structure of **Hg-59** (Wang et al. 2015)

complex/pseudorotaxane **2** ⊂ **1** was then used for Hg^{2+} tracking. Fluorescence titration experiments in the presence of other cations in 300 μM $(CH_3)_2CO$ showed that there was a massive enhancement of the absorption maximum of **1** upon the incremental addition of 1.0 equiv. of Hg^{2+} coupled with a bathochromic shift from 326 to 329 nm. This was being accrued to the coordination of Hg^{2+} with the thymine moieties in **1**, leading to the formation of $T-Hg^{2+}-T$ pairings between **1** and Hg^{2+}. TPE derivatives are known to only display strong fluorescence after aggregation; otherwise, they exhibit zero or low fluorescence when existent in a highly dispersed state. Springing from the AIE properties of **2**, the derived supramolecular polymer exhibited strong fluorescence which was exploited for Hg^{2+} detection and removal. Linearity of fluorescence response in the range 0 – 180 μM was observed, and the analytical detection limit was 2.3 μM. The applicability of the **2** ⊂ **1** supramolecular system in removing Hg^{2+} from real water samples was successfully tested.

Taking advantage of supramolecular self-assembly, a new sensitive and selective probe, (E)-1-((5-(4-nitrophenyl) furan-2-yl)methylene) semicarbazone (**Hg-60**) (Fig. 51), was derived from fusing 5-(4-nitrophenyl)-2-furan (the fluorophore) with semicarbazide groups (Qu et al. 2014). In DMSO/H_2O (8:2, v/v) HEPES buffer (pH = 7.2) solution, there was a dampening of the fluorescence intensity of the probe (20 μM) when Hg^{2+} (1 equiv.) was added in the presence of Fe^{3+}, Hg^{2+}, Ag^{+}, Ca^{2+}, Cu^{2+}, Co^{2+}, Ni^{2+}, Cd^{2+}, Pb^{2+}, Zn^{2+}, Cr^{3+}, and Mg^{2+} (20 μM). This observation was ascribed to the supramolecular self-assembly breaking and the cooperation reaction occurrence. The detection limit of **Hg-60** for Hg^{2+} determination was 2.084 nM, whilst Job's plot analysis furnished a 1:2 stoichiometric ratio between **Hg-60** and Hg^{2+} in **Hg-60**–Hg^{2+}. Test strips of the probe successfully tracked Hg^{2+} in solution.

Hg^{2+} probes based on carbohydrate-appended resorufin fluorophore

Ma and co-workers, with the employment of a carbohydrate-based Ferrier carbocyclisation reaction, designed a water-soluble fluorescent probe, **Hg-61** (Fig. 52), for the monitoring of Hg^{2+} through a 'turn on' mode of its fluorescence intensity (Ma et al. 2012). The probe's stability was established within the wide pH range of 3.4–9.3; the best operational pH value of the designated probe was 7.4. Meanwhile, 15-min response time for the sensing of Hg^{2+} by the reported probe was achieved. The experimental pH range employed for the analytical experiments is 3.4–9.3. In pure

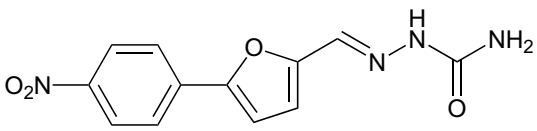

Hg-60

Fig. 51 Structure of **Hg-60** (Qu et al. 2014)

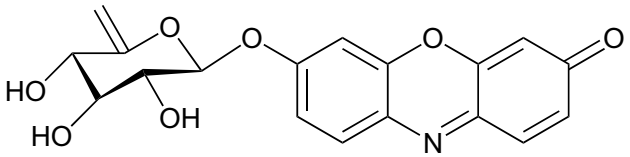

Hg-61

Fig. 52 Structure of Probe **Hg-61** (Ma et al. 2012)

H_2O (20 µM, pH 6.0), the compound maintained no fluorescent character. However, when the pH changed to > 6.96 by the addition of PBS buffer, there was a sudden appearance of vibrant fluorescence intensity with an accompanying colour variation from colourless to purple. This is due to the formation of *O*-anionic compound from the resorufin in the probe. The incremental additions of Hg^{2+} (0–1.0 µM) incited a 25-fold enhancement of the compound's fluorescence intensity. However, the addition of a dozen of cations including Ca^{2+}, Cd^{2+}, Co^{2+}, Cu^{2+}, Mg^{2+}, Mn^{2+}, Zn^{2+}, Ag^{2+}, Pb^{2+}, Fe^{3+}, Fe^{2+}, Ni^{2+} did not alter the fluorescence intensity significantly under the similar investigation conditions. The limit of detection of Probe **Hg-61** for Hg^{2+} was quantified as 0.15 µM or 30 µg/L. The potent value of Compound **Hg-61** was realised in its application to track Hg^{2+} analyte ion in the A549 cell line of a 5-day-old zebrafish and human lung adenocarcinoma epithelial origins (Fig. 53).

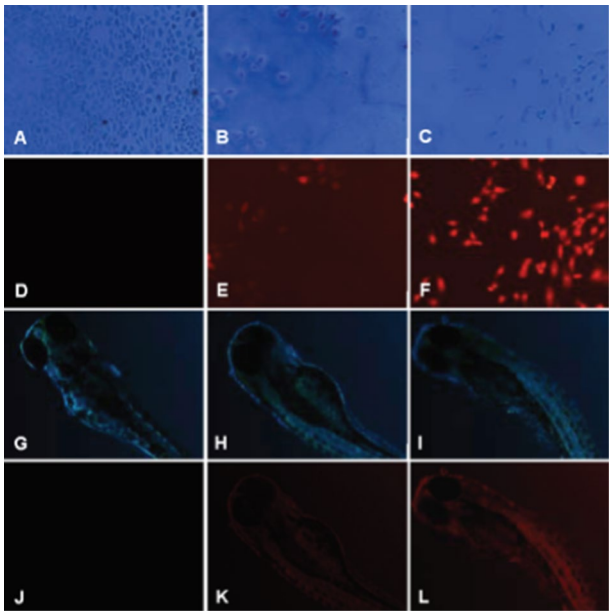

Fig. 53 Hg^{2+} fluorescence images in A549 cells and zebrafish with Probe **Hg-61**. Bright-field transmission image (AC) and fluorescence image (DF) of A549 cells pre-treated with 20, 20, and 100 µM of Probe **Hg-61** for 24 h and then incubated with 0, 10, and 50 µM of Hg^{2+} for 60 min, respectively (under green light excitation). Zebrafish bright-field transmission image (G–I) and fluorescence image (J–L) pretreated with 30, 30, and 60 µM of Probe **Hg-61** for 120 min followed by incubation with 0, 15, and 30 µM of Hg^{2+} for 30 min, respectively (under green light excitation) (Ma et al. 2012)

Small-molecule Hg^{2+} probes based on polymer-embedded fluorophore

A novel water-soluble non-conjugated fluorescent polymer dots (PDs), G-PEI PDs, synthesised by reacting polyethylenimine (PEI) and glutathione (GSH) was disclosed from Luo's laboratory in 2018 (2018). In Britton–Robinson buffer (0.04 M, pH 5.0), a selective, quenched fluorescence intensity was observed in the presence of Hg^{2+} amongst the sixteen cations, fourteen anions and natural organic matter humid acid analysed. The fluorescence titration data gave the analytical detection limit as 32 nM, meaning the probe could effectively monitor Hg^{2+} in the nanomolar concentration range. The probe displayed a linear response proportionally (0.1–100 µM) was reversible in its sensing mode and could track Hg^{2+} in river water samples.

Geng et al. reported a novel water-soluble polymer, **Hg-62** (Fig. 54), prepared from linking a poly (vinyl alcohol) (PVA) with rhodamine B hydrazide and hexamethylenediisocyanate (Geng et al. 2014). The compound was successfully employed as both colourimetric and fluorescent probe for sensitive and selective tracking of Hg^{2+} in the mutual presence of other various alkali, alkaline earth, and transition cations, viz Co^{2+}, Ag^{+}, Cd^{2+}, Ni^{2+}, Pb^{2+}, Cr^{3+}, Cu^{2+}, Fe^{3+}, K^{+}, Ba^{2+}, Mg^{2+}, Fe^{2+}, and Zn^{2+} ions in aqueous media. The pH range 5.57–11.09 was found to be the stable pH range at which the probe works most effectually. Hg^{2+} addition to Probe **Hg-62′**s solution led to a notable visual colour change (from colourless to pink) and a great amplification of Probe **Hg-62′**s fluorescence intensity (an 11-fold enhancement) compared with the metal ions that imposed almost zero effect. The sensing of the analyte ion occurred just after a short period of about 5 min after the addition of Hg^{2+}. The linear range of detection of Hg^{2+} by the synthesised compound **Hg-62** was $(0–8.0)\times10^{-5}$ mol/L and the corresponding detection limit was calculated to be 5.72×10^{-7} mol/L.

Li and the members of his team reported the sensing properties of a conjugated polymer, Probe **Hg-63** (Fig. 55), which demonstrated its ability to sequester Hg^{2+} in the midst of several other cations like Li^{+}, Ba^{2+}, Hg^{2+}, K^{+}, Na^{+}, Mg^{2+}, Pb^{2+}, Fe^{2+}, Co^{2+}, Ca^{2+}, Mn^{2+}, Fe^{3+}, Cu^{2+}, Cd^{2+}, Cr^{3+}, Ni^{2+}, Al^{3+}, and Zn^{2+} (Ding et al. 2017). Analysis of the fluorescence properties of Probe **Hg-63** in THF showed that these cations had no influence on the fluorescence of the probe except for Hg^{2+}, which showed an 11.8-fold increment. Probe **Hg-63′**s detection limit for Hg^{2+} tracking was calculated to be 1.0×10^{-6} M.

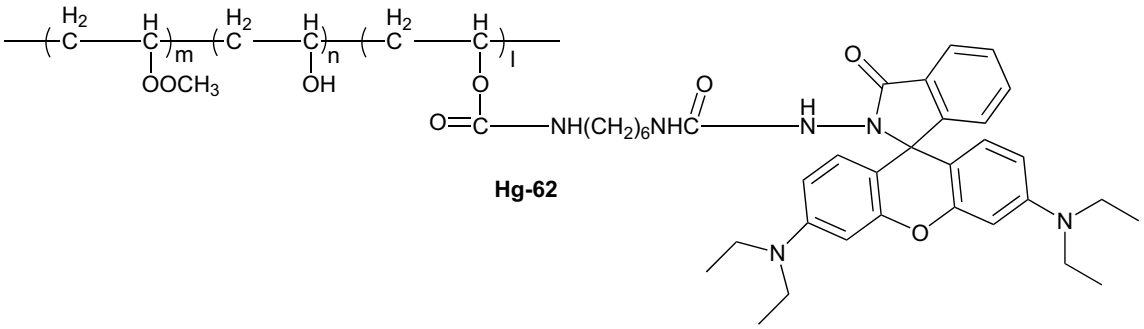

Fig. 54 Structure of Probe **Hg-62** (Geng et al. 2014)

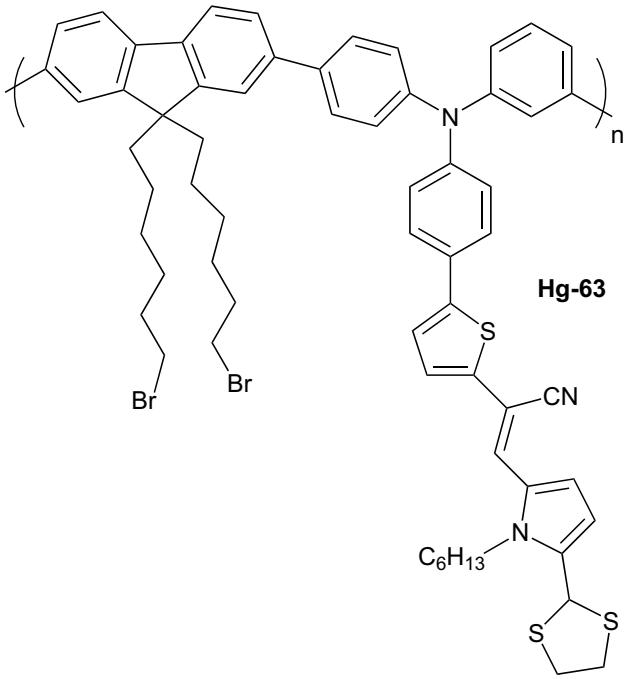

Fig. 55 Structure of Probe **Hg-63** (Ding et al. 2017)

The successful report of a conjugated polymer which took advantage of aggregation-induced emission enhancement (AIEE) for the sensing of Hg^{2+} was documented by Shan and colleagues (2018). The probe's fluorescence intensity was suppressed upon the addition of Hg^{2+} in the midst of common cations like Ag^{+}, Cr^{3+}, Al^{3+}, Fe^{3+}, Ca^{2+}, Ni^{2+}, Co^{2+}, Pb^{2+}, Cu^{2+}, Zn^{2+}, Mg^{2+}, Fe^{2+}, Mn^{2+}, Cd^{2+}, Ba^{2+}, Li^{+}, Na^{+} and K^{+}, explained as due to the strong interaction of Hg^{2+} with the thioketal groups in the probe moiety. The analytical detection limit for the sensing operation was 2.3×10^{-7} mol L^{-1}.

Hg^{2+} probes based on metal-organic frameworks (MOFs) and covalent-organic frameworks (COFs)

In 2016, Ding's group reported a novel, superb thioether-functionalised hydrazone-linked fluorescent covalent-organic framework, COF-LZU8, with superior Hg^{2+} recognition property unequalled by many other thioether-functionalised probes (Ding et al. 2016). The report of the probe was the very first instance of the application of COF in tracking and removing cations—the sensing operation took advantage of the extended π-conjugation framework which is capable of enhancing the fluorescence signal intensity. Insight into the strong interaction between the sulphur atoms of the thioether groups in the probe moiety and Hg^{2+} was furnished by X-ray photoelectron spectroscopy and solid-state NMR. Real-time fluorescence response towards various analytical cations in acetonitrile showed that the probe effectively monitored Hg^{2+} by displaying a quenched fluorescence with a corresponding colour change.

A metal-organic framework (MOF)-based probe developed from butyne-functionalised UiO-66@Butyne (UiO-66@Butyne was synthesised by reacting terephthalic acid having two side chains to generate Butyne functionalisation, BDC@butyne, and then, MOF formation was carried out in the solvothermal method with $ZrCl_4$ in *N*,*N*-dimethylformamide as the solvent) was employed as a very selective and sensitive probe for tracking Hg^{2+} (Samanta et al. 2018). The probe experienced a quenched fluorescence towards Hg^{2+} in the presence of other metal ions (Ba^{2+}, Cd^{2+}, Co^{2+}, Cu^{2+}, Zn^{2+}, Cr^{3+}, Fe^{3+}, Mg^{2+}, Mn^{2+}, Ni^{2+}, and Sr^{2+}) in an aqueous medium. None of these metal ions modulate the fluorescence intensity of the reported probe, affirming the singular response of the probe towards Hg^{2+}. This sole detection of Hg^{2+} is ascribed to the oxymercuration reaction between UiO-66@Butyne and Hg^{2+} in H_2O, leading to the formation of UiO-66@OH, which displays a comparatively lesser fluorescence than the probe. The probe effectively monitored Hg^{2+} at levels as low as 10.9 nM.

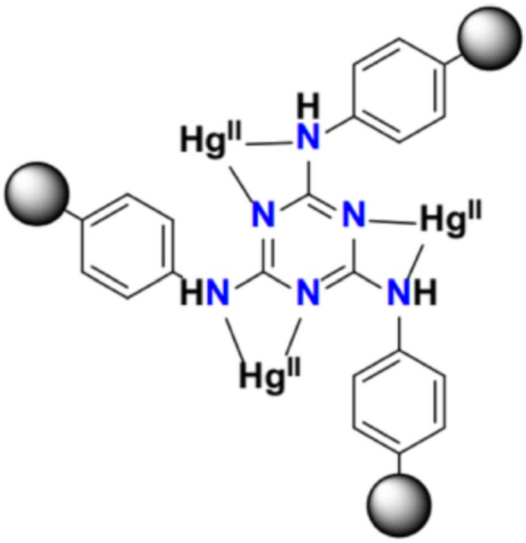

Fig. 56 Possible chelating coordination mode for the Hg^{2+} ion in **Hg-64** (Liu et al. 2018)

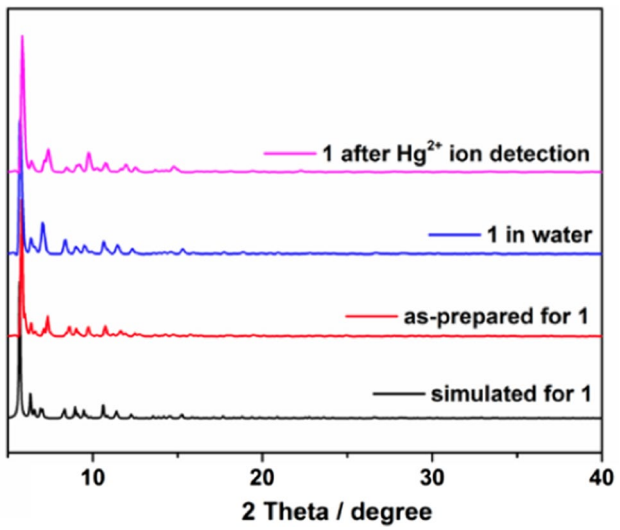

Fig. 57 Powder X-ray diffraction (PXRD) patterns of **Hg-64** (Liu et al. 2018)

A new cluster-based metal-organic framework [**Hg-64**, $(Me_2NH_2)Cd_3(OH)(H_2O)_3(TATAB)_2](DMA)_6$ (DMA = *N*,*N*-dimethylacetamide)] was synthesised for Hg^{2+} monitoring (Liu et al. 2018). As shown in Fig. 56, the probe anchors $[(Me_2NH_2)Cd_3(OH)(H_2O)_3(TATAB)_2](DMA)_6$ (DMA = *N*,*N*-dimethylacetamide) with triazine backbones and uses the 4,4′,4″-s-triazin-1,3,5-triyltri-p-aminobenzoic acid (H_3TATAB) as the organic spaces. The probe sensitively and selectively recognised Hg^{2+} in the presence of other cations in an aqueous medium (3 mL) via an 'on–off' mode and a red shift of the emission peak. Figure 57 gives the X-ray diffraction patterns, which supported the chelating interaction of the probe with Hg^{2+}.

Probe **Hg-65** (Fig. 58) was developed from metal-organic frameworks (MOF) and was favourably engaged for the monitoring of Hg^{2+} in a sensitive, selective, and reversible manner (Wu et al. 2015). The cadmium-based probe system was the first example of a ratiometric probe constructed from MOF. In the competitive environment of other cations, only Hg^{2+} led to the quenching of the probe's fluorescence; there existed only minimal interference in the sensing of Hg^{2+} by other cations under the same testing condition in an aqueous medium. Interesting was that the probe displayed a very minuscule detection limit of 2 nM.

Mercuric (II) (Hg^{2+}) Nanoprobes

The use of carbon dots (CDs) as ratiometric fluorescent probes was reported by Li's group (2019). All detection operations were done at pH = 2.5. The ratiometric fluorescence intensity at F_{414}/F_{565} exhibits broad linearity in the range of 30–60 μM. The detection limit of 60 nM was calculated with a rapid response time of 30 s obtained. Bano and co-workers reported carbon quantum dots as sensitive nanoprobes for Hg^{2+} monitoring via an 'on–off' mode (Bano et al. 2018). All detection operations were done at pH = 7 in the presence of co-existing metal ions. The detection limit of 6 nM was calculated, and the potential of the probe's real-time monitoring of Hg^{2+} in pond water samples was determined.

The excellent affinity property of thymine with Hg^{2+} was exploited in the design of novel, water-soluble, thymine-modified graphitic carbon nitride quantum dots, T-gCNQDs, which are employed as a fluorescent nanoprobe for Hg^{2+} detection (Achadu and Revaprasadu 2018). Thymine functionalisation amplified the fluorescence of the QDs, and the interaction of thymine with Hg^{2+} through the formation of a T-Hg^{2+}-T complex gives the basis for Hg^{2+} tracking. Optical detection in phosphate buffer (10 mM, pH 7.2) resulted in the dampening of the fluorescence intensity of the probe by Hg^{2+} in the joint existence of other cations (Ca^{2+}, Ni^{2+}, Cu^{2+}, Fe^{2+}, Co^{2+}, Mn^{2+}, Pb^{2+}, Al^{3+}, Na^{+}, K^{+}, Cd^{2+}, Cr^{3+}, Mg^{2+}, and Ag^{+}). Broad linearity of detection (1.0–500 nM) was observed with a detection limit of 0.15 nM calculated. The probe is applicable for Hg^{2+} monitoring in tap and pond water samples.

A colourimetric probe designed based on the Hg^{2+}-induced deprotection and morphology transition of 1-dodecanethiol ($C_{12}H_{25}SH$)-capped silver nanoprisms (Ag NPRs) in the presence of I^{-} at ambient temperature was reported by Chen et al. (2013a). The reported compound was unresponsive to pH changes in the range of 3.6–5.9. In HAc/NaAc buffer solutions (10 mM, pH 5.0), the probe detected Hg^{2+} sensitively and selectively with a magnificent 100-time

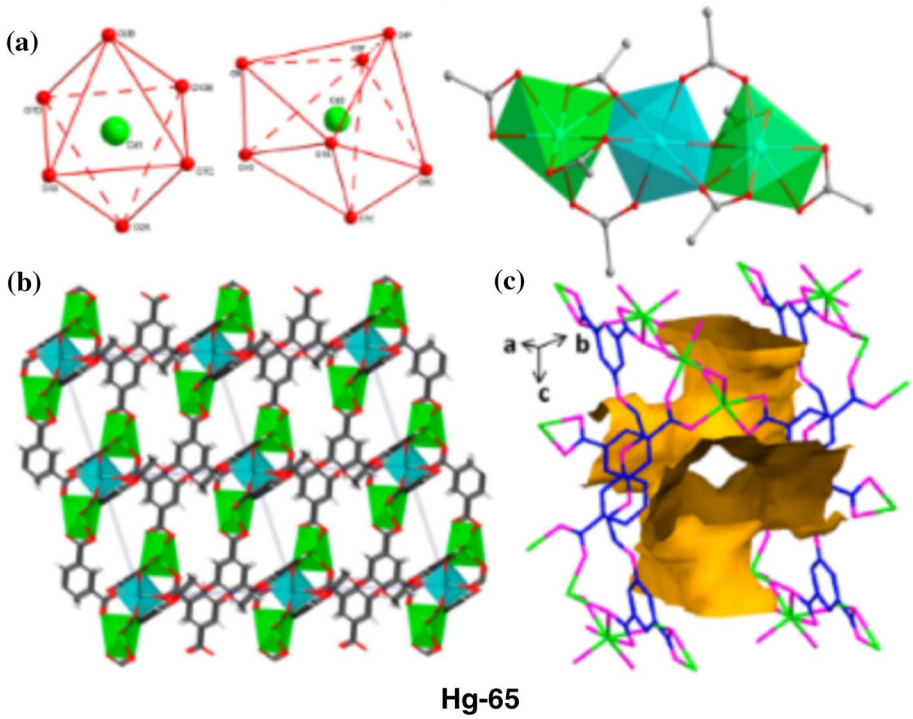

Fig. 58 Structure of MOF Probe **Hg-65** showing: **a** Cd^{2+} ions' coordination environment in **Hg-65**, whose building unit is Cd-EDDA, where EDDA = ethane-1,2-diylbis(oxy)]diisophthalic acid, **b** the crystal packing view of Hg-60 along the 'a' direction, and **c** the channel structure of **Hg-65** (Wu et al. 2015). Copyright (2015) American Chemical Society

fluorescence intensity increment ('turn on') noticed upon the addition of Hg^{2+}, whereas the addition of the other cations like Fe^{2+}, Cu^{2+}, Zn^{2+}, Mn^{2+}, Cd^{2+}, Pb^{2+}, Mg^{2+}, Ba^{2+}, Co^{2+}, and Ag^{+} induced a rather benign influence on the probe's fluorescence intensity under the same optimised testing conditions. The upward shift of the fluorescence intensity was explained as due to the presence of a strong affinity between the thiol groups in the probe molecule and Hg^{2+}. A rapid response time of 15 min (which showed stability even up to 30 min) was calculated for the detection of Hg^{2+} by the designated probe. A linear relationship between the increasing additions of Hg^{2+} to the probe's solution was proposed, and the calculated detection limit was 3.3 nM. Interestingly, the probe was employed for Hg^{2+} tracking in drinking water, tap water, and pond water samples with excellent recoveries achieved.

Huang et al. designed and synthesised a water-soluble fluorescent probe, based on fluorescence quantum dot (Mn: CdS/ZnS) functionalised 33-mer thymine-rich single-stranded DNA (strand A) and gold nanoparticles (GNPs) functionalised 10-mer single-stranded DNA (strand B), for Hg^{2+} sensing (Huang et al. 2013b). In 0.01 M PBS buffer, the initially weak fluorescence intensities of strands A and B experienced dramatic upward catapults ('turn on') upon Hg^{2+} addition (1.0 μM) in the sample solution, whilst the other cations like Mn^{2+}, Ba^{2+}, Ni^{2+}, Cu^{2+}, Ca^{2+}, Cr^{2+}, Co^{2+}, Cd^{2+}, Mg^{2+}, Zn^{2+}, Al^{3+}, Fe^{3+}, Pb^{2+}, Ag^{+}, and Au^{3+} (10 μM) left no influence on the probe's fluorescence intensity. The authors showed that the designated probe responded to Hg^{2+} detection within two linear ranges, i.e. $(0–1)\times10^{-9}$ M and 1×10^{-9} – 1×10^{-8} M. The calculated detection limit was obtained down to 0.18 nM. The probe demonstrated reversibility in its detection property, and ultimately, it was successfully applied for the tracking of Hg^{2+} both in tap and lake water samples.

Huang and co-workers constructed a simple, green fluorescent nitrogen-doped carbon nanoparticles (FNCPs)-based probe, using strawberry juice as the source of carbon (Huang et al. 2013c). The reported probe that bears both carboxylic and amino groups showed ultra-high sensitivity and selectivity for Hg^{2+} via fluorescence quenching. The linear ranges of Hg^{2+} detection fell within two broad ranges: 10–100 nM and 1–50 μM. It was shown that the monitoring of Hg^{2+} by the designed compound was complete at about 10 min. In 1 mL of phosphate solution (25 mM, pH 7.4), the addition of Hg^{2+} to the probe's solution engendered a massive quenching of the fluorescence intensity ('turn off') in the midst of 15 cations such as Ca^{2+}, Ag^{+}, Ni^{2+}, Cr^{3+}, Al^{3+}, Cu^{2+}, Ba^{2+}, Fe^{3+}, Pb^{2+}, Zn^{2+}, Fe^{2+}, Co^{2+}, Mg^{2+}, Mn^{2+}, or Cd^{2+}. Meanwhile, the other various tested cations left the fluorescence intensity unchanged. The calculated limit of detection (LOD) was 3 nM. The practical usage of the probe was demonstrated successfully as given by its efficacy to measure Hg^{2+} concentration in lake water samples.

The preparation of the water-soluble, 'green' fluorescent carbon nanoparticles (CPs)-based probe that uses sweet potatoes as the carbon source was reported by Lu et al. (2012). The probe was obtained via the hydrothermal technique and houses both hydroxyl and carboxylic or carbonyl moieties in its architectural skeleton. The employment of

the probe for the sensitive and selective monitoring of Hg^{2+} via a fluorescence dampening mode was envisaged. The best working pH range of the described probe was 1.0–7.0. The detection of Hg^{2+} traversed over two linear concentration ranges of 0.5–10 and 500–4×10^4 nM, and the calculated detection limit was 0.23 nM. It was proposed that electron or energy transfer was responsible for the quenching phenomenon of the probe's fluorescence intensity ('turn off') observed by Hg^{2+} addition in PBS (pH 7.0; $\lambda_{ex} = 360$ nm) when jointly existent with other cations such as Ag^+, Ca^{2+}, Fe^{3+}, Co^{2+}, Cd^{2+}, Cu^{2+}, Mg^{2+}, Mn^{2+}, Pb^{2+}, Ni^{2+}, and Zn^{2+}, which impinged no monumental influence on the probe's fluorescence intensity. The sensing of Hg^{2+} by the CPs probe was successfully recovered by the addition of Cys. As a proof of concept, the efficaciousness of the CPs probe for Hg^{2+} tracking in the real environmental system was successfully demonstrated in lake water samples.

Lu's group documented bovine serum albumin (BSA), assembled in a silver nanocarbon (BSA–Ag NCs), which functions as a novel ratiometric fluorescence probe for the monitoring of Hg^{2+}. Experimental results furnished excellent linearity of the fluorescence response for the tracking of Hg^{2+} within the concentration range of 0–2.5 mg mL^{-1} (Lu et al. 2013). Meanwhile, the detection limit of 4.87×10^8 M was obtained from the Benesi–Hildebrand plot analysis, a much lower value than those of ratiometric fluorescent probes of organic origins. Upon the addition of Hg^{2+}, the fluorescence intensity of the reported compound at 634 nm was reduced ('turn off'); an elevation at 480 nm with a concomitant colour variation from light yellow to colourless and a sharp red to blue fluorescence was observed. The anti-interference property of the designed Ag NC probe compound was good, implying that the monitoring of Hg^{2+} by the probe was not significantly interfered by several other cations such as Na^+, Ag^+, Ca^{2+}, Co^{2+}, Cd^{2+}, Ni^{2+}, Mg^{2+}, Pb^{2+}, Cu^{2+}, Zn^{2+}, Al^{3+}, and Fe^{3+} investigated, with the exception of Ag^+ that induced a minor disturbance.

Paramanik et al. designed an Au nanocluster–CdTe quantum dots nanocomposite probe, utilised for the recognition of Hg^{2+} (Paramanik et al. 2013). Desirably, the addition of cations like Co^{2+}, Fe^{3+}, Mg^{2+}, Mn^{2+}, Ni^{2+}, Pb^{2+}, Sr^{2+}, Zn^{2+}, Cd^{2+}, Ca^{2+}, and Cu^{2+} did not leave any meaningful impact on the fluorescence intensity of the reported probe, except for Hg^{2+} that quenched the fluorescence dramatically ('turn off') (about 74%-fold) at 553 nm. Although Cu^{2+} impinged a 26% quenching of the probe's fluorescence, the effect was rather insignificant compared to that posed by Hg^{2+}. The calculated detection limit of Hg^{2+} recognition by the probe is 9 nM.

Singh et al. constructed a new Biginelli-based organic nanoparticle-based compound (Singh et al. 2013). The designated molecule, Probe **Hg-66** (Fig. 59), which employs both a conformational change and an intramolecular charge-transfer process, was used as a fluorescent probe for the sensitive and selective monitoring of Hg^{2+} in an aqueous medium. In Tris buffer (pH = 7.4, 1 mM) solution, the sequential addition of Hg^{2+} to the solution of the probe suppressed its fluorescence intensity massively ('turn off') in the co-presence of other rival cations investigated. The limit of detection was obtained down to 1 nM. The response time for Hg^{2+} detection by the probe was 3 min.

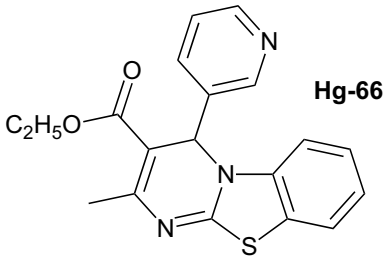

Fig. 59 Structure of Biginelli-based organic nanoparticle-based Probe **Hg-66** (Singh et al. 2013)

The usage of mercury-specific DNA (MSD-DNA)-functionalised gold nanoparticles (AuNPs), as probe for Hg^{2+} tracking was described by Tan's group (Tan et al. 2013). The concentration range of Hg^{2+} detection by these probe molecules was determined to be 0.02–1.0 μM. Experimental results revealed a lowering of the fluorescence intensity of the probe ('turn off') upon the incremental addition of Hg^{2+} in the presence of other cations (including Co^{2+}, Fe^{3+}, Mn^{2+}, Ca^{2+}, Mg^{2+}, Cr^{3+}, Cu^{2+}, Ni^{2+}, and Pb^{2+}) assessed. The sensing experiments furnished the limit of detection of as 16 nM. Noteworthy is that the monitoring of Hg^{2+} in actual river water samples was realised by the synthesised AuNPs–MSD-based probe.

Inspired by a time-gated fluorescence resonance energy transfer (TGFRET) detection technique, Huang and his team members again attained the fluorescence detection of Hg^{2+} by employing water-soluble ssDNA functionalised quantum dots (which constituted the energy-transfer donor unit) and gold nanoparticles (which served as the energy-transfer acceptor moiety) (Huang et al. 2013a). The analysis of the experimental results showed that there was a significant quenching of the reported compound's fluorescence intensity ('turn off') in a linear fashion (i.e. 1×10^{-9}–1×10^{-8} M) upon the addition of varying Hg^{2+} concentrations. By contrast, the addition of various investigated cations left an insignificant effect on the fluorescence intensity of the compound. Moreover, a suitably low detection limit of 0.49 nM or 0.1 ppb was obtained. Desirably, the compound was shown to successfully track Hg^{2+} in tap water, river, and lake water samples with excellent results achieved.

Via a hydrothermal treatment, Li et al. developed water-soluble nitrogen-doped carbon quantum dots (N-CQDs) for

the detection of Hg^{2+} through selective and sensitive fluorescence dampening approach (Li et al. 2015). The fluorescence intensities of the developed N-CQDs experienced stability in the broad pH range of 4.0–10.0. N-CQDs' fluorescence was invariably unperturbed upon the addition of other cations of seventeen different kinds, except for a large fluorescence suppression caused by Hg^{2+} ('turn off'). The linear concentration range of Hg^{2+} detection was from 10 nM–20 mM, with a detection limit of 8.60 nM or 1.72 ppb estimated. The probe's lost fluorescence intensity was regained (about 79-fold regeneration) after I^- was added in the presence of ten other different anions. This result demonstrated the ability of the probes to also monitor I^- within a linear detection range of 0.50 mM– 40 mM or 63.50–5080 mg L^{-1} observed with a detection limit of 0.354 mM or 45.0 mg L^{-1} calculated.

Li and his research group gave an account of a water-soluble graphene oxide (GO) probe, functionalised with single-stranded DNA aptamer, and employed for a label-free Hg^{2+} tracking via a fluorescence quenching phenomenon (Li et al. 2013). In PBS solution (10 mM Na_2HPO_4/NaH_2PO_4, 0.3 M NaCl, 0.1 mM ethylenediamine, pH = 7.0), the probe's initially strong fluorescence intensity at 488 nm excitation wavelength was largely and concomitantly suppressed ('turn off') upon the addition of Hg^{2+} when several cations like Ag^+, K^+, Cd^{2+}, Ca^{2+}, Cu^{2+}, Ni^{2+}, Pb^{2+}, Co^{2+}, and Fe^{3+} were present. The linear tracking range of the probe was noted to be from 1 nM–50 nM, and the quenching phenomenon was observed to lapse only for *ca.* 5 min. The estimated detection limit was sufficiently low down to 0.92 nM or 0.18 ppb.

The works of Zhang et al. (2015b) described a sensitive, fluorometric labelled ss-DNA for tracking Hg^{2+}. The fluorescence increment in the developed bioassay was induced by graphene oxide (GO) and exonuclease (exo) III. The detection limit and response time of the assay were calculated to be 0.1 nM and 8 min, respectively. Mediated by Hg^{2+}, there was a formation of a well-folded dsDNA by the FAM-labelled ssDNA which became digested by Exo III, leading to the release of FAM-labelled mononucleotide and Hg^{2+}. The FAM-labelled mononucleotide was not accumulated onto the GO surface, resulting in increased fluorescence intensity. The released Hg^{2+} then induced a new cycle of this whole process. In this way, a minuscule quantity of Hg^{2+} can engender a plethora of enzyme digestion reactions and form a massively amplified fluorescence signal. The assay could excellently monitor Hg^{2+} in lake water samples.

For a collection of other nanomaterial-based probes developed for Hg^{2+} monitoring, readers are referred to the brilliant review article by Duan and Zhan (2015).

Other sterling instances of the report of fluorescent, colourimetric, and/or ratiometric probes for Hg^{2+} monitoring exist in the literature, but owing to space limitation, these are reserved for the author's future review assignments.

Important generalisations

From the foregoing careful discussion on various kinds of fluorescent, colourimetric, and/or ratiometric Hg^{2+}-selective probes developed from diverse fluorophore motifs, these important generalisations are made:

- Probes such as Probes **Hg-1**, **Hg-7**, **Hg-8**, and **Hg-13** appended with solubilising groups like the amino group, $–NH_2$, tend to be more soluble in water than those without this functionality. Moreover, amino group-appended probes possess enhanced quantum yield than their counterparts without this functional group.
- For ages, there has been a heavy reliance on the use of nitrogen-centric motifs for the construction of Hg^{2+} probes, but the need for nitrogen coordination for signalling processes usually encounters some inadequacies. Besides an exclusive reliance on nitrogen coordination chemistry, there is always a possibility of false-positive signalling owing to protonation or pH sensitivity. This limitation has been largely tackled by a research focus shifting towards the employment of sulphur-incorporating groups, although this also is not without its restraints.
- Hg^{2+} being a soft Lewis acid and equally possessing a strong thiophilic affinity has prompted many reported Hg^{2+}-selective probes typically to employ sulphur as a soft donor atom to facilitate a tight binding to the metal as part of the fluorescence probe architectures. Reported probes that employ this strategy include Probes **Hg-4**, **Hg-6**, **Hg-7**, to mention a few. Only a few probes for Hg^{2+} based on alkynes have been developed according to the π electrophilicity of Hg^{2+}. Furthermore, their signalling modes are due to the irreversible chemical reactions of alkynes as opposed to reversible interactions. This impedes their practical applications. As a basic requirement, ideal probes should possess a reversibility property (Dong et al. 2017).
- Most longstanding strategies employed for the design of Hg^{2+}-selective probes are based on the complexation or chemical reaction between the probes and Hg^{2+}. The reaction-based design includes Hg^{2+}-induced desulphurisation and desulphurisation which ensues in cyclisation to the heterocycle, mercuration, and Hg^{2+}-promoted hydrolysis reactions. Comprised in the latter category is a typical reaction-based strategy tagged 'Hg^{2+}-promoted deprotection of thioacetals' which has been taken advantage of to generate a host of probes. Reported probes which makes use of this design strategy include Probes **Hg-14, Hg-15, Hg-21–Hg-25, Hg-53, Hg-57**, **Hg-58**, etc.
- There is increasing gravitation towards the use of red to near-infrared (NIR) probes (which possess > 600 nm) owing to their merits of profound tissue penetration,

reduced photodamage to biological models and lowered interference ensuing from background autofluorescence of biomolecules in living systems. This is particularly relevant to the construction of rhodamine probes since the absorption and emission wavelengths of most rhodamine derivatives are < 600 nm, placing a restraint on their biological applications. Instances of NIR probes reported in this review include the case of Probe **Hg-32**.

- Probes, such as Probes **Hg-9**, **Hg-32**, **Hg-48**, **Hg-56**, **Hg-65**, and others that make use of ratiometric fluorescence signalling mode are more desirable and gaining increasing research attention than those with a single fluorescence response wavelength. Basically, ratiometric probes operate by making use of the ratio of the emission intensity at two different wavelengths. Ratiometric detection strategy eradicates uncertainties mostly due to environmental conditions like polarity, pH, temperature, and non-homogeneity of distribution of fluorescent indicators in cells. Sterling instances of such probes include the squaraines-based probes which possess long excitation and emission wavelengths (have sharp absorption around *ca.* 640 nm).
- Inorganic quantum dots are gaining grounds as alternative fluorophores due to their good photobleaching anti-resistance and possession of high quantum yields and wide light-absorption band. Unfortunately, inorganic quantum dots typically contain Se, Cd, Pb, or other toxic elements (Das and Tan 2008). Carbon QDs have replaced inorganic QDs as the former possess greater photostability and reduced toxicity. Recently, graphene oxide (GO), which contains carbon (being environmental-friendly, earth-abundant, and inexpensive), has emerged as a new fluorophore because of its good water solubility, strong photoluminescence, great mechanical strength, facile surface alteration, and the ability for bio-conjugation.
- A rapid response time is highly essential for either an on-site or online field monitoring. Good response times have been achieved by many of the reported probes, including Probes **Hg-10**, **Hg-13**, **Hg-14**, **Hg-15**, **Hg-16**, **Hg-32**, **Hg-41**, **Hg-61**, etc.
- In all analytical detection sense, fluorescence 'turn on' probes are more sought after than their fluorescence 'turn off' counterparts since the former usually display lower background and higher sensitivity than the latter (Wang et al. 2013).

Conclusions

In this review, fluorescent, colourimetric, and/or ratiometric probes based on the molecular motifs of synthetic small organic molecules, supramolecules, polymers, metal-organic frameworks, covalent-organic frameworks, and nanoparticles have been discussed in the context of the detection of mercuric (II) (Hg^{2+}), giving recent updates within the timeframe of 2011–2019. Probes that exhibit fluorescence or colourimetric variation in response to various analytes are preferable to other types of probes, as they emit easily recognisable optical response by fluorimeters or simply by naked eyes. The main features highlighted in the reported probes in this review were the parameters of the most suitable solvent system, optimum pH value/range, interference property, detection limit, and association constant. The environmental and/or biological utilities of these probes are also discussed wherever possible. Even though research works on the detection of Hg^{2+} have been very successful thus far, there still exist a couple of lingering obstacles which need tackling for the achievement of further advancements in the science of Hg^{2+} detection.

Presently, specific instances of Hg^{2+}-selective probes that possess the simultaneous qualities of supersensitivity and selectivity, rapid response time, convenience of preparation, low toxicity, and above all, water solubility are rare. Meanwhile, many organic probes require laborious synthetic methods, whilst probes based on quantum dots (QDs) exhibit toxicity. Besides, a large proportion of these probes possess very short fluorescence lifetime and utilise visible light emission which cannot be used in in vivo sensing. Other challenges are irreversible Hg^{2+} complexation, poor selectivity, and long response time. Perhaps the greater challenge, now, is the difficulty in designing and synthesising probes that could overcome all these challenges.

The spin–orbit coupling which induces a 'heavy atom' effect makes Hg^{2+} intrinsically a quencher of fluorescence. This phenomenon, within the convention of sole diagnostic monitoring of Hg^{2+}, is undesirable owing to the reason that some other heavy cations like Cu^{2+}, Pb^{2+}, Cd^{2+}, and Ag^{+} can also induce similar effect, interfering with the detection of Hg^{2+} and thereby leading to confusing observation and interpretation of experimental phenomena and results. As such, more 'turn on', interference-free Hg^{2+}-selective probes should be developed (as opposed to the diverse 'turn off' ones that exist in several bodies of literature) by researchers in this field.

If only these considerations would be favourably addressed, more and better Hg^{2+}-selective probes would be designed, developed, and reported from various labs from across the world, with the possibility that the future of Hg^{2+} detection would brighter than it is now.

Acknowledgements The author highly appreciates the reviewers for their valuable comments which were used to improve the manuscript significantly. The author's heart goes with everyone during this period of the outbreak of the coronavirus disease (COVID-19) pandemic that brought the whole world to its knees.

References

Abdelhamid HN, Wu H (2015) Reduced graphene oxide conjugate thymine as a new probe for ultrasensitive and selective fluorometric determination of mercury (II) ions. Microchim Acta 182(9–10):1609–1617. https://doi.org/10.1007/s00604-015-1461-4

Achadu OJ, Revaprasadu N (2018) Microwave-assisted synthesis of thymine-functionalized graphitic carbon nitride quantum dots as a fluorescent nanoprobe for mercury(II). Microchim Acta 185:461. https://doi.org/10.1007/s00604-018-3004-2

Aderinto SO, Imhanria S (2018) Fluorescent and colourimetric 1, 8-naphthalimide-appended chemosensors for the tracking of metal ions: selected examples from the year 2010 to 2017. Chem Papers 72:1823–1851. https://doi.org/10.1007/s11696-018-0411-0

Aderinto SO, Zhang H, Wu H, Chen C, Zhang J, Peng H, Yang Z, Wang F (2016) Synthesis and studies of two proton–receptor fluorescent probes based on 1,8-naphthalimide. Color Technol 133:40–49. https://doi.org/10.1111/cote.12250

Allendorf MD, Bauer CA, Bhaktaa RK, Houk RJT (2009) Luminescent metal–organic frameworks. Chem Soc Rev 38:1330–1352. https://doi.org/10.1039/b802352m

Ando S, Koide K (2011) Development and applications of fluorogenic probes for mercury (II) based on vinyl ether oxymercuration. J Am Chem Soc 133(8):2556–2566. https://doi.org/10.1021/ja108028m

Arbeloa IL, Ojeda PR (1981) Molecular forms of rhodamine B. Chem Phys Lett 79(2):347–350. https://doi.org/10.1016/0009-2614(81)80219-9

Arivazhagan C, Borthakur R, Ghosh S (2015) Ferrocene and triazole-appended rhodamine based multisignaling sensors for Hg^{2+} and their application in live cell imaging. Organometallics 34(7):1147–1155. https://doi.org/10.1021/om500948c

Arya SK, Bhansali S (2011) Lung cancer and its early detection using biomarker-based biosensors. Chem Rev 111:6783–6809. https://doi.org/10.1021/cr100420s

Athey PS, Kiefer GE (2002) A new, facile synthesis of 1,4,7,10-tetraazacyclododecane: cyclen. J Org Chem 67:4081–4085. https://doi.org/10.1021/jo016111d

Baeyer A (1871) Ueber eine neue Klasse von Farbstoffen. Ber Dtsch Chem Ges 4:555–558. https://doi.org/10.1002/cber.18710040209

Bano D, Kumar V, Singh VK, Hasan SH (2018) Green synthesis of fluorescent carbon quantum dots for the detection of mercury(II) and glutathione. New J Chem 42:5814–5821. https://doi.org/10.1039/C8NJ00432C

Bhalla V, Kumar RM, Sharma PR, Kaur T (2012) New Fluorogenic sensors for Hg^{2+} ions: through-bond energy transfer from pentaquinone to rhodamine. Inorg Chem 51:2150–2156. https://doi.org/10.1021/ic201990q

Bicker KL, Wiskur SL, Lavigne JJ (2011) Chemosensors: principles, strategies, and applications. In: Wang B, Anslyn BE (eds) Chemosensors: principles, strategies, and applications. Wiley, New York, pp 275–295

Bigdeli A, Ghasemi F, Moayed SA, Shahrajabiana M, Fahimi-Kashani N, Jafarinejad S, Nejad MAF, Hormozi-Nezhad MR (2019) Ratiometric fluorescent nanoprobes for visual detection: design principles and recent advances—a review. Anal Chim Acta 1079(4):30–58. https://doi.org/10.1016/j.aca.2019.06.035

Bravo AG, Cosio C, Amouroux D, Zopfi J, Chevalley PA, Spangenberg JE, Ungureanu V-G, Dominik J (2014) Extremely elevated methyl mercury levels in water, sediment and organisms in a Romanian reservoir affected by release of mercury from a chlor-alkali plant. Water Res 49:391–405. https://doi.org/10.1016/j.watres.2013.10.024

Carocci A, Rovito N, Sinicropi MS, Genchi G (2013) Mercury toxicity and neurodegenerative effects. Rev Environ Contam Toxicol 229:1–18. https://doi.org/10.1007/978-3-319-03777-6_1

Carter KP, Young AM, Palmer AE (2014) Fluorescent sensors for measuring metal ions in living systems. Chem Rev 114:4564–4601. https://doi.org/10.1021/cr400546e

Ceresole M (1888) Production of new red coloring-matter. US Patent 377:349

Chan J, Dodani SC, Chang CJ (2012) Reaction-based small-molecule fluorescent probes for chemoselective bioimaging. Nat Chem 4:973–984. https://doi.org/10.1038/nchem.1500

Choi MG, Kim YH, Namgoong JE, Chang SK (2009) Hg^{2+}-selective chromogenic and fluorogenic chemodosimeter based on thiocoumarins. Chem Commun. https://doi.org/10.1039/B905612B

Chen L, Park SJ, Wu D, Kim HM, Yoon J (2019) A two-photon fluorescent probe for colorimetric and ratiometric monitoring of mercury in live cells and tissues. Chem Comm 55:1766–1769. https://doi.org/10.1039/c8cc08608g

Cheng H-B, Li Z, Huang Y-D, Liu L, Wu H-C (2017) Pillararene-based aggregation-induced-emission-active supramolecular system for simultaneous detection and removal of mercury(II) in water. ACS Appl Mater Interfaces 9:11889–11894. https://doi.org/10.1021/acsami.7b00363

Chen G, Guo Z, Zeng G, Tang L (2015) Fluorescent and colorimetric sensors for environmental mercury detection. Analyst 140:5400–5443. https://doi.org/10.1039/C5AN00389J

Chen L, Fu X, Lu W, Chen L (2013a) Highly sensitive and selective colorimetric sensing of Hg^{2+} based on the morphology transition of silver nanoprisms. ACS Appl Mater Interfaces 5(2):284–290. https://doi.org/10.1021/am3020857

Chen X, Meng X, Wang S, Cai Y, Wu Y, Feng Y, Zhu M, Guo Q (2013b) A rhodamine-based fluorescent probe for detecting Hg^{2+} in a fully aqueous environment. Dalton Trans 42:14819–14825. https://doi.org/10.1039/C3DT51279G

Chen X, Pradhan T, Wang F, Kim JS, Yoon J (2012) Fluorescent chemosensors based on spiroring-opening of xanthenes and related derivatives. Chem Rev 112:1910–1956. https://doi.org/10.1021/cr200201z

Chen X, Tian X, Shin I, Yoon J (2011) Fluorescent and luminescent probes for detection of reactive oxygen and nitrogen species. Chem Soc Rev 40:4783–4804. https://doi.org/10.1039/C1CS15037E

Chu KH, Zhou Y, Fang Y, Wang LH, Li JY, Yao C (2013) Rhodamine–pyrene conjugated chemosensors for ratiometric detection of Hg^{2+} ions: Different sensing behavior between a spirolactone and a spirothiolactone. Dyes Pigm 98:339–434. https://doi.org/10.1016/j.dyepig.2013.02.019

Clegg RM (1996) Fluorescence resonance energy transfer. In: Wang XF, Herman B (eds) Fluorescence imaging spectroscopy and microscopy, vol 137. Wiley, New York, pp 179–251

Coronado E, Galan-Mascaros JR, Marti-Gastaldo C, Palomares E, Durrant JR, Vilar R, Gratzel M, Nazeeruddin MdK (2005) Reversible colorimetric probes for mercury sensing. J Am Chem Soc 127(35):12351–12356. https://doi.org/10.1021/ja0517724

Costa FN, Korn MGA, Brito GB, Ferlin S, Fostier AH (2016) Preliminary results of mercury levels in raw and cooked seafood and their public health impact. Food Chem 192:837–841. https://doi.org/10.1016/j.foodchem.2015.07.081

Das GK, Tan TTY (2008) Rare-earth-doped and codoped Y_2O_3 nanomaterials as potential bioimaging probes. J Phys Chem C 112:11211–11217. https://doi.org/10.1021/jp802076n

Dilek G, Akkaya EU (2000) Novel squaraine signalling Zn(II) ions: three-state fluorescence response to a single input. Tetrahedron Lett 41:3721–3724. https://doi.org/10.1016/S0040-4039(00)00474-3

Ding J, Li H, Wang C, Yang J, Xie Y, Peng Q, Li Q, Li Z (2015) "Turn-on" fluorescent probe for mercury (II): high selectivity and sensitivity and new design approach by the adjustment of the π-bridge. ACS Appl Mater Interfaces 7(21):11369–11376. https://doi.org/10.1021/acsami.5b01800

Ding S-Y, Dong M, Wang Y-W, Chen Y-T, Wang H-Z, Su C-Y, Wang W (2016) Thioether-based fluorescent covalent organic framework for selective detection and facile removal of Mercury(II). J Am Chem Soc 138:3031–3037. https://doi.org/10.1021/jacs.5b10754

Ding J, Li H, Xie Y, Peng Q, Li Q, Li Z (2017) Reaction-based conjugated polymer fluorescent probe for mercury (II): good sensing performance with "turn-on" signal output. Polym Chem 8:2221–2226. https://doi.org/10.1039/C7PY00035A

Dong WK, Akogun SF, Zhang Y, Sun YX, Dong XY (2017) A reversible "turn-on" fluorescent sensor for selective detection of Zn^{2+}. Sens Actuators 238:723–734. https://doi.org/10.1016/j.snb.2016.07.047

dos Remedios CG, Miki M, Barden JA (1987) Fluorescence resonance energy transfer measurements of distances in actin and myosin: a critical evaluation. J Muscle Res Cell Motil 8(2):97–117. https://doi.org/10.1007/BF01753986

Duan J, Zhan J (2015) Recent developments on nanomaterials-based optical sensors for Hg^{2+} detection. Sci China Mater 58:223–240. https://doi.org/10.1007/s40843-015-0031-8

Duke RM, Veale EB, Pfeffer FM, Kruger PE, Gunnlaugsson T (2010) Colorimetric and fluorescent anion sensors: an overview of recent developments in the use of 1, 8-naphthalimide-based chemosensors. Chem Soc Rev 39:3936–3953. https://doi.org/10.1039/B910560N

Durand J, Kojic L, Wang Y, Lee P, Cynader MS, Gu Q (2000) Confocal imaging of N-methyl-D-aspartate receptors in living cortical neurons. Neuroscience 97(1):11–23. https://doi.org/10.1016/S0306-4522(99)00595-3

Egawa T, Koide Y, Hanaoka K, Komatsu T, Terai T, Nagano T (2011) Development of a fluorescein analogue, Tokyo Magenta, as a novel scaffold for fluorescence probes in red region. Chem Commun 47:4162–4164. https://doi.org/10.1039/C1CC00078K

Fan J, Chen C, Lin Q, Fu N (2012) A fluorescent probe for the dual-channel detection of Hg^{2+}/Ag^{+} and its Hg^{2+}-based complex for detection of mercapto biomolecules with a tunable measuring range. Sens Actuators B Chem 173:874–881. https://doi.org/10.1016/j.snb.2012.08.004

Fang Y, Zhou Y, Li J, Rui Q, Yao C (2015) Naphthalimide-Rhodamine based chemosensors for colorimetric and fluorescent sensing Hg^{2+} through different signaling mechanisms in corresponding solvent systems. Sens Actuators B Chem 215:350–359. https://doi.org/10.1016/j.snb.2015.03.080

Feng X, Ding X, Jiang D (2012) Covalent organic frameworks. Chem Soc Rev 41:6010–6022. https://doi.org/10.1039/c2cs35157a

Förster T (1965) Delocalized excitation and excitation transfer. In: Sinanoglu O (ed) Modern quantum chemistry, vol 3. Academic Press Incorporated, New York, pp 93–137

Freeman R, Finder T, Willner I (2009) Multiplexed analysis of Hg^{2+} and Ag^{+} ions by nucleic acid functionalized CdSe/ZnS quantum dots and their use for logic gate operations. Angew Chem Int Ed 48:7818–7821. https://doi.org/10.1002/anie.200902395

Frisbie SH, Mitchell EJ, Sarkar B (2015) Urgent need to reevaluate the latest World Health Organization guidelines for toxic inorganic substances in drinking water. Environ Health 14:63. https://doi.org/10.1186/s12940-015-0050-7

Gao B, Gong W-T, Zhang Q-L, Ye J-W, Ning G-L (2012) A selective "turn-on" fluorescent sensor for Hg^{2+} based on "reactive" 7-hydroxycoumarin compound. Sens Actuators B Chem 162:391–395. https://doi.org/10.1016/j.snb.2011.12.060

Geng T-M, Wang Y, Huang R-Y (2014) Fluorescence sensors for selective detection of Hg^{2+} Ion using a water-soluble poly(vinyl alcohol) bearing rhodamine B moieties. J Fluoresc 24:1207–1213. https://doi.org/10.1007/s10895-014-1402-3

Georgiev NI, Bojinov VB, Nikolov PS (2011) The design, synthesis and photophysical properties of two novel 1, 8-naphthalimide fluorescent pH sensors based on PET and ICT. Dyes Pigm 88:350–357. https://doi.org/10.1016/j.dyepig.2010.08.004

Ghasemi F, Hormozi-Nezhad MR, Mahmoudi M (2018) A new strategy to design colorful ratiometric probes and its application to fluorescent detection of Hg (II). Sens Actuators B 259:894–899. https://doi.org/10.1016/j.snb.2017.12.141

Gibb H, Oleary KG (2014) Mercury exposure and health impacts among individuals in the artisanal and small-scale gold mining community: a comprehensive review. Environ Health Perspect 122:667–672. https://doi.org/10.1289/ehp.1307864

Gierczyk, B. (2013). NMR Studies of Crown Ether–Cyclodextrin Complexes. In: Annual reports on NMR spectroscopy, vol 80, pp 1–31. Academic Presshttps://doi.org/10.1016/B978-0-12-408097-3.00001-9

Gong Y-J, Zhang X-B, Chen Z, Yuan Y, Jin Z, Mei L, Zhang J, Tan W, Shen G-L, Yu R-Q (2012) An efficient rhodamine thiospirolactam-based fluorescent probe for detection of Hg^{2+} in aqueous samples. Analyst 137:932–938. https://doi.org/10.1039/C2AN15935J

Grynkiewicz G, Poenie M, Tsien RY (1985) A new generation of Ca^{2+} indicators with greatly improved fluorescence properties. J Biol Chem 260:3440–3450

Gu B, Huang L, Mi N, Yin P, Zhang Y, Tu X, Luo X, Luo S, Yao S, (2015) An ESIPT-based fluorescent probe for highly selective and ratiometric detection of mercury (II) in solution and in cells. Analyst 140:2778–2784. https://doi.org/10.1039/C5AN00273G

Gunnlaugsson T, Glynn M, Tocci GM, Kruger PE, Pfeffer FM (2006) Anion recognition and sensing in organic and aqueous media using luminescent and colorimetric sensors. Coord Chem Rev 250:3094–3117. https://doi.org/10.1016/j.ccr.2006.08.017

Guo H, Aleyasin H, Dickinson BC, Haskew-Layton RE, Ratan RR (2014) Recent advances in hydrogen peroxide imaging for biological applications. Cell Biosci 4:64. https://doi.org/10.1186/2045-3701-4-64

Guo W, Yuan J, Wang E (2009) Oligonucleotide-stabilized Ag nanoclusters as novel fluorescence probes for the highly selective and sensitive detection of the Hg^{2+} ion. Chem Commun. https://doi.org/10.1039/B821518A

Guo Y, An J, Tang H, Peng M, Suzenet F (2015) Selective and "turn-off" fluorimetric detection of mercury (II) based on coumarinyldithiolane and coumarinyldithiane in aqueous solution. Mater Res Bull 63:155–163. https://doi.org/10.1016/j.materresbull.2014.12.015

Gupta A, Kumar N (2016) A review of mechanisms for fluorescent ''turn-on'' probes to detect Al^{3+} ions. RSC Adv 6:106413–106434. https://doi.org/10.1039/C6RA23682K

Haugland R P, Kang H C (1998) U.S. Patent 4(774):339

Herschel Sir JFW (1845) On a case of superficial colour presented by a homogeneous liquid internally colorless. Phil Trans R Soc London 135:143–145. https://doi.org/10.1098/rspl.1843.0039

Hoyle I, Handy RD (2005) Dose-dependent inorganic mercury absorption by isolated perfused intestine of rainbow trout, *Oncorhynchus mykiss*, involves both amiloride-sensitive and energy-dependent pathways. Aquat Toxicol 72:147–159. https://doi.org/10.1016/j.aquatox.2004.11.015

Hu JH, Li JB, Qi J, Chen JJ (2015) Highly selective and effective mercury (II) fluorescent sensors. New J Chem 39:843–848. https://doi.org/10.1039/C4NJ01147C

Hu Z-Q, Zhuang W-M, Li M, Liu M-D, Wen L-R, Li C-X (2013) Highly sensitive and selective turn-on fluorescent chemodosimeter for Hg^{2+} based on thiorhodamine 6G-amide and its

applications for biological imaging. Dyes Pigm 98:286–289. https://doi.org/10.1016/j.dyepig.2013.03.002
Huang D, Niu C, Ruan M, Wang X, Zeng G, Deng C (2013a) Highly sensitive strategy for Hg^{2+} detection in environmental water samples using long lifetime fluorescence quantum dots and gold nanoparticles. Environ Sci Technol 47:4392–4398. https://doi.org/10.1021/es302967n
Huang D, Niu C, Wang X, Lv X, Zeng G (2013b) "Turn-On" fluorescent sensor for Hg^{2+} based on single-stranded DNA functionalized Mn:CdS/ZnS quantum dots and gold nanoparticles by time-gated mode. Anal Chem 85(2):1164–1170. https://doi.org/10.1021/ac303084d
Huang H, Lv J-J, Zhou D-L, Bao N, Xu Y, Wang A-J, Feng J-J (2013c) One-pot green synthesis of nitrogen-doped carbon nanoparticles as fluorescent probes for mercury ions. RSC Adv 3:21691–21696. https://doi.org/10.1039/C3RA43452D
Jia Y, Li J (2015) Molecular assembly of Schiff base interactions: construction and application. Chem Rev 115(3):1597–1621. https://doi.org/10.1021/cr400559g
James SL (2003) Metal-organic frameworks. Chem Soc Rev 32:276–288. https://doi.org/10.1039/b200393g
Jones LJ, Upson RH, Haugland RP, Panchuk-Voloshina N, Zhou M, Haugland RP (1997) Quenched BODIPY dye-labeled casein substrates for the assay of protease activity by direct fluorescence measurement. Anal Biochem 251(2):144–152. https://doi.org/10.1006/abio.1997.2259
Kappe T (1994) The early history of calixarene chemistry. J Incl Phenom Mol Recognit Chem 19:3–15
Kaur A, Kolanowski JL, New EJ (2016) Reversible fluorescent probes for biological redox states. Angew Chem 55(5):1602–1613. https://doi.org/10.1002/anie.201506353
Kaura N, Kumar S (2011) Colorimetric metal ion sensors. Tetrahedron 67(48):9233–9264. https://doi.org/10.1016/j.tet.2011.09.003
Keller RCA, Silvius JR, De Kruijff B (1995) Characterization of the resonance energy transfer couple coumarin-BODIPY and its possible applications in protein-lipid research. Biochem Biophys Res Commun 207:508–514. https://doi.org/10.1006/bbrc.1995.1217
Kim HM, Cho BR (2015) Small-molecule two-photon probes for bioimaging applications. Chem Rev 115(11):5014–5055. https://doi.org/10.1021/cr5004425
Kim HN, Guo Z, Zhu W, Yoon J, Tian H (2011) Recent progress on polymer-based fluorescent and colorimetric chemosensors. Chem Soc Rev 40:79–93. https://doi.org/10.1039/C0CS00058B
Kim HN, Lee MH, Kim HJ, Kim JS, Yoon J (2008) A new trend in rhodamine-based chemosensors: application of spirolactam ring-opening to sensing ions. Chem Soc Rev 37:1465–1472. https://doi.org/10.1039/B802497A
Kim HN, Ren WX, Kim JS, Yoon J (2012) Fluorescent and colorimetric sensors for detection of lead, cadmium, and mercury ions. Chem Soc Rev 41:3210–3244. https://doi.org/10.1039/C1CS15245A
Kim HM, Cho BR (2009) Two-photon probes for intracellular free metal ions, acidic vesicles, and lipid rafts in live tissues. Acc Chem Res 42:863–872. https://doi.org/10.1021/ar800185u
Kim PKM, Zamora R, Petrosko P, Billiar TR (2001) The regulatory role of nitric oxide in apoptosis. Int Immunopharmacol 1:1421–1441. https://doi.org/10.1016/S1567-5769(01)00088-1
Kim SH, Kim JH, Cui JZ, Gal YS, Jin SH, Koh K (2002) Absorption spectra, aggregation and photofading behaviour of near-infrared absorbing squarylium dyes containing perimidine moiety. Dyes Pigm 55(1):1–7. https://doi.org/10.1016/S0143-7208(02)00051-7
Koo YEL, Fan W, Hah H, Xu H, Orringer D, Ross B, Rehemtulla A, Philbert MA, Kopelman R (2007) Photonic explorers based on multifunctional nanoplatforms for biosensing and photodynamic therapy. Appl Opt 46:1924–1930. https://doi.org/10.1364/AO.46.001924
Kukrer B, Akkaya EU (1999) Red to near IR fluorescent signalling of carbohydrates. Tetrahedron Lett 40(51):9125–9128. https://doi.org/10.1016/S0040-4039(99)01890-0
Kumar KS, Ramakrishnappa T, Balakrishna RG, Pandurangappa M (2014) A fluorescent chemodosimeter for hg^{2+}based on a spirolactam ring-opening strategy and its application towards mercury determination in aqueous and cellular media. J Fluoresc 24(1):67–74. https://doi.org/10.1007/s10895-013-1271-1
Kumar M, Puri A (2012) A review of permissible limits of drinking water. Indian J Occup Environ Med 16(1):40–44. https://doi.org/10.4103/0019-5278.99696
Kumar M, Reja SI, Bhalla V (2012) A charge transfer amplified fluorescent Hg^{2+} complex for detection of picric acid and construction of logic functions. Org Lett 14(23):6084–6087. https://doi.org/10.1021/ol3029753
Krishna TR, Parent M, Werts MHV, Moreaux L, Gmouh S, Charpak S, Caminade A-M, Majoral J-P, Blanchard-Desce M (2006) Water-soluble dendrimeric two-photon tracers for in vivo imaging. Angew Chem Int Ed 45:4645–4648. https://doi.org/10.1002/anie.200601246
La YK, Hong JA, Jeong YJ, Lee J (2016) A 1, 8-naphthalimide-based chemosensor for dual-mode sensing: colorimetric and fluorometric detection of multiple analytes. RSC Adv 6:84098–84105. https://doi.org/10.1039/C6RA20100H
Lakowicz JR (1999) Principles of fluorescence spectroscopy, 2nd edn. Plenum Publishing Corporation, New York, p 692
Li J, Yim D, Jang W-D, Yoon J (2017) Recent progress in the design and applications of fluorescence probes containing crown ethers. Chem Soc Rev 46:2437–2458. https://doi.org/10.1039/C6CS00619A
Li B, Ma H, Zhang B, Qian J, Cao T, Feng H, Li W, Dong Y, Qin W (2019) Dually emitting carbon dots as fluorescent probes for ratiometric fluorescent sensing of pH values, mercury(II), chloride and Cr(VI) via different mechanisms. Microchim Acta 186:341. https://doi.org/10.1007/s00604-019-3437-2
Lee H, Hong K-I, Jang W-D (2018) Design and applications of molecular probes containing porphyrin derivatives. Coord Chem Rev 354:46–73. https://doi.org/10.1016/j.ccr.2017.06.008
Lee MH, Kim JS, Sessler JL (2015) Small molecule-based ratiometric fluorescence probes for cations, anions, and biomolecules. Chem Soc Rev 44:4185–4191. https://doi.org/10.1039/C4CS00280F
Li C-Y, Xu F, Li Y-F, Zhou K, Zhou Y (2012) A fluorescent chemosensor for Hg^{2+} based on naphthalimide derivative by fluorescence enhancement in aqueous solution. Anal Chim Acta 717:122–126. https://doi.org/10.1016/j.aca.2011.12.018
Li G, Gao G, Cheng J, Chen X, Zhao Y, Ye Y (2016) Two new reversible naphthalimide-based fluorescent chemosensors for Hg^{2+}. Luminescence 31:992–996. https://doi.org/10.1002/bio.3063
Li M, Zhou X, Ding W, Guo S, Wu N (2013) Fluorescent aptamer-functionalized graphene oxide biosensor for label-free detection of mercury(II). Biosens Bioelectron 41:889–893. https://doi.org/10.1016/j.bios.2012.09.060
Li Z, Yu H, Bian T, Zhao Y, Zhou C, Shang L, Liu Y, Wu L-Z, Tung C-H, Zhang T (2015) Highly luminescent nitrogen-doped carbon quantum dots as effective fluorescent probes for mercuric and iodide ions. J Mater Chem C 3:1922–1928. https://doi.org/10.1039/C4TC02756F
Lin Y-W, Huang C-C, Chang H-T, Lin Y-W, Huang C-C, Chang H-T (2011) Gold nanoparticle probes for the detection of mercury, lead and copper ions. Analyst 136:863–871. https://doi.org/10.1039/C0AN00652A
Liu B-H, Liu D-X, Yang K-Q, Dong S-J, Li W, Wang Y-J (2018) A new cluster-based metal-organic framework with triazine backbones for selective luminescent detection of mercury(II) ion. Inorg Chem Comm 90:61–64. https://doi.org/10.1016/j.inoche.2018.02.008

Liu J, Sun YQ, Wang P, Zhang J, Guo W (2013a) Construction of NIR and ratiometric fluorescent probe for Hg^{2+} based on a rhodamine-inspired dye platform. Analyst 138:2654–2660. https://doi.org/10.1039/C3AN00061C

Liu Y, Chen M, Cao T, Sun Y, Li C, Liu Q (2013b) A cyanine-modified nanosystem for in vivo upconversion luminescence bioimaging of methylmercury. J Am Chem Soc 135(26):9869–9876. https://doi.org/10.1021/ja403798m

Liu Y, Lv X, Zhao Y, Chen M-L, Liu J, Wang P, Guo W (2012) A naphthalimide–rhodamine ratiometric fluorescent probe for Hg^{2+} based on fluorescence resonance energy transfer. Dyes Pigm 92:909–915. https://doi.org/10.1016/j.dyepig.2011.07.020

Liu H, Liu C, Yang X, Zeng S, Xiong Y, Xu W (2008) Uniformly sized-cyclodextrin molecularly imprinted microspheres prepared by a novel surface imprinting technique for ursolic acid. Anal Chim Acta 628:87–94. https://doi.org/10.1016/j.aca.2008.08.042

Lodeiro C, Pina F (2009) Luminescent and chromogenic molecular probes based on polyamines and related compounds. Coord Chem Rev 253:1353–1383. https://doi.org/10.1016/j.ccr.2008.09.008

Loudet A, Burgess K (2007) BODIPY dyes and their derivatives: syntheses and spectroscopic properties. Chem Rev 107(11):4891–4932. https://doi.org/10.1021/cr078381n

Lu D, Zhang C, Fan L, Wu H, Shuang S, Dong C (2013) A novel ratiometric fluorescence probe based on BSA assembled silver nanoclusters for mercuric ion selective sensing. Anal Methods 5:5522–5527. https://doi.org/10.1039/C3AY40901E

Lu W, Qin X, Liu S, Chang G, Zhang Y, Luo Y, Asiri AM, Al-Youbi AO, Sun X (2012) Green synthesis of carbon nanodots as an effective fluorescent probe for sensitive and selective detection of mercury (II) ions. Anal Chem 84:5351–5357. https://doi.org/10.1007/s11051-012-1344-0

Luo D, Liu SG, Li NB, Luo HQ (2018) Water-soluble polymer dots formed from polyethylenimine and glutathione as a fluorescent probe for mercury(II). Microchim Acta 185:284. https://doi.org/10.1007/s00604-018-2817-3

Luo S, Zhang E, Su Y, Cheng T, Shi C (2011) A review of NIR dyes in cancer targeting and imaging. Biomaterials 32:7127–7138. https://doi.org/10.1016/j.biomaterials.2011.06.024

Ma X, Wang J, Shan Q, Tan Z, Wei G, Wei D, Du Y (2012) A "Turn-on" fluorescent Hg^{2+} chemosensor based on ferrier carbocyclization. Org Lett 14(3):820–823. https://doi.org/10.1021/ol2033477

Maçôas E, Marcelo G, Pinto S, Cañeque T, Cuadro AM, Vaquerob JJ, Martinhoa JMG (2011) A V-shaped cationic dye for nonlinear optical bioimaging. Chem Commun 47:7374–7376. https://doi.org/10.1039/C1CC12163D

Mahato P, Saha S, Das P, Agarwalla H, Das A (2014) An overview of the recent developments on Hg^{2+} recognition. RSC Adv 4:36140–36174. https://doi.org/10.1039/C4RA03594A

Maity SB, Banerjee S, Sunwoo K, Kim JS, Bharadwaj PK (2015) A fluorescent chemosensor for Hg^{2+} and Cd^{2+} ions in aqueous medium under physiological pH and its applications in imaging living cells. Inorg Chem 54(8):3929–3936. https://doi.org/10.1021/acs.inorgchem.5b00106

Mandal AK, Suresh M, Das P, Suresh E, Baidya M, Ghosh SK (2012) Recognition of Hg^{2+} ion through restricted imine isomerization: crystallographic evidence and imaging in live cells. Org Lett 14(12):2980–2983. https://doi.org/10.1021/ol3009733

Marme N, Knemeyer J -P, Sauer M, Wolfrum J, (2003) Inter-and intramolecular fluorescence quenching of organic dyes by tryptophan. Bioconjugate Chem 14(6):1133–1139. https://doi.org/10.1021/bc0341324

Martinez-Finley EJ, Aschner M (2014) Recent advances in mercury research. Curr Envir Health Rpt 1:163–171. https://doi.org/10.1007/s40572-014-0014-z

Mason WT (1999) Fluorescent and luminescent chemosensors for biological activity, 2nd edn. Academic Press, London

Moon JO, Choi MG, Sun TH, Choe J-I, Chang S-K (2013) Synthesis of thionaphthalimides and their dual Hg^{2+}-selective signaling by desulfurization of thioimides. Dyes Pigm 96:170–175. https://doi.org/10.1016/j.dyepig.2012.08.007

Moro AJ, Cywinski PJ, Körsten S, Mohr GJ (2010) An ATP fluorescent chemosensor based on a Zn (II)-complexed dipicolylamine receptor coupled with a naphthalimide chromophore. Chem Commun 46:1085–1087. https://doi.org/10.1039/B919661G

Nolan EM, Lippard SJ (2008) Tools and tactics for the optical detection of mercuric ion. Chem Rev 108:3443–3480. https://doi.org/10.1021/cr068000q

Oswald B, Simon L, Lehmann G, Terpetsching E, Wolfbeis OS (2000) Red laser-induced fluorescence energy transfer in an immunosystem. Anal Biochem 280(2):272–277. https://doi.org/10.1006/abio.2000.4553

Paramanik B, Bhattacharyya S, Patra A (2013) Detection of Hg^{2+} and F^- ions by using fluorescence switching of quantum dots in an Au-cluster–CdTe QD nanocomposite. Chem Eur J 19:5980–5987. https://doi.org/10.1002/chem.201203576

Park S-H, Kwon N, Lee J-H, Yoon J, Shin I (2020) Synthetic ratiometric fluorescent probes for detection of ions. Chem Soc Rev 49:143–179. https://doi.org/10.1039/C9CS00243J

Praveen L, Babu J, Reddy MLP, Varma RL (2012) Unfolding with mercury: anthracene-oxyquinoline dyad as a fluorescent indicator for Hg(II). Tetrahedron Lett 53(31):3951–3954. https://doi.org/10.1016/j.tetlet.2012.03.053

Qin S, Chen B, Huang J, Han Y (2018) A thiocoumarin-based colorimetric and ratiometric fluorescent probe for Hg^{2+} in aqueous solution and its application in live-cell imaging. New J Chem 42:12766–12772. https://doi.org/10.1039/c8nj01491d

Qu W-J, Gao G-Y, Shi B-B, Wei T-B, Zhang Y-M, Lin Q, Yao H (2014) A highly selective and sensitive fluorescent chemosensor for mercury ions based on the mechanism of supramolecular self-assembly. Sens Actuators B 204:368–374. https://doi.org/10.1016/j.snb.2014.07.101

Quang DT, Hop NV, Luyen N, Thu HP, Oanh DY, Hien NK, Hieu NV, Lee MH, Kim JS (2013) A new fluorescent chemosensor for Hg^{2+} in aqueous solution. Luminescence 28(2):222–225. https://doi.org/10.1002/bio.2368

Reddie KG, Humphries WH, Bain CP, Payne CK, Kemp ML, Murthy N (2012) Fluorescent coumarin thiols measure biological redox couples. Org Lett 14(3):680–683. https://doi.org/10.1021/ol203105c

Renzoni A, Zino F, Franchi E (1998) Mercury levels along the food chain and risk for exposed populations. Environ Res 77:68–72. https://doi.org/10.1006/enrs.1998.3832

Rice KM, Walker EM Jr, Wu M, Gillette C, Blough ER (2014) Environmental mercury and its toxic effects. J Prev Med Public Health 47(2):74–83. https://doi.org/10.3961/jpmph.2014.47.2.74

Ritchie CM, Johnsen KR, Kiser JR, Antoku Y, Dickson RM, Petty JT (2007) Ag nanocluster formation using a cytosine oligonucleotide template. J Phys Chem C 111:175–181. https://doi.org/10.1021/jp0648487

Rothemund P (1936) A new porphyrin synthesis: the synthesis of porphin[1]. J Am Chem Soc 58(4):625–627. https://doi.org/10.1021/ja01295a027

Rudd ND, Wang H, Fuendes-Fernandez EMA, Teat SJ, Chen F, Hall G, Chabal YJ, Li J (2016) Highly efficient luminescent metal–organic framework for the simultaneous detection and removal of heavy metals from water. ACS Appl Mater Interfaces 8(44):30294–30303. https://doi.org/10.1021/acsami.6b10890

Rui Q-Q, Zhou Y, Fang Y, Yao C (2016) Spirolactone and spirothiolactone rhodamine-pyrene probes for detection of Hg^{2+} with different sensing properties and its application in living cells.

Spectrochim Acta A Mol Biomol Spectrosc 159:209–218. https://doi.org/10.1016/j.saa.2016.01.024
Rurack K, Kollmannsberger M, Daub J (2001) A highly efficient sensor molecule emitting in the near infrared (NIR): 3, 5-distyryl-8-(p-dimethylaminophenyl) difluoroboradiaza-s-indacene. New J Chem 25:289–292. https://doi.org/10.1039/B007379M
Samanta A, Vendrell M, Dasa R, Chang Y-T (2010) Development of photostable near-infrared cyanine dyes. Chem Commun 46:7406–7408. https://doi.org/10.1039/C0CC02366C
Samanta P, Desai AV, Sharma S, Chandra P, Ghosh SK (2018) Selective Recognition of Hg^{2+} ion in Water by a Functionalized Metal−Organic Framework (MOF) Based Chemodosimeter. Inorg Chem 57:2360–2364. https://doi.org/10.1021/acs.inorgchem.7b02426
Sathyamoorthi G, Boyer JH, Allik TH, Chandra S (1994) Laser active cyanopyrromethene–BF_2 complexes. Heteroat Chem 5(4):403–407. https://doi.org/10.1002/hc.520050413
Schade SZ, Jolley ME, Sarauer BJ, Simonson LG (1996) BODIPY–α-Casein, a pH-independent protein substrate for protease assays using fluorescence polarization. Anal Biochem 243(1):1–7. https://doi.org/10.1006/abio.1996.0475
Shan Y, Yao W, Liang Z, Zhu L, Yang S, Ruan Z (2018) Reaction-based AIEE-active conjugated polymer as fluorescent turn on probe for mercury ions with good sensing performance. Dyes Pigm 156:1–7. https://doi.org/10.1016/j.dyepig.2018.03.060
Shan FS, Lai JP, Sun H, Zhang P, Luo C, He YH, Feng H-R (2016) A facile, fast responsive and highly selective mercury(II) probe characterized by the fluorescence quenching of 2,9-dimethyl-1,10-phenanthroline and two new metal–organic frameworks. RSC Adv 6:66215–66223. https://doi.org/10.1039/C6RA13514E
Shang L, Dong D (2008) Facile preparation of water-soluble fluorescent silver nanoclusters using a polyelectrolyte template. Chem Commun. https://doi.org/10.1039/B717728C
Shellaiah M, Rajan YC, Balu P, Murugan A (2015) A pyrene based Schiff base probe for selective fluorescence turn-on detection of Hg^{2+} ions with live cell application. New J Chem 39:2523–2531. https://doi.org/10.1039/C4NJ02367F
Shen Y, Chen C-F (2012) Helicenes: Synthesis and Applications. Chem Rev 112:1463–1535. https://doi.org/10.1021/cr200087r
Singha S, Jun YW, Sarkar S, Ahn KH (2019) An endeavor in the reaction-based approach to fluorescent probes for biorelevant analytes: challenges and achievements. Acc Chem Res 52:2571–2581. https://doi.org/10.1021/acs.accounts.9b00314
Singh A, Raj T, Aree T, Singh N (2013) Fluorescent Organic nanoparticles of biginelli-based molecules: recognition of Hg^{2+} and Cl^- in an aqueous medium. Inorg Chem 52(24):13830–13832. https://doi.org/10.1021/ic402763z
Song S, Qin Y, He Y, Huang Q, Fan C, Chen H-Y (2010) Functional nanoprobes for ultrasensitive detection of biomolecules. Chem Soc Rev 39:4234–4243. https://doi.org/10.1039/c000682n
Srivastava P, Razi SS, Ali R, Gupta RC, Yadav SS, Narayan G, Misra A (2014) Selective naked-eye detection of Hg^{2+} through an efficient turn-on photoinduced electron transfer fluorescent probe and its real applications. Anal Chem 86:8693–8699. https://doi.org/10.1021/ac501780z
Stokes GG (1845) On the change of refrangibility of light. Phil Trans R Soc London 142:463–562. https://doi.org/10.1098/rstl.1852.0022
Shyamal M, Maity S, Maity A, Maity R, Roy S, Misra A (2018) Aggregation induced emission based "turn-off" fluorescent chemosensor for selective and swift sensing of mercury (II) ions in water. Sens Actuators B 263:347–359. https://doi.org/10.1016/j.snb.2018.02.130
Taki M, Akaoka K, Iyoshi S, Yamamoto Y (2012) Rosamine-based fluorescent sensor with femtomolar affinity for the reversible detection of a mercury ion. Inorg Chem 51(24):13075–13077. https://doi.org/10.1021/ic301822r
Tan D, He Y, Xing X, Zhao Y, Tang H, Pang D (2013) Aptamer functionalized gold nanoparticles based fluorescent probe for the detection of mercury (II) ion in aqueous solution. Talanta 113:26–30. https://doi.org/10.1016/j.talanta.2013.03.055
Thoresen LH, Kim H, Welch MB, Burghart A (1998) Burgess K (1998) Synthesis of 3, 5-Diaryl-4, 4-difluoro-4-bora-3a, 4a-diaza-s-indacene (BODIPY®) dyes. Synlett 11:1276–1278
Tian M, Liu L, Li Y, Hu R, Liu T, Liu H, Wang S, Li Y (2014) An unusual OFF–ON fluorescence sensor for detecting mercury ions in aqueous media and living cells. Chem Commun 50:2055–2057. https://doi.org/10.1039/C3CC47915C
Traverso G, Diehl F, Hurst R, Shuber A, Whitney D, Johnson C, Levin B, Kinzler KW, Vogelstein B (2003) Multicolor *in vitro* translation. Nat Biotechnol 21:1093–1097. https://doi.org/10.1038/nbt857
Treibs A, Kreuzer F-H (1968) Difluorboryl-Komplexe von Di- und Tripyrrylmethenen. Justus Liebigs Annalen der Chemie banner 718(1):208–223. https://doi.org/10.1002/jlac.19687180119
Tung C-H (2004) Fluorescent peptide probes for in vivo diagnostic imaging. Pept Sci 76(5):391–403. https://doi.org/10.1002/bip.20139
U.S. Environmental Protection Agency (1989) Risk Assessment, Management and Communication of Drinking Water Contamination, US EPA 625/4-89/024, EPA; Washington, DC, 1989; World Health Organisation. Mercury in drinking-water: Background document for development of WHO guidelines for drinking-water quality, 2005
U.S. Environmental Protection Agency (2001) National Primary Drinking Water Standards; Report EPA 816-F-01-007, EPA, Washington DC WHO (World Health Organization)
Un H-I, Huang C-B, Huang C, Jia T, Zhao X-L, Wang C-H, Xu L, Yang H-B (2014) A versatile fluorescent dye based on naphthalimide: highly selective detection of Hg^{2+} in aqueous solution and living cells and its aggregation-induced emission behaviour. Org Chem Front 1:1083–1090. https://doi.org/10.1039/C4QO00185K
Umezawa K, Nakamura Y, Makino H, Citterio D, Suzuki K (2008) Bright, color-tunable fluorescent dyes in the visible near-infrared region. J Am Chem Soc 130:1550–1551. https://doi.org/10.1021/ja077756j
Urbano A (2003) Recent developments in the synthesis of helicene-like molecules. Angew Chem Int Ed 42:3986–3989. https://doi.org/10.1002/anie.200301667
Vedamalai M (2012) Wu SP (2012) A BODIPY-based highly selective fluorescent chemosensor for Hg2+ ions and its application in living cell imaging. Eur J Org Chem 6:1158–1163. https://doi.org/10.1002/ejoc.201101623
Vonlanthen M, Connelly CM, Deiters A, Linden A, Finney NS (2014) Thiourea-based fluorescent chemosensors for aqueous metal ion detection and cellular imaging. J Org Chem 79:6054–6060. https://doi.org/10.1021/jo500710g
Wagner BD (2009) The use of coumarins as environmentally-sensitive fluorescent probes of heterogeneous inclusion systems. Molecules 14(1):210–237. https://doi.org/10.3390/molecules14010210
Wang F, Xu Y, Aderinto SO, Peng H, Zhang H, Wu H (2017) A new highly effective fluorescent probe for Al^{3+} ions and its application in practical samples. J Photochem Photobiol A Chem 332:273–282. https://doi.org/10.1016/j.jphotochem.2016.09.004
Wang A, Yang Y, Yu F, Xue L, Hu B, Fan W, Dong Y (2015) A highly selective and sensitive fluorescent probe for quantitative detection of Hg^{2+} based on aggregation-induced emission features. Talanta 132:864–870. https://doi.org/10.1016/j.talanta.2014.10.048
Wang F, Nam S-W, Guo Z, Park S, Yoon J (2012) A new rhodamine derivative bearing benzothiazole and thiocarbonyl moieties as a highly selective fluorescent and colorimetric chemodosimeter

for Hg^{2+}. Sens Actuators B Chem 161:948–953. https://doi.org/10.1016/j.snb.2011.11.070

Wang H, Wang Y, Jin J, Yang R (2008) Gold nanoparticle-based colorimetric and "turn-on" fluorescent probe for mercury (II) ions in aqueous solution. Anal Chem 80:9021–9028. https://doi.org/10.1021/ac801382k

Wang Y, Chen J-T, Yan X-P (2013) Fabrication of transferrin functionalized gold nanoclusters/graphene oxide nanocomposite for turn-on near-infrared fluorescent bioimaging of cancer cells and small animals. Anal Chem 85:2529–2535. https://doi.org/10.1021/ac303747t

Weissleder R, Ntziachristos V (2003) Shedding light onto live molecular targets. Nat Med 9:123–128. https://doi.org/10.1038/nm0103-123

Welder F, Paul B, Nakazumi H, Yagi S, Colyer CL (2003) Symmetric and asymmetric squarylium dyes as noncovalent protein labels: a study by fluorimetry and capillary electrophoresis. J Chromatogr B 793(1):93–105. https://doi.org/10.1016/S1570-0232(03)00367-2

Weng J, Mei Q, Ling Q, Fan Q, Huang W (2012) A new colorimetric and fluorescent ratiometric sensor for Hg^{2+} based on 4-pyren-1-yl-pyrimidine. Tetrahedron 68:3129–3134. https://doi.org/10.1016/j.tet.2011.12.071

Wu C, Wang J, Shen J, Bi C, Zhou H (2017) Coumarin-based Hg^{2+} fluorescent probe: synthesis and turn-on fluorescence detection in neat aqueous solution. Sens Actuators B 243:678–683. https://doi.org/10.1016/j.snb.2016.12.046

Wu P, Liu Y, Liu Y, Wang J, Li Y, Liu W, Wang J (2015) Cadmium-based metal–organic framework as a highly selective and sensitive ratiometric luminescent sensor for mercury (II). Inorg Chem 54(23):11046–11048. https://doi.org/10.1021/acs.inorgchem.5b01758

Xu H, Suslick KS (2010) Water-Soluble fluorescent silver nanoclusters. Adv Mater 22:1078–1082. https://doi.org/10.1002/adma.200904199

Xu H, Li Q, Wang L, He Y, Shi J, Tang B, Fan C (2014) Nanoscale optical probes for cellular imaging. Chem Soc Rev 43:2650–2661. https://doi.org/10.1039/c3cs60309a

Xu N-Z, Liu M-M, Ye M-A, Zhou Y, Wu G-Z, Yao C (2017) A Rhodamine-naphthalimide conjugated chemosensor for ratiometric detection Hg^{2+} in actual aqueous samples. J Lumin 188:135–140. https://doi.org/10.1016/j.jlumin.2017.03.067

Yang Y, Zhao Q, Feng W, Li F (2013) Luminescent chemodosimeters for bioimaging. Chem Rev 113:192–270. https://doi.org/10.1021/cr2004103

Yu Z, Tian Z, Li Z, Luo Z, Li Y, Li Y, Ren J (2016) A new chromogenic and fluorogenic chemosensor for Hg (II) with high selectivity based on the Hg^{2+}-promoted deprotection of thioacetals. Sens Actuators B Chem 223:172–177. https://doi.org/10.1016/j.snb.2015.09.082

Yuan L, Lin W, Yang Y, Chen H (2012) A unique class of near-infrared functional fluorescent dyes with carboxylic-acid-modulated fluorescence ON/OFF switching: rational design, synthesis, optical properties, theoretical calculations, and applications for fluorescence imaging in living animals. J Am Chem Soc 134:1200–1211

Zarlaida F, Adli M (2017) Gold and silver nanoparticles and indicator dyes as active agents in colorimetric spot and strip tests for mercury (II) ions: a review. Microchim Acta 184:45–58. https://doi.org/10.1007/s00604-016-1967-4

Zhai D, Zhang K, Zhang Y, Sun H, Fan G (2012) Mesoporous silica equipped with europium-based chemosensor for mercury ion detection: synthesis, characterization, and sensing performance. Inorgan Chim Acta 387:396–400. https://doi.org/10.1016/j.ica.2012.02.035

Zhang H, Tong C, Sha J, Liu B, Lü C (2015a) Fluorescent mesoporous silica nanoparticles functionalized graphene oxide: a facile FRET-based ratiometric probe for Hg^{2+}. Sens Actuators B Chem 206:181–189. https://doi.org/10.1016/j.snb.2014.09.051

Zhang X, Yin J, Yoon J (2014) Recent advances in development of chiral fluorescent and colorimetric sensors. Chem Rev 114:4918–4959. https://doi.org/10.1021/cr400568b

Zhang Y, Chen H, Chen D, Wu D, Chen Z, Zhang J, Chen X, Liu SH, Yin J (2016) A colorimetric and ratiometric fluorescent probe for mercury (II) in lysosome. Sens Actuators B Chem 224:907–914. https://doi.org/10.1016/j.snb.2015.11.018

Zhang Y, Tang L, Yang F, Sun Z, Zhang GJ (2015b) Highly sensitive DNA-based fluorometric mercury (II) bioassay based on graphene oxide and exonuclease III-assisted signal amplification. Microchim Acta 182:1535–1541. https://doi.org/10.1007/s00604-015-1482-z

Zhang Y, Yuan S (2018) Luminescent sensors based on metal-organic frameworks. Coord Chem Rev 354(1):28–45. https://doi.org/10.1016/j.ccr.2017.06.007

Zhang Z, Chen Y, Xu D, Yang L, Liu A (2013) A new 1,8-naphthalimide-based colorimetric and "turn-on" fluorescent Hg^{2+} sensor. Spectrochim Acta Mol Biomol Spectrosc 105:8–13. https://doi.org/10.1016/j.saa.2012.11.113

Zheng Z-Q, Bian Q-N, Zhang X-J (2013) Advances in modifying fluorescein and rhodamine fluorophores as fluorescent chemosensors. Chem Comm 49:429–447. https://doi.org/10.1039/C2CC35997A

Zhou Y, Chu K, Zhen H, Fang Y, Yao C (2013) Visualizing Hg^{2+} ions in living cells using a FRET-based fluorescent sensor. Spectrochim Acta Part A: Mol. Biomol Spectrosc 106:197–202. https://doi.org/10.1016/j.saa.2012.12.092

Zhou Y, Tang L, Zeng G, Zhang C, Zhang Y, Xie X (2016) Current progress in biosensors for heavy metal ions based on DNAzymes/DNA molecules functionalized nanostructures: a review. Sens Actuators B Chem 223:280–294. https://doi.org/10.1016/j.snb.2015.09.090